

**THE USE OF MICROTREMOR MEASUREMENTS FOR SEISMIC HAZARD  
STUDIES IN THE GREATER VANCOUVER REGIONAL DISTRICT (GVRD)**

by

DENNIS TEO

B.A.Sc., The University of British Columbia, 1997

A THESIS SUBMITTED IN PARTIAL FULFILLMENT OF  
THE REQUIREMENTS FOR THE DEGREE OF  
**MASTER OF APPLIED SCIENCE**

in

THE FACULTY OF GRADUATE STUDIES

Department of Civil Engineering

We accept this thesis as conforming  
to the required standard



THE UNIVERSITY OF BRITISH COLUMBIA

November 1999

©Dennis Teo, 1999

In presenting this thesis in partial fulfilment of the requirements for an advanced degree at the University of British Columbia, I agree that the Library shall make it freely available for reference and study. I further agree that permission for extensive copying of this thesis for scholarly purposes may be granted by the head of my department or by his or her representatives. It is understood that copying or publication of this thesis for financial gain shall not be allowed without my written permission.

Department of CIVIL ENGINEERING

The University of British Columbia  
Vancouver, Canada

Date 25 NOVEMBER 1999

# ABSTRACT

---

The Greater Vancouver Regional District (GVRD) in the province of British Columbia is located in one of the most seismically active regions of Canada. In this thesis, a method for assessing the seismic hazard potential at GVRD sites using the characteristics of microtremors is evaluated. These characteristics, site predominant periods and relative amplification ratios, were determined by analyzing records of microtremors. The feasibility of using the microtremor characteristics for hazard estimation was investigated.

The stability of the characteristics of microtremors at a site is crucial for assessing seismic hazard potential. For the GVRD region, the site predominant periods of microtremors were found to be stable over time. On the other hand, the peak Fourier spectral amplitudes and horizontal-to-vertical spectral ratios tend to fluctuate over time in response to the strength of the input sources. Comparison of spectral characteristics of microtremors and those of low-level earthquake ground motions showed that microtremor measurements can be used effectively to delineate the periods of peak response of sites. At deeper sites (>150 m) the periods of peak response from microtremors may reflect either the dominant response due to resonance in one of the upper strata or the excitation of one of the higher periods at the sites instead of the fundamental periods of these sites. The relative amplification ratio was found to be an inconsistent indicator for comparing the relative seismic amplification potential of sites.

# TABLE OF CONTENTS

---

ABSTRACT.....	ii
TABLE OF CONTENTS .....	iii
LIST OF TABLES .....	vi
LIST OF FIGURES .....	vii
ACKNOWLEDGEMENTS.....	x
DEDICATION.....	xi
CHAPTER 1 INTRODUCTION.....	1
1.1 Background Information .....	1
1.2 Scope and Objectives of This Study .....	4
1.3 Outline of Thesis.....	5
CHAPTER 2 MICROTREMORS: THEORY AND PRACTICE .....	6
2.1 Theory of Microtremors.....	6
2.2 Past and Current Research .....	10
CHAPTER 3 NAKAMURA'S METHOD.....	15
3.1 Background on Nakamura's Method.....	15
3.2 Recent Studies of Nakamura's Method .....	21
CHAPTER 4 STABILITY OF MICROTREMOR CHARACTERISTICS .....	28
4.1 Stability Test of Microtremor Measurements.....	28
4.1.1 Determination of Stability of Site Periods and Amplification Ratios using Average Fourier Spectra .....	29
4.1.2 Determination of Stability of Site Periods and Amplification Ratios using Nakamura's Procedure...	30
4.1.3 Conclusions.....	31

CHAPTER 5	UBC'S MICROTREMOR MEASUREMENT TECHNIQUE AND DATA ANALYSIS.....	37
	5.1 Introduction.....	37
	5.2 Microtremor Measurements and Typical Testing Procedures ..	37
	5.2.1 Equipment used for Microtremor Measurements .....	38
	5.2.2 Deciding Sensor Locations .....	39
	5.2.3 Typical Testing Procedure.....	40
	5.3 Method for Determining Site Predominant Periods and Relative Amplification Ratios.....	46
	5.3.1 Channel Data Extraction.....	46
	5.3.2 Determination of Site Predominant Periods and Relative Amplification Ratios .....	47
CHAPTER 6	APPLICATION OF MICROTREMOR MEASUREMENTS – CASE STUDIES .....	52
	6.1 Geology of the Fraser Delta.....	52
	6.2 Comparison of Microtremor Measurements with Earthquake Ground Motions at station MNY .....	56
	6.2.1 Background Information on the Earthquake Ground Motions .....	56
	6.2.2 Comparison of Spectral Characteristics between Microtremors and Earthquake Ground Motions.....	57
	6.3 Lulu Island, New Westminister .....	61
	6.3.1 Site Predominant Periods and Estimated Depths of Surface Layer .....	61
	6.3.2 Relative Amplification Ratios.....	64
	6.4 Richmond.....	75
	6.4.1 Site Predominant Periods and Estimated Depths of Surface Layer .....	75
	6.4.2 Relative Amplification Ratios.....	78
	6.5 Conclusions.....	89
CHAPTER 7	SUMMARY, CONCLUSIONS AND RECOMMENDATIONS FOR FUTURE RESEARCH.....	91
	7.1 Summary.....	91
	7.2 Conclusions.....	92

7.2.1	Stability of Dynamic Characteristics of Microtremors .....	92
7.2.2	Surface Microtremor Measurements .....	92
7.2.3	Analytical Analysis and Interpretation .....	93
7.3	Recommendations for Future Research .....	94
NOMENCLATURE .....		96
ABBREVIATIONS .....		98
REFERENCES .....		99
APPENDIX A	MICROTREMOR MEASUREMENTS .....	102
A.1	Overview .....	102
A.2	Equipment Check List.....	102
A.3	Preparation and Storage of Sensors .....	103
A.5	Setup of Data Acquisition System .....	105
A.6	Typical Testing Procedures.....	106
APPENDIX B	MICROTREMOR DATA FILE CONVERSION .....	116
B.1	Description.....	116
B.2	Conversion Procedures .....	116
APPENDIX C	MICROTREMOR DATA ANALYSIS – PROGRAM OPERATING INSTRUCTIONS AND DOCUMENTATION .....	119
C.1	Description.....	119
C.2	Installation And System Requirements.....	132
C.2.1	Installation of DADiSP 4.1 .....	132
C.2.2	Installation of DADiSP Macro Files.....	132
C.3	Program Execution.....	133
C.3.1	Storing the Data Files for Batch Processing .....	133
C.3.2	Running the Programs .....	134
C.3.3	Example of Experimental Analytical Results .....	134

## LIST OF TABLES

---

Table 6.1	Definition of Geological Settings in the Fraser Delta.....	55
Table 6.2(a)	Earthquake Source Information (after Hao <i>et al.</i> , 1998).....	58
Table 6.2(b)	Earthquake Peak Ground Accelerations Recorded at station MNY (after Hao <i>et al.</i> , 1998).....	58
Table 6.3(a)	Site Predominant Periods, Estimated Depths of Surface Layer(s), Relative Amplification Ratios and Number of Storeys of Buildings likely to experience the most damage under strong shaking along Wood Street in Lulu Island, New Westminster, British Columbia.....	67
Table 6.3(b)	Site Predominant Periods, Estimated Depths of Surface Layer(s), Relative Amplification Ratios and Number of Storeys of Buildings likely to experience the most damage under strong shaking along Ewen Avenue in Lulu Island, New Westminster, British Columbia.....	67
Table 6.4(a)	Site Predominant Periods, Estimated Depths of Surface Layer(s), Relative Amplification Ratios and Number of Storeys of Buildings likely to experience the most damage under strong shaking along Shell Road in Richmond, British Columbia.....	81
Table 6.4(b)	Site Predominant Periods, Estimated Depths of Surface Layer(s), Relative Amplification Ratios and Number of Storeys of Buildings likely to experience the most damage under strong shaking along Westminster Highway in Richmond, British Columbia.....	82

## LIST OF FIGURES

---

Figure 2.1	Present Understanding about Low-strain Ground Motions (modified from Seo, 1997) .....	7
Figure 2.2(a)	Microtremor Average Fourier Response Spectrum with one distinct peak .....	9
Figure 2.2(b)	Microtremor Average Fourier Response Spectrum with more than one distinct peak .....	9
Figure 2.3	Comparison of Spectra between Microtremors and Strong Motion during the 1985 Mexico earthquake for several Strong Motion Stations (after Seo, 1997) .....	14
Figure 3.1	Comparison of Response Spectra of Microtremors During Quiet Interval and Passage of a Train (after Nakamura, 1989) .....	19
Figure 3.2	Stability of Site Predominant Frequency from Nakamura's Method (after Nakamura, 1989) .....	19
Figure 3.3	Range of $R_B$ values for various sites in Japan (after Nakamura, 1989) ...	20
Figure 3.4	Schematic of the Multiple Source Model used for Noise Simulation (after Lachet and Bard, 1994) .....	25
Figure 3.5	Shape of the Source Functions used in Time Domain (after Lachet and Bard, 1994) .....	26
Figure 3.6	Comparison of H/V Peak Frequencies for Noise Simulation and those for Vertically Incident Shear Waves (after Lachet and Bard, 1994) .....	27
Figure 3.7	Comparison of H/V Peak Amplitudes for Noise Simulation and the Maximum Amplitudes of the Transfer Function for Vertically Incident Shear Waves (modified after Lachet and Bard, 1994) .....	27
Figure 4.1	Location of MNY Station .....	32
Figure 4.2	Variations of Predominant Frequencies from Average Fourier Spectra over time .....	33
Figure 4.3	Variations of Peak Amplitudes from Average Fourier Spectra over time .....	34
Figure 4.4	Variations of Predominant Frequencies from Nakamura's Method over time .....	35
Figure 4.5	Variations of Peak Amplitudes from Nakamura's Method over time .....	36

Figure 5.1	Flow chart of Microtremor Data Acquisition and Analysis.....	42
Figure 5.2	Response Characteristics of Velocity Sensors used for Microtremor Measurements .....	43
Figure 5.3	Arrangement of Data Acquisition System .....	44
Figure 5.4	Typical Arrangement of Sensors (Top view).....	44
Figure 5.5	Examples of Measured Microtremor Records with: (a) limited or no signal saturation, (b) some signal saturation, and (c) too much signal saturation .....	45
Figure 5.6	An Example of An Analyzed Record of Microtremor Measurement at Shell Road (1999) .....	50
Figure 5.7	Location of the Reference Hard Ground Site: Station K05 .....	51
Figure 6.1	Map of the Fraser Delta area showing Surface Geology and Depths of Holocene Deposits (after Hao <i>et al.</i> , 1998).....	54
Figure 6.2	Acceleration Records and Fourier Spectra of the 1996 Duvall, Washington Earthquake measured at station MNY (after Hao <i>et al.</i> , 1998).....	59
Figure 6.3	Acceleration Records and Fourier Spectra of the 1997 Georgia Strait, British Columbia Earthquake measured at station MNY (after Hao <i>et al.</i> , 1998) .....	60
Figure 6.4	Locations of Microtremor Measurement Stations along Wood Street and Ewen Avenue in Lulu Island, New Westminster, British Columbia .....	66
Figure 6.5	Distribution of $V_{S30}$ in Lulu Island, New Westminster and Richmond from Seismic Cone Penetration Tests carried out by Geological Survey of Canada (after Hunter <i>et al.</i> , 1998).....	68
Figure 6.6	An Example of Records of Microtremor Measurements at Sites along Wood Street in Lulu Island (1998) .....	69
Figure 6.7	An Example of Records of Microtremor Measurements at Sites along Ewen Avenue in Lulu Island (1998).....	70
Figure 6.8	Distribution of Site Predominant Periods (in seconds) along Wood Street and Ewen Avenue in Lulu Island, New Westminster, B.C.....	71
Figure 6.9	Distribution of Estimated Depths (in metres) of Surface Layer(s) based on $V_S$ of 200 m/s along Wood Street and Ewen Avenue in Lulu Island, New Westminster, B.C.....	72

Figure 6.10	Distribution of Shear Wave Velocities and Soil Profiles with Depth at Borehole station FD97-1 (after Geological Survey of Canada, 1998).....	73
Figure 6.11	Distribution of Relative Amplification Ratios along Wood Street and Ewen Avenue in Lulu Island, New Westminster, B.C.....	74
Figure 6.12	Locations of Microtremor Measurement Stations and Distribution of Site Predominant Periods (in seconds) along Shell Road and Westminster Highway in Richmond, B.C.....	80
Figure 6.13	An Example of Records of Microtremor Measurements at Sites along Shell Road in Richmond (1998) .....	83
Figure 6.14	An Example of Records of Microtremor Measurements at Sites along Westminster Highway in Richmond (1998) .....	84
Figure 6.15	Distribution of Estimated Depths (in metres) of Surface Layer(s) based on $V_s$ of 185 m/s along Shell Road and Westminster Highway in Richmond, B.C. ....	85
Figure 6.16	Distribution of Shear Wave Velocities and Soil Profiles with Depth at Borehole station FD94-4 near station K20 (after Geological Survey of Canada, 1998) .....	86
Figure 6.17	Distribution of Relative Amplification Ratios along Shell Road and Westminster Highway in Richmond, B.C.....	87
Figure 6.18	Plot of Relative Amplification Ratios versus Estimated Depths of Surface Layer(s).....	88
Figure A.1	Sensors used to measure vibrations in Horizontal (Sensors on Left and Right) and Vertical (Sensor in the middle) directions .....	111
Figure A.2	Sensor (with case removed) used to measure vibrations in the Horizontal direction .....	112
Figure A.3	Sensor (with case removed) used to measure vibrations in the Vertical direction .....	113
Figure A.4	Amplifier Model TA-406.....	114
Figure A.5	Main Menu of Data Acquisition Program .....	115
Figure C.1	DADiSP Worksheet Layout.....	135
Figure C.2	An Example of An Analyzed Record of Microtremor Measurement at Station K15 in U.B.C. (1998) .....	136
Figure C.3	Location of Microtremor Measurement Station K15.....	137

## ACKNOWLEDGEMENTS

---

I would like to thank my supervisors, Dr. W.D.L. Finn and Dr. C. Ventura for their constant guidance, patience and encouragement throughout this research. Without their timely advice and understanding this thesis work would not have been successful. Their thoughts and constructive suggestions during their review of early drafts of this thesis are greatly appreciated.

I am deeply indebted to Dr X.-S. Hao. His invaluable assistance in performing microtremor measurements and spectral analysis is gratefully appreciated. I would also like to thank Dr P. Monahan for providing invaluable information on geological conditions of several sites studied in this thesis. Finally, I would like to thank the Geological Survey of Canada for providing the CD-ROM which contains the geological and seismic data of various sites in the Fraser River Delta.

I would like to express my sincere gratitude to Dr L. Finn, Dr C. Ventura, Dr P.M. Byrne, Dr Y.P. Vaid, Dr J.A. Howie and Dr J. Fannin for enriching my knowledge of Geotechnical/Earthquake engineering through their excellent courses.

Also, I would like to thank Mr. Howard Nichol, the U.B.C.'s earthquake lab technician, for safekeeping of the microtremor data acquisition system. In addition, I would like to thank Mr. Pei-Chin Tsai who provided invaluable assistance during the field tests.

Finally, I would like to thank Dr. W.D.L. Finn and Dr. C. Ventura who reviewed the final draft of this thesis.

The financial support provided by the University of British Columbia is acknowledged with deep appreciation. This includes a Graduate Research Assistantship, as well as International Graduate Student Tuition Fee Scholarships.

*This thesis is dedicated to my parents...*

*Thank you for your constant support, guidance and  
love without which this thesis could not have been  
possible.*

# CHAPTER 1

## INTRODUCTION

---

### 1.1 BACKGROUND INFORMATION

The Greater Vancouver Regional District (GVRD) in south-western British Columbia, Canada is situated in one of the most seismically active regions of Canada. Because significant earthquakes are expected to occur in the GVRD region in the future (Finn, 1996) and will most likely affect the economy of the province adversely, it is of great importance to assess the distribution of seismic hazard potential in the region.

Local site or geological conditions greatly influence the damage potential of incoming seismic waves from major earthquakes (Finn, 1994; Seo, 1997). For example, the 1985 Michoacan earthquake caused extensive damage to structures with periods close to site periods in Mexico City. The peak accelerations of the input motions in rock of less than 0.05 g were amplified by about 5 times on the clay soils of the old lakebed on which Mexico City is located. Seismic hazard assessment provides a means of quantifying or estimating the effects of local geological conditions on potential seismic response of sites. There are several methods for assessing the seismic hazard potential of sites. One method is by performing site-specific, detailed dynamic analyses based on earthquake records and soil properties from site characterizations. Typical site investigation methods include the standard penetration tests (SPT), seismic cone penetration tests (SCPT), shear wave velocity ( $V_s$ ) measurements, as well as retrieval and testing of soil samples. The dynamic analysis approach is, however, too costly and time-consuming, and is thus only

performed for important projects. An alternative approach for effective mapping of seismic hazard potential on a regional basis is to use code-based amplification or foundation factors. Amplification factors are factors assigned to soil zones based on descriptions of soils from geological maps and soils data available from site investigations for specific projects. They reflect damage associated with different soil conditions in the field, and in an approximate way integrate the effects of possible soil amplification and soil-structure resonance (Finn, 1997). Examples of seismic response characterizations which make use of amplification factors include the *1994 NEHRP Guidelines; Foundation Factors, F (NBCC, 1995)* and *Definition of Site Classes and Amplification Factors (Borcherdt, 1994)* (Finn, 1997). However, this method of seismic hazard mapping requires data from site investigations and can be time-consuming and costly when such data is not available already.

In this thesis a method for mapping seismic hazard potential based on the characteristics of microtremors recorded at a site is investigated. Microtremors are *low-strain* or weak ground motions caused by human activities, operating machinery, and traffic. They propagate through the ground and are amplified at periods synchronous with the predominant periods of site response. Microtremors have been used to estimate predominant site periods and relative amplification factors for microzonation purposes (Nakamura, 1989; Hao *et al.*, 1994; Seo, 1992, 1995 and 1997). Seismic hazard mapping or seismic microzonation based on characteristics of microtremors has some significant advantages over the more conventional methods. Microtremor measurements are performed on the ground surface so no borings or insitu tests are required. As a result, a

large number of sites can be evaluated in a relatively short time. Microtremor measurements can therefore provide a fast and cheap way of assessing dynamic characteristics of the ground for seismic hazard studies.

The characterization of site response to strong earthquake incoming motions using parameters based on weak motion response parameters such as those from microtremor measurements is favourable because of the ease of obtaining such response and wider availability of weak seismic motion data. Weak motions are defined as motions which elicit mainly elastic response from the site (Finn, 1994). Past characterization of sites for weak motion response (Borcherdt and Gibbs, 1976; Borcherdt, 1991) have shown that ground motion characteristics such as local shear wave velocity or site periods strongly correlate with the site conditions or the type of geologic units. Studies carried out by Borcherdt (1990, 1991) and Borcherdt *et al.* (1991) showed that response estimated based on weak motion characterization appeared to be generally applicable to seismic response during the 1989 Loma Prieta earthquake in San Francisco Bay area. For instance, the average horizontal spectral amplifications were found to be consistent with those of the weak motion response to within one standard deviation for the San Francisco Bay Mud sites and within two standard deviations for alluvial sites (Finn, 1994). The difference in the responses of strong motions and weak motions can be attributed to the nonlinear response of the soil sites during strong earthquake shaking. The nonlinear effect can cause significant damping effects or deamplifications to the soil response. Hence the response predicted using the weak motion data would correctly predict enhanced ground motions during strong shaking but would also overestimate the amplification response of

the strong motion. The characterization of strong motion response by weak motion parameters is therefore useful in indicating the relative seismic hazard potential or sites but in many cases these parameters cannot be used to directly quantify strong motion response.

## **1.2 SCOPE AND OBJECTIVES OF THIS STUDY**

The objective of this thesis is to assess the effectiveness of microtremor measurements as a basis for mapping seismic hazard potential of sites. In order to accomplish this, a feasibility study was carried out by comparing the dynamic characteristics of microtremors with those based on geological and seismic data. The dynamic characteristics of interest explored in this thesis are the site predominant periods and relative amplification ratios. The site predominant period is the period of peak response whereas the relative amplification ratios is the corresponding peak amplitude of the horizontal-to-vertical spectral ratio at a site normalized using that of a reference hard ground site. This thesis covers several aspects of microtremors, including theoretical background, instruments used for measurement, guidelines for microtremor measurements, method of data analysis, and illustrations of the application of microtremor microzonation using case studies. The stability of microtremor characteristics at a given site over time is also investigated.

Microtremor measurements for this study were conducted at selected sites in the Fraser Delta of the GVRD, specifically in Lulu Island, New Westminster and in Richmond. The microtremor data acquisition and analysis system of the University of British Columbia's

Civil Engineering Department was utilized to perform the microtremor measurements. The measured microtremor records were analyzed and maps showing the distribution of site predominant periods and relative amplification ratios were developed. The results from microtremor measurements were compared with available seismic response data to determine the validity of the microtremor results.

### 1.3 OUTLINE OF THESIS

This thesis is comprised of seven chapters and three appendices. The second chapter presents the theory of microtremors and background information on the use of microtremor characteristics. The third chapter describes Nakamura's H/V method, and presents a discussion of its validity and applicability. **Chapter Four** discusses the importance of stability of microtremor characteristics, and presents the results of stability tests carried out at a measurement station in Vancouver. **Chapter Five** describes the microtremor measurement procedures and analyses of the microtremor records obtained during the course of this study. Discussion of the results and case studies are presented in **Chapter Six**. Finally, summary, conclusions and recommendations for future research are presented in the final chapter.

**Appendix A** includes details of the microtremor data acquisition system presently used at U.B.C. **Appendix B** contains details on microtremor data file conversions. Finally, **Appendix C** contains descriptions and operating instructions for data analysis using DADiSP software. A sample result of data analysis is also shown in **Appendix C**.

## CHAPTER 2

# MICROTREMORS: THEORY AND PRACTICE

---

### 2.1 THEORY OF MICROTREMORS

The ground surface layers are normally exposed to two kinds of low-strain ground motions or tremors, the so-called microseisms and microtremors (Kanai *et al.*, 1960). Microseisms are caused by natural agents (storms, sea waves, wind) and microtremors are caused by artificial agents (automobiles, machines, human activities). The microtremors normally predominate in the period range shorter than two seconds, and reflect ground motion characteristics of soft sediment layers. The microtremors measured at a site tend to show a fairly stable predominant period over time, but the microtremor amplitudes change between day and night times. Microseisms usually appear in the period range longer than about three seconds, and may provide useful information about deeper site structures. The features of the microseisms -- both amplitude and period characteristics -- are affected by the weather conditions. Present understanding about low-strain ground motions is illustrated in **Figure 2.1**.

Theoretically, microtremor measurements can be used to produce an accurate estimation of ground vibration characteristics (Nakamura, 1989; Hao, 1992; Seo, 1995). The characteristics of the measured ground motions reflect the dynamic characteristics of the subsurface soil conditions and the properties of the source of ground motions. Ground vibration is essentially amplified at periods almost identical to the site predominant periods of the surface soil layers as the incident ground motion passes through the soil

layers. Hence, characteristics of measured microtremors can be used to quantify the effects of local geological conditions on site response, and provide information on the amplification characteristics of a site.

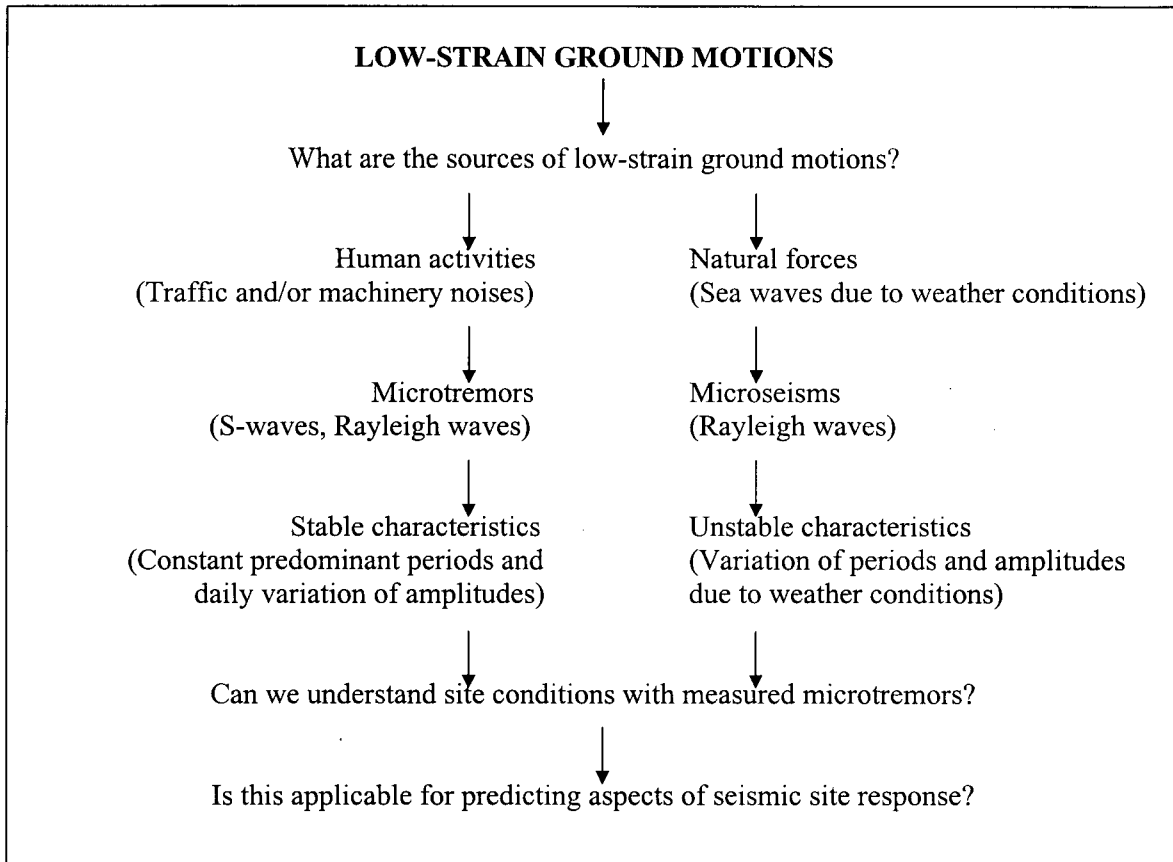


**Figure 2.1** Present Understanding about Low-strain Ground Motions (modified from Seo, 1997).

The usefulness of microtremor observations can be illustrated by considering a Fourier response spectrum processed from a measured microtremor record. Examples of a microtremor Fourier response spectrum with one distinct peak and a Fourier spectrum with more than one distinct peak are shown in **Figures 2.2(a)** and **(b)**. The Fourier spectrum reveals the dynamic characteristics of the site at which the microtremor measurement was carried out. The peak of the spectrum indicates the site predominant period of the surface layer at which ground shaking is likely to experience the most amplification. Soft and deep layers would generally have long periods, whereas hard and thin layers would have short periods. Two or more pronounced peaks might appear in the response spectrum, as illustrated by **Figure 2.2(b)**, indicating that the site is resonating at two or more frequencies of the ground motions. If the multiple peaks are present in a narrow frequency band, it may be due to improper signal processing of the collected data (Bendat and Piersol, 1993).

The peak spectral amplitudes may contain strong source effects in the input ground motions (Nakamura, 1989; Hao *et al.*, 1994). In which case, they are not suitable as a means of comparison of relative amplification potential between sites. The source effects on peak amplitudes can be reduced substantially using ratios of horizontal-to-vertical spectral components (Nakamura, 1989) to determine periods of peak response. Normalization of the peak amplitudes of the spectral ratios by the peak amplitude of a reference rock site gives the relative amplification ratio between a soft soil site and a hard ground site. The relative amplification ratio may provide a basis for comparing the relative amplification potential of different sites under earthquake shaking.

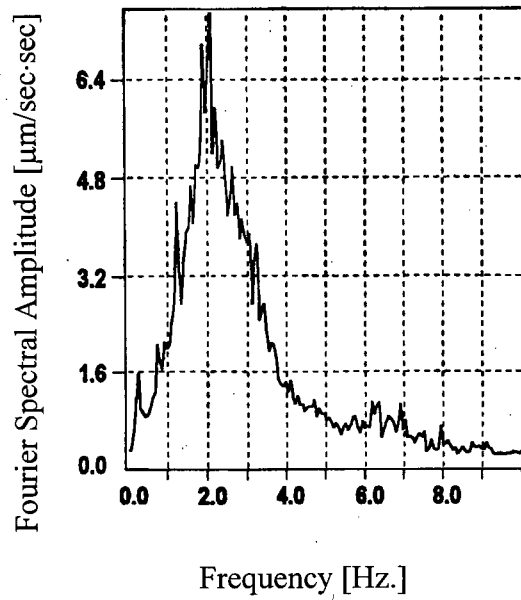


**Figure 2.2(a)** Microtremor Average Fourier Response Spectrum with one distinct peak.

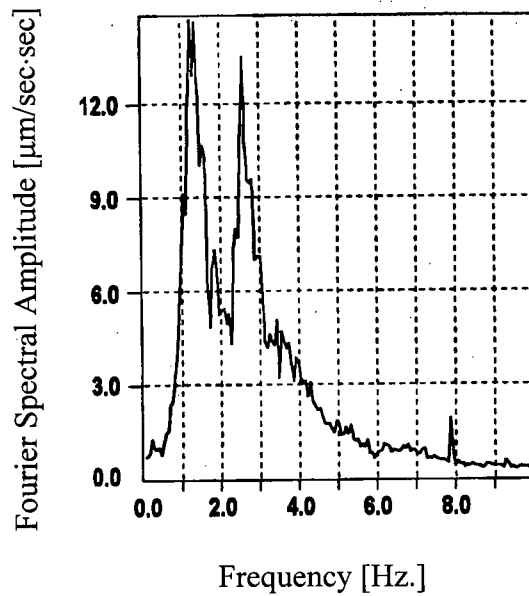


**Figure 2.2(b)** Microtremor Average Fourier Response Spectrum with more than one distinct peak.

## 2.2 PAST AND CURRENT RESEARCH

Research on the use of microtremors for microzonation purposes has been carried out and documented over the last few decades. Significant progress has been made on the use of microtremors for seismic hazard studies since Kanai and his associates first used microtremor measurements to determine dynamic characteristics, specifically microtremor patterns and periods, of sites for microzonation purposes (Kanai *et al.*, 1954; Kanai and Tanaka, 1960).

Udwadia and Trifunac (1978) investigated the feasibility of using microtremors to determine site amplification characteristics for earthquake shaking by comparing data from strong motion earthquake records and microtremor measurements at El Centro, California. They found little correlation between the amplification characteristics of the ground motions due to earthquake shaking and microtremor excitation, and hence concluded that microtremors are mostly affected by source characteristics and wave propagation effects. In addition, they found that the amplitudes of microtremor motions were stationary over durations of 5 to 10 minutes but not so over a period of a day. The main problem was the source effects of the input motions which made the interpretation of microtremor data extremely difficult. Also, the microtremors reflect elastic ground response whereas moderate to strong earthquake shaking induces nonlinear soil behaviour which changes the dynamic characteristics of the site.

Aki (1988) reviewed the problems associated with the determination of frequency dependent, site specific, amplification factors using microtremors. He concluded that the

inability to separate source effects from site effects is a major obstacle to the effective use of microtremor measurements for evaluation of site characteristics. Since the sources are likely to be different for different sites, it is difficult to determine even the relative amplifications reliably. Hence, the effective use of microtremor measurements in determining the site response characteristics would require a method of removing or minimizing source effects. Such a procedure was proposed by Nakamura (1989) based on horizontal-to-vertical spectral ratios. Periods of peak response based on these ratios were very stable and source effects were minimized. This method will be discussed in the next chapter.

Kagami, Duke, Liang and Ohta (1982) examined the usefulness of long-period microtremors for earthquake engineering problems at sites with extremely deep soil deposits. Extensive microtremor observations were carried out in Niigata Plain, Japan, and in Los Angeles, California, where depths to the basement rock are several kilometers. The result of Fourier analysis showed that the amplitude of microtremors in the long-period range increased systematically from the outcrop of basement rock to the deep deposit site, with the increase corresponding to the depth to basement rock. This result supports the use of microtremors for relative amplitude estimation. Note that the long-period tremors referred to above are microtremors, not microseisms.

Seo (1997) investigated whether microtremors could be used to assess the dynamic characteristics of earthquake strong motions. Microtremor measurements were made in the Mexico basin just after the 1985 Mexico earthquake. **Figure 2.3** shows a comparison

between microtremor Fourier response spectra and strong motion acceleration spectra from the 1985 earthquake at several stations in Mexico City. Although the spectral shapes are dissimilar, the site periods from measured microtremors and strong motions are essentially identical on soft sediment sites (SCT, CDAO, and CDAF). These sites responded essentially elastically within the range of ground motion amplitudes and hence nonlinear effects were low. Stable microtremor periods have also been found in Japan around the damaged Kobe-Hanshin area of the 1995 Hyogoken-Nanbu earthquake. On firm hill sites in Mexico City, such as UNAM, VIV and TAC, site periods from microtremors and strong motion shaking are not similar. This evidence suggests that the application of microtremor measurements in delineating the predominant periods of sites may be effective on soft sites but not necessarily on hard sites.

The studies described above represent a sampling of research conducted on microtremors. Based on these studies, the following observations can be made regarding the use of microtremors for seismic hazard assessment:

- Source effects have a major impact on the site frequency (or period) and amplitude of microtremors. Therefore the effective use of microtremor data for microzonation purposes will only be possible with the removal of source effects.
- The source effects may be removed or minimized using a method proposed by Nakamura (1989).
- Even in the absence of source effects, site periods and site amplification factors estimated from microtremor measurements may not be applicable to the sites during strong shaking because of nonlinear response of the soil layer(s).

- Microtremors may not generate peak response at the fundamental period of the site but at other periods.
- Based on comparisons of strong motion records and measured microtremors, it appears that microtremor measurements may be useful in providing information on low-strain site periods and other site amplification characteristics.

In conclusion, microtremor measurements may be used to quantify the effects of local geological conditions on ground motions and provide a basis for comparing the relative damage potential of sites if source effects can be removed from site measurements. In the next chapter, a method for removing the source effects will be introduced.

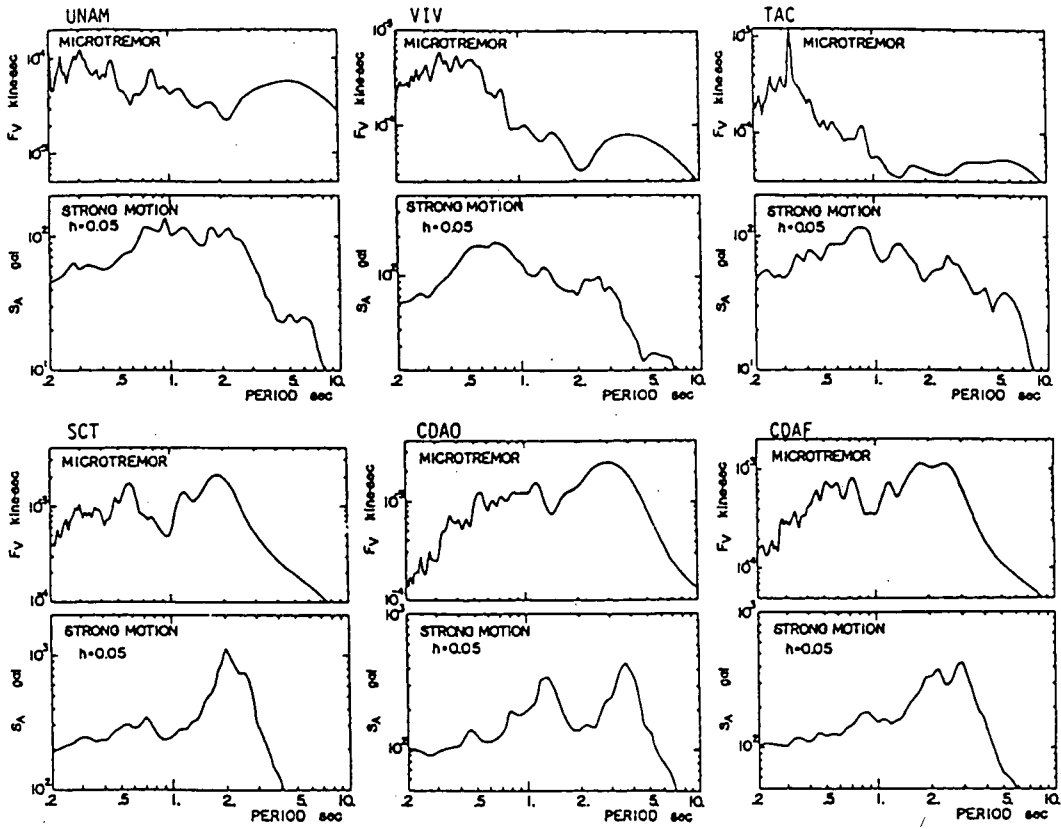


**Figure 2.3** Comparison of Spectra between Microtremors and Strong Motions during the 1985 Mexico earthquake for several Strong Motion Stations (after Seo, 1997).

## CHAPTER 3

# NAKAMURA'S METHOD

---

This chapter presents the Nakamura's method (§3.1) for the interpretation of microtremor measurements and discusses its general validity (§3.2).

### 3.1 BACKGROUND ON NAKAMURA'S METHOD

Nakamura proposed a method of estimating the dynamic characteristics of surface layers by measuring solely the microtremors at the ground surface. In the past microtremor measurements had to be conducted during a relative quiet time span to minimize source effects which can cause substantial fluctuation in the predominant periods of microtremors. Such effects can be seen at sites such as Tabata in Japan where microtremors were recorded on an hourly basis over a 30-hour period at each site (Nakamura, 1989). **Figure 3.1** shows the Fourier response spectra of microtremors measured at three different times at a Tabata site. Microtremor measurements were taken during the passage of a train, at an intermission of train operation during the day and during a quiet time at 3:00 AM. The signature of a local source such as a passing train is clearly evident in **Figure 3.1**. The Fourier spectrum of the microtremors including the frequency or period of peak responses was radically altered by the passing train. Nakamura then applied his proposed method, in which site response is characterized by the ratio of horizontal to vertical spectra at the site, to the hourly data over a 24-hour period at the Tabata site. **Figure 3.2** shows the Fourier response spectral ratios of microtremors measured over the 24 hours. The predominant frequency of the site was

essentially stable and was not changed by source effects. These results and those from other recent applications of Nakamura's method, e.g., Hao *et al.* (1994), show that Nakamura's method can be effective in stabilizing periods of peak response and minimizing source effects. The background on Nakamura's method is presented below.

The dynamic characteristics observed at a point include all of the wave motion radiation characteristics  $F(f)$  at the focal region, the dynamic characteristics  $T(f)$  of the wave motion propagation route up to the observation point, and the dynamic characteristics  $S(f)$  of the surface layers at the observation point, where  $f$  denotes frequency (Nakamura, 1989). The surface sources,  $F(f)$ , were assumed to generate mostly Rayleigh waves and affect both the horizontal and vertical motions in the surface layer equally. This is the key assumption of the method. For each observation point and different low-strain earthquake/ground motions, the surface layer characteristics  $S(f)$  are essentially the same even when the radiation characteristics  $F(f)$  and/or propagation characteristics  $T(f)$  are different. The stability of the dynamic characteristics of the surface layer(s) is what makes microtremor analysis a useful tool for determining site characteristics.

The dynamic characteristics of surface layers can be estimated from the transfer function for horizontal motions at a site. Surface microtremor measurements provide spectral ratios of horizontal-to-vertical components of the surface layer which may be used to assess the transfer function for horizontal motions at a site. As a result, the transfer function of surface layers may be assessed from surface measurements of microtremors alone. This is explained as follows.

The transfer function for horizontal motions at a site,  $S_T$ , is defined as:

$$S_T = \frac{S_{HS}}{S_{HB}}$$

where  $S_{HS}$  and  $S_{HB}$  are the spectral ordinates of the horizontal motions at the surface and the hard base layer respectively. The transfer function for vertical motions,  $E_S$ , is defined as:

$$E_S = \frac{S_{VS}}{S_{VB}}$$

where  $S_{VS}$  and  $S_{VB}$  are the frequency-dependent spectral ordinates of the vertical motions at the surface and the hard base layer respectively. A key assumption here is that there is no amplification in the vertical ground motions. If there are no Rayleigh waves or source effects,  $E_S = 1$ ;  $E_S$  will become larger than 1 with increasing effects of Rayleigh waves (Nakamura, 1989).

The effects of source or Rayleigh waves are compensated by the modified transfer function,  $S_{TT}$ , for the site which incorporates the effects of the horizontal and vertical transfer functions.  $S_{TT}$  is defined as:

$$S_{TT} = \frac{S_T}{E_S}$$

If there are no source effects,  $E_S = 1$  and  $S_{TT}$  is the same as the horizontal transfer function, i.e.,  $S_{TT} = S_T$ . In the scenario that there are source effects,  $E_S$  is greater than 1.

The  $S_{TT}$  can then be written as:

$$S_{TT} = \frac{S_T}{E_S} = \frac{S_{HS}/S_{HB}}{S_{VS}/S_{VB}} = \frac{S_{HS}/S_{VS}}{S_{HB}/S_{VB}} = \frac{R_S}{R_B}$$

where  $R_S = \frac{S_{HS}}{S_{VS}}$  and  $R_B = \frac{S_{HB}}{S_{VB}}$ .  $R_S$  and  $R_B$  are obtained by dividing the spectral ordinates of the horizontal microtremor spectrum by those of the vertical microtremor spectrum, with the subscripts  $S$  and  $B$  correspond to the surface and the hard base layer respectively. In order to use surface microtremor measurements to assess the transfer functions of sites, it is necessary that  $S_{TT}$  is approximately equal to  $R_S$ , where  $R_S$  is the horizontal-to-vertical spectral ratio from surface microtremor measurements. Test results from detailed studies at the Kanonomiya and Tabata sites in Japan showed that the horizontal-to-vertical spectral ratios at the bedrock,  $R_B$ , were approximately 1.0 for a relatively wide frequency range, as indicated by **Figure 3.3**, i.e., on the firm substrate, wave propagation is essentially even in all directions. This is summarized as follows:

$$R_B \cong 1 \text{ and therefore, } S_{TT} \cong R_S$$

Hence, the transfer function of surface layers may be estimated from surface measurements of microtremors alone. A more reliable  $S_{TT}$  can be estimated by multiplying  $R_S$  with  $1/R_B$  when geological data of the ground is provided since  $R_B$  contains the characteristics unique to the point and is free from the effect of Rayleigh waves. In this thesis, it was assumed that  $R_B$  fluctuates within a much narrower range than  $R_S$  and thus does not significantly affect the relative amplitudes of the spectral ratios in  $R_S$  (Finn, 1992). Considering that  $R_B$  is essentially constant at 1.0 over a significant period range of engineering interest as described above, this assumption is reasonable.

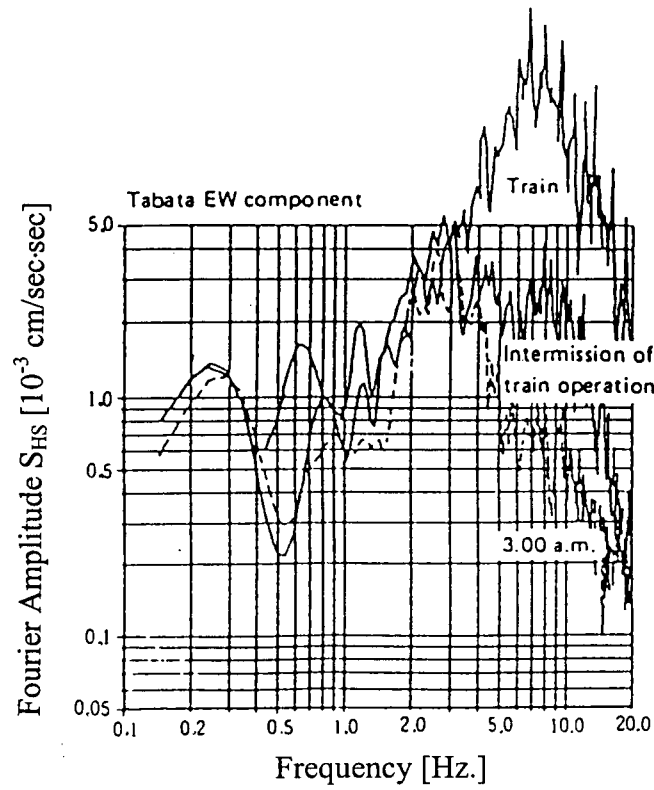


**Figure 3.1** Comparison of Response Spectra of Microtremors during Quiet Interval and Passage of a Train (after Nakamura, 1989).

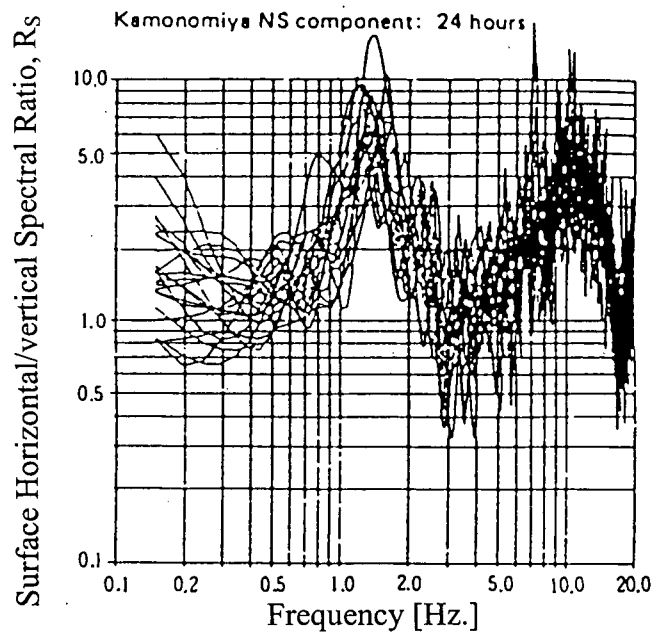


**Figure 3.2** Stability of Site Predominant Frequency from Nakamura's Method (after Nakamura, 1989).

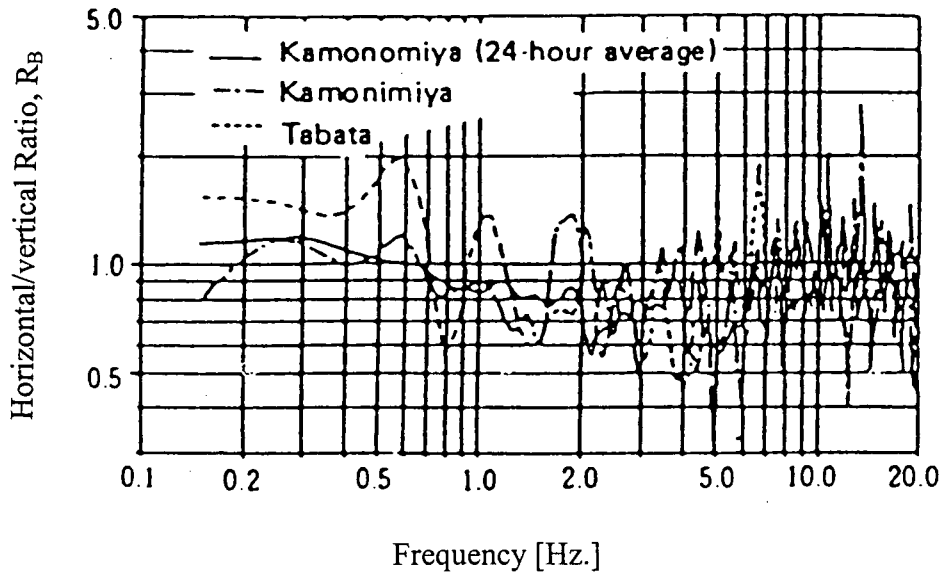


**Figure 3.3** Range of  $R_B$  values for various sites in Japan (after Nakamura, 1989).

### 3.2 RECENT STUDIES OF NAKAMURA'S METHOD

Lachet and Bard (1994) performed a numerical analysis of Nakamura's method using urban noise simulation to investigate both the amplitude and position of the peak of the horizontal-to-vertical (or H/V) spectral ratios and their relation to vertical shear wave resonance in the surface layer(s) for different source types and for varying geological structures. The results of both studies are discussed as follows.

Firstly, Lachet and Bard (1994) investigated the position of the H/V peak and its sensitivity to different source types and geological conditions. Nakamura (1989) stated that the position of the H/V peak indicates the period of peak response when it is independent of the source characteristics. The sensitivity of the location of the peak of H/V ratios to source characteristics and different geological structures was investigated using a multiple source model as shown in **Figure 3.4**. The multiple source model used sources consisting of explosions and a unidirectional force to simulate urban noises with different source functions. The shapes of the different source functions such as step, Ricker and pseudo-Dirac in the time domain are as shown in **Figure 3.5**. The measured records were analyzed using Nakamura's method. Lachet and Bard found that the position of the peak of H/V ratios remains constant regardless of the source types or functions used in the simulations. This result supported Nakamura's claim that the position of the H/V peak is independent of the source characteristics.

The influence of the geological conditions on the H/V peak position was investigated using six simple theoretical models of geological structures with varying shear velocity

contrast and thickness of the soil layers, and a few more complex, real geological structures. Lachet and Bard found that for different cases representing different geological conditions, the H/V peaks locate at different frequency positions. They concluded that the H/V peaks represent distinct geological structures. Lachet and Bard (1994) also compared the frequency corresponding to the H/V peak,  $f_n$ , to that of the resonance site frequency corresponding to the vertical  $S_V$  wave resonance,  $f_s$ . The results of comparison between  $f_n$  and  $f_s$  are shown in **Figure 3.6**. There was good agreement between  $f_n$  and  $f_s$  where the data of  $f_n$  versus  $f_s$  aligned along the fitting line  $f_n = f_s$ . They therefore concluded that the peak position of the H/V ratios is probably a reliable indicator of the frequency (or period) of peak response of the ground surface layer for different geological conditions.

Lachet and Bard further investigated whether the amplification of seismic motion due to resonance of ground surface layer(s) might be estimated from the maximum spectral amplitude of the H/V ratio. **Figure 3.7** shows the comparison between the amplitude of the H/V peaks ( $A_n$ ) obtained and the maximum amplitude of the amplification function for vertically incident S waves ( $A_s$ ) at several sites; the dotted line is the fitting line of  $A_s = A_n$ . It is clear that there was poor agreement between the H/V peak amplitude and the maximum amplitudes for the vertically incident shear waves. Moreover, investigations on the influence of variations of Poisson's ratio and source-receiver distance on the H/V peak amplitude have also shown that the amplitude of the H/V peak was very sensitive to variations in these parameters. As a result, Lachet and Bard concluded that very poor

correlation exists between the amplitude of the H/V peak and the actual amplification value under  $S_V$  wave incidence.

Based on the results discussed above, the main conclusions regarding Nakamura's method are summarized as follows:

- The position of the peak of H/V ratios is independent of the source characteristics or excitation function. This shows that Nakamura's method is effective in removing the source effects from microtremor measurements.
- The frequencies from the H/V peak positions derived from noise simulation were similar to the resonance frequencies from vertically incident  $S_V$  waves. Hence, the peak of H/V ratios from Nakamura's method gives a reliable indication of the resonance frequency or frequency of peak response of the surface layer.
- The peak amplitudes of the H/V ratios from Nakamura's method were found to correlate poorly with the maximum amplitudes at resonance frequency of the vertically incident  $S_V$  waves in addition to being very sensitive to Poisson's ratio in the sedimentary structure and the source-receiver distance. The poor or lack of correlation between the peak amplitudes from Nakamura's method and those at fundamental resonance from vertically incident shear waves suggests that Nakamura's method provides information on spectral amplification characteristics of peak response but not necessarily those at fundamental resonance of the sites. This is especially true for sites with deep surface layers (>200 metres) overlying the bedrock such as at many sites in Richmond. A case study on amplification response of Richmond sites, including such a deep site is presented and discussed in §6.4.

In conclusion, Nakamura's method is effective in minimizing the source effects from site effect quantification using microtremor measurements. It can therefore provide a reliable estimate of the predominant frequency (or period) and potential amplification characteristics at peak response of a given site. The peak horizontal-to-vertical spectral ratios are dependent upon the strength of input motions. They may be normalized using the spectral ratio of a reference hard ground site, and used as a basis for comparing the relative amplification potential between sites under strong shaking. The next chapter describes tests at a site in GVRD to investigate the stability of site periods and amplification characteristics of microtremors. Issues on stability of site predominant period and peak amplitude of horizontal-to-vertical spectral ratios estimated using Nakamura's method are addressed.

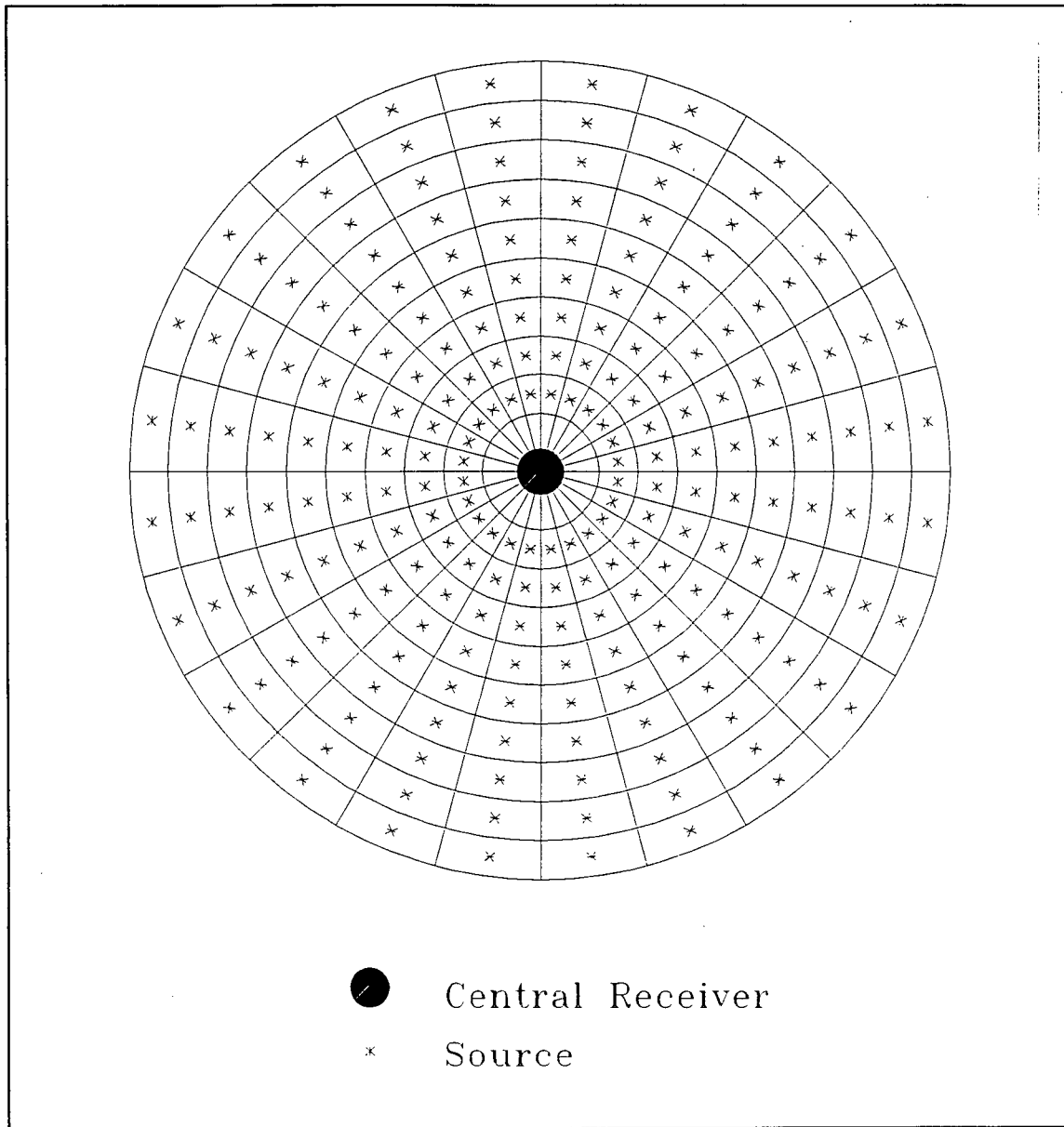


**Figure 3.4** Schematic of the Multiple Source Model used for Noise Simulation (after Lachet and Bard, 1994).

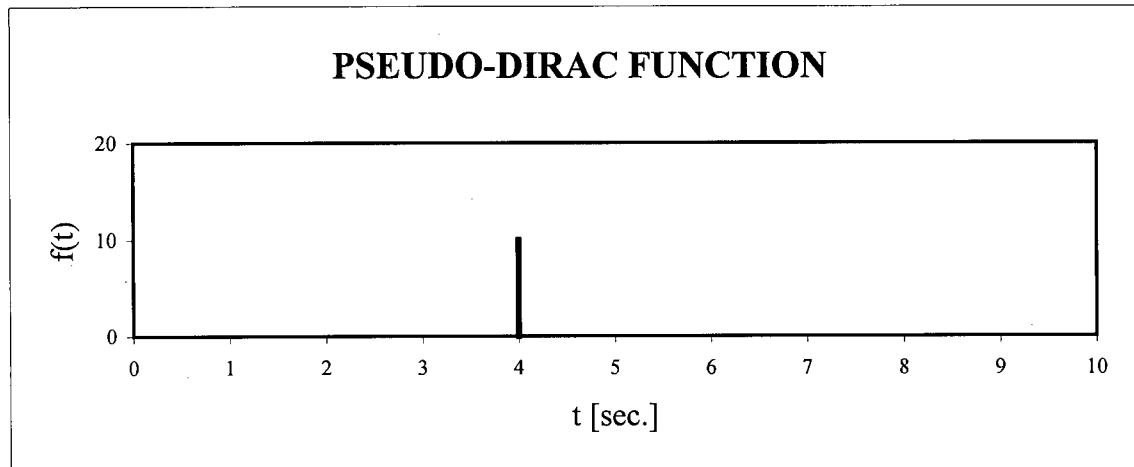
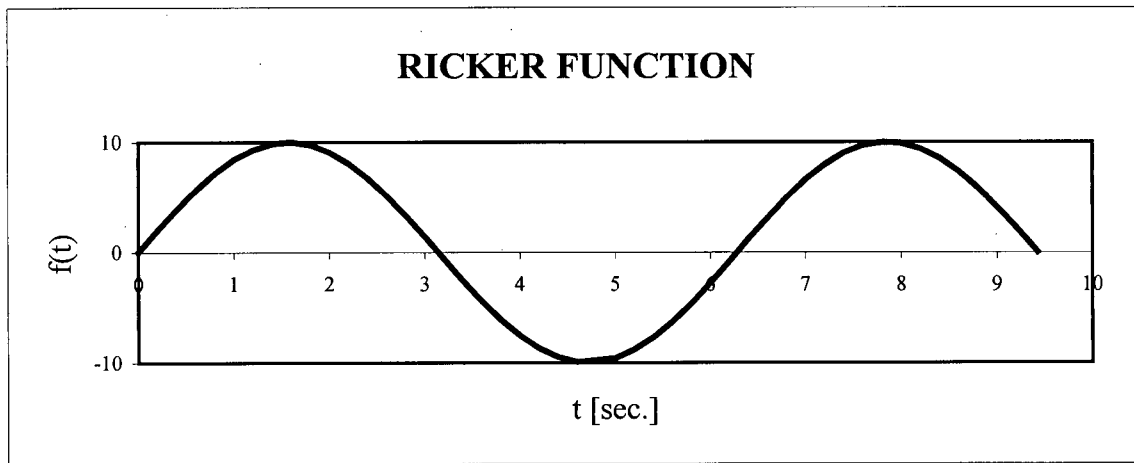
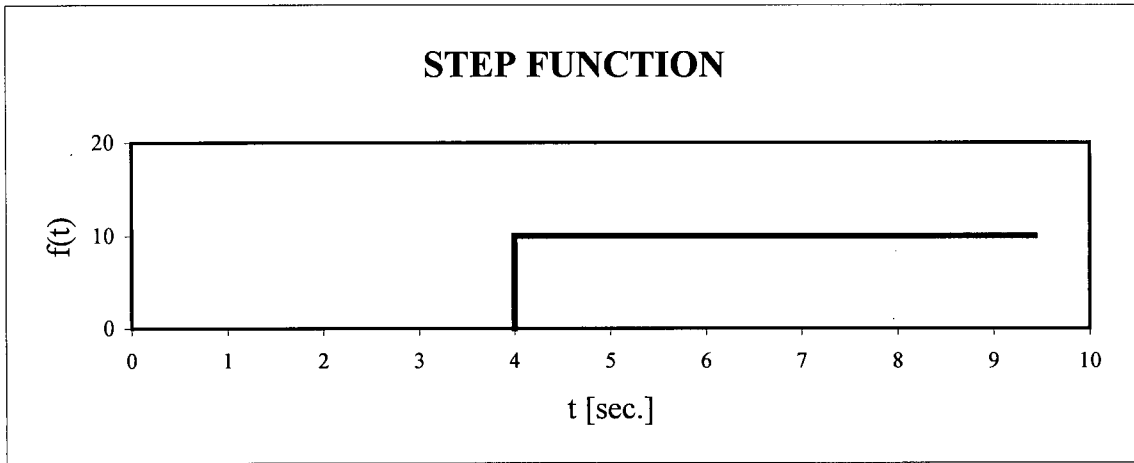


**Figure 3.5** Shape of the Source Functions used in Time Domain (after Lachet and Bard 1994).

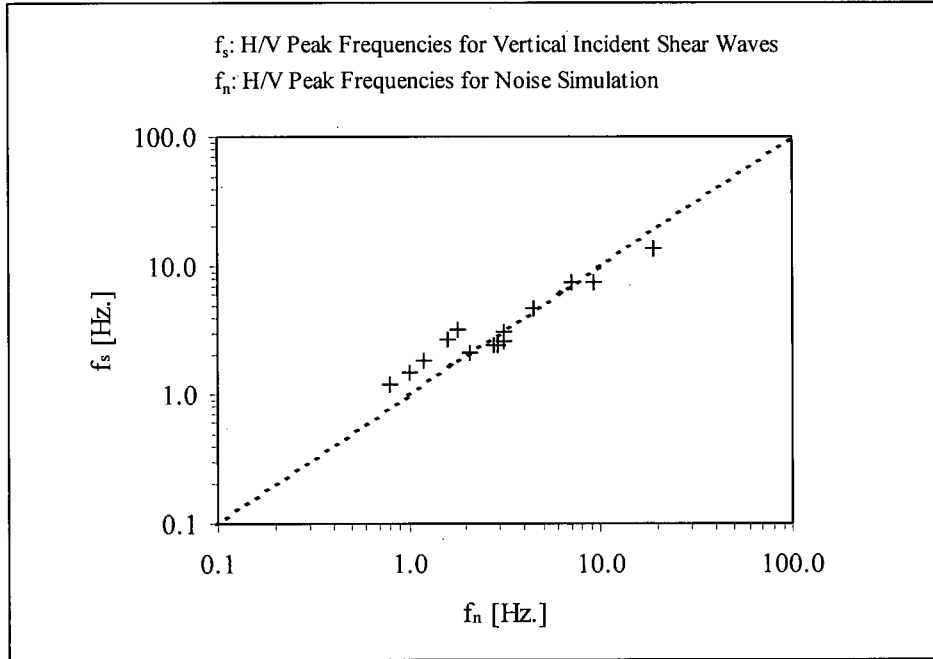


**Figure 3.6** Comparison of H/V Peak Frequencies for Noise Simulation and those for Vertically Incident Shear Waves (after Lachet and Bard, 1994).

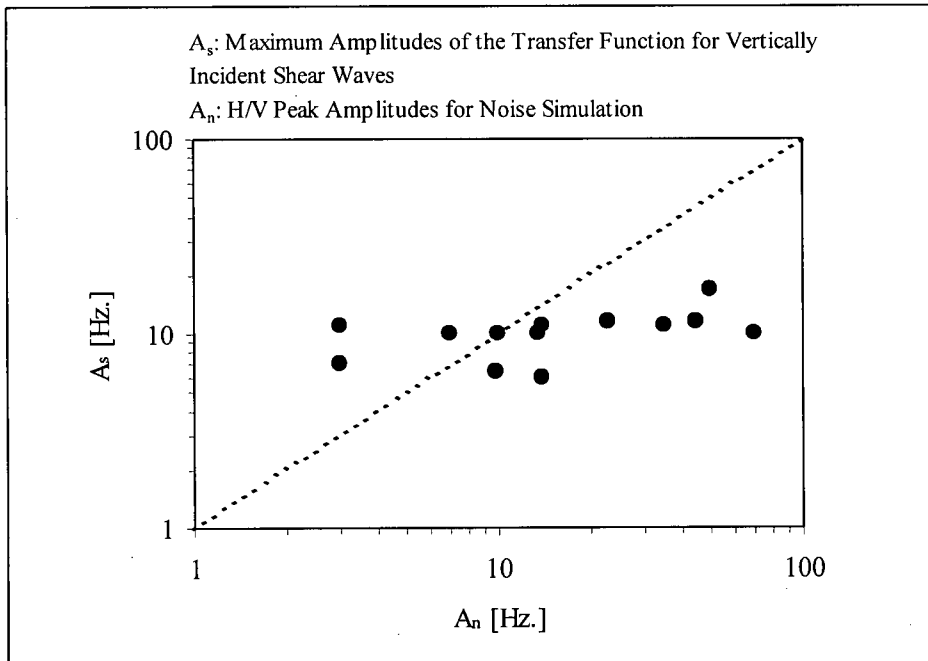


**Figure 3.7** Comparison of H/V Peak Amplitudes for Noise Simulation and the Maximum Amplitudes of the Transfer Function for Vertically Incident Shear Waves (modified after Lachet and Bard, 1994).

## CHAPTER 4

# STABILITY OF MICROTREMOR CHARACTERISTICS

---

The results of a stability test carried out in the GVRD region are discussed and presented in this chapter. The stability test was carried out by Hao *et al.*, 1997 to assess the spectral stability of microtremor characteristics in the GVRD region. Details of the test can be found in the report entitled "Microtremor Measurements in the Vancouver Regional District, Canada" (Hao, Finn, Ventura, Seo, Samano, 1998).

### 4.1 STABILITY TEST OF MICROTREMOR MEASUREMENTS

A key requirement for effective use of microtremor measurements for seismic hazard studies is the stability of microtremor characteristics over time. Stability is evaluated by examining the variations in predominant periods and amplification ratios at a particular site over a long period of time.

Continuous measurements were carried out by Hao *et al.* at strong motion station MNY in Vancouver from 12 A.M., 23 September 1997 to 10 A.M., 1 October 1997. The location of station MNY which is about 5 km northeast of the Vancouver International Airport is shown in **Figure 4.1**. Weather and meteorological conditions were nearly constant during the period of measurements, with some rainy periods from September 25 to October 1, 1997. A total of 96 measurements each with duration of 300 seconds were taken every 2 hours during an 8-day period. Each record consisted of measurements in

two orthogonal horizontal directions – N00E and N90E – and the vertical direction of the ground motions. The predominant frequencies and the corresponding spectral amplitudes of the microtremors were determined using two methods as described below.

#### **4.1.1 DETERMINATION OF STABILITY OF SITE PERIODS AND AMPLIFICATION RATIOS USING AVERAGE FOURIER SPECTRA**

A detailed analysis of all records of the stability test was performed to determine the most amplified frequencies and the corresponding peak spectral amplitudes based on average Fourier response spectra. The Fourier spectra were obtained by dividing each record into eight segments and then taking the average of the results. **Figure 4.2** shows the distribution of peak frequencies along the north-south direction (NS), the east-west (EW) direction, and the average peak frequencies over the test period. The results of the analysis show that the predominant frequency was nearly constant at  $2.3$  to  $2.4 \pm 0.25$  Hz (with the exception of a few outliers) for the entire duration of the test. Both the NS and EW directions give very similar site predominant frequencies. **Figure 4.3** shows the distribution of peak amplitudes along the NS and EW directions, and the average peak amplitudes over the test period. The amplitudes varied widely from day-time to night-time, ranging from a high of  $0.009$  cm/sec-sec during the day-time to a low of  $0.0007$  cm/sec-sec at night-time. Also, the amplitudes were much smaller during weekends compared to those during the weekdays during the test period, probably due to decreased traffic activities in the area. This is clearly shown in **Figure 4.3** where September 28<sup>th</sup> to September 29<sup>th</sup>, 1999 was the weekend. The results on peak amplitudes show that the peak amplitudes varied in accordance to the strength of the input motions or sources.

#### 4.1.2 DETERMINATION OF STABILITY OF SITE PERIODS AND AMPLIFICATION RATIOS USING NAKAMURA'S PROCEDURE

Nakamura's method was also used to determine the frequencies of peak response and the corresponding peak amplitudes of the spectral ratios. The distribution of the site predominant frequencies and peak amplitudes of the Fourier spectral ratios along the NS and EW directions, and the average site predominant frequency over the test period are shown in **Figures 4.4** and **4.5** respectively. The site predominant frequency was found to be nearly constant at  $2.2 \pm 0.15$  Hz along the NS and EW directions, with both directions giving very similar average site predominant frequencies. It is similar to that found using the average Fourier response spectra but Nakamura's method gives a smaller standard deviation of 0.15 Hz compared to 0.25 Hz from the average Fourier spectra. The variation of amplitudes of spectral ratios was somewhat smaller than from the average Fourier spectra, varying from a high of 0.009 cm/sec-sec during day-time to a low of 0.003 cm/sec-sec at night-time. In addition, the peak amplitudes during the weekends were observed to be smaller than those during the weekdays. These results again indicate that the peak amplitudes were dependent upon the strength of the input motions, even though the source effects had been minimized using Nakamura's method.

### 4.1.3 CONCLUSIONS

Based on the results of the stability test at station MNY, it can be concluded that the site predominant period is a stable characteristic of microtremor measurements, regardless of the orientation of measurements (NS or EW). Both Nakamura's method and the Fourier response spectra give similar site predominant period likely because there were no strong source effects at the MNY site. Nakamura's method did however give a smaller standard deviation in the determination of the site predominant period. The main advantage of Nakamura's method is that it gives good results of site periods of peak response even if there are strong source effects, as evidenced by results of microtremor measurements at Tabata site in Japan (§3.1).

The peak amplitudes from both Fourier spectra and Nakamura's spectral ratios tend to fluctuate over time in relation to the strength of the input motions or sources. Nakamura's method did give a narrower range of variation in the peak spectral ratio amplitudes compared to that of the Fourier spectra. Finally, based on the results from the stability test, it can be concluded that Nakamura's method does fairly well stabilize the site predominant frequencies and the corresponding peak amplitudes of the measured microtremors.

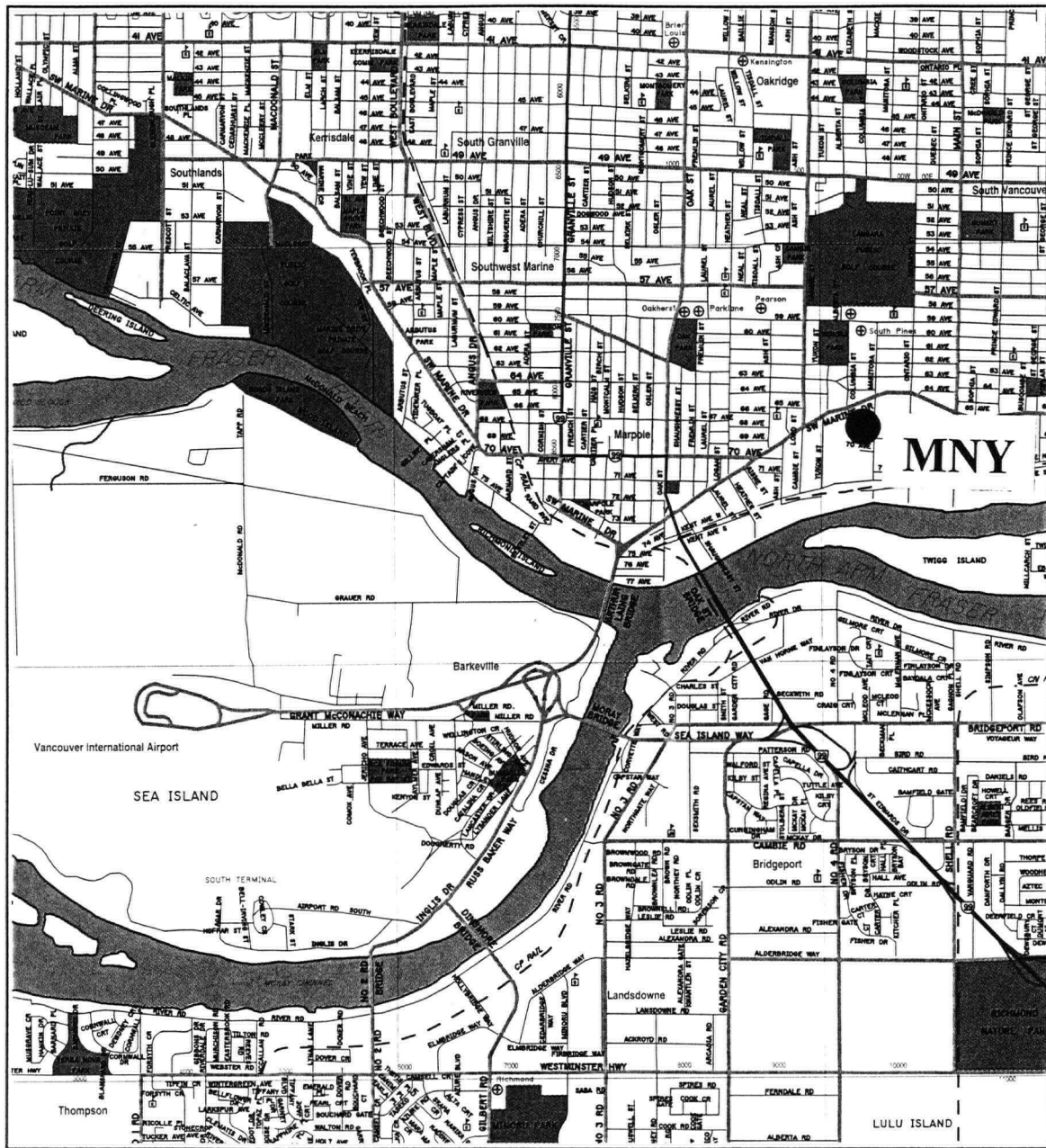
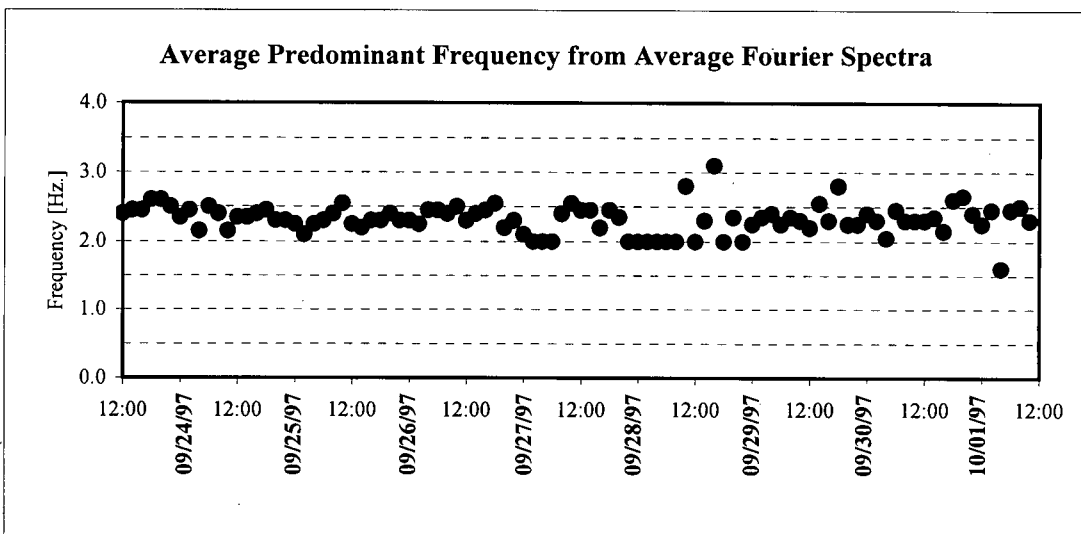
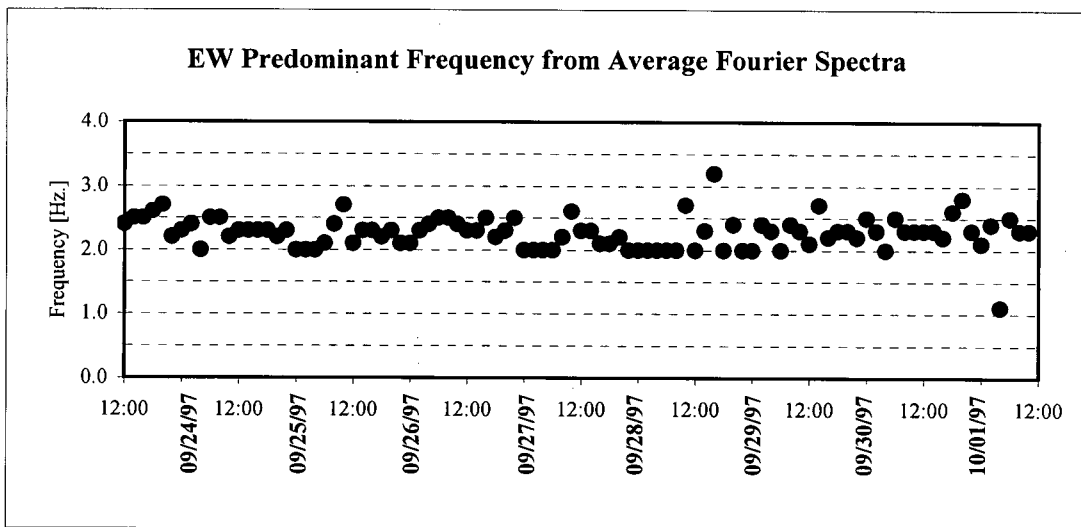
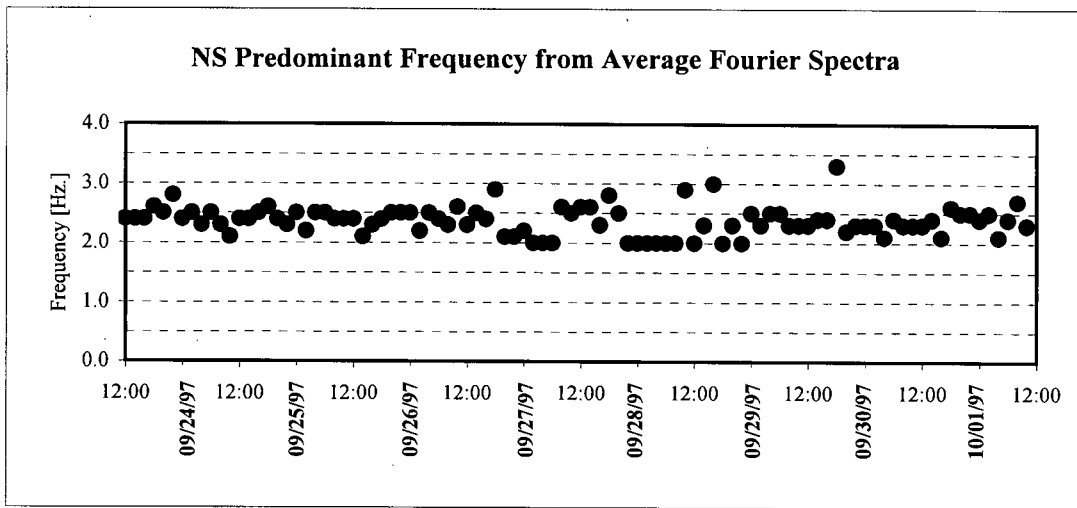
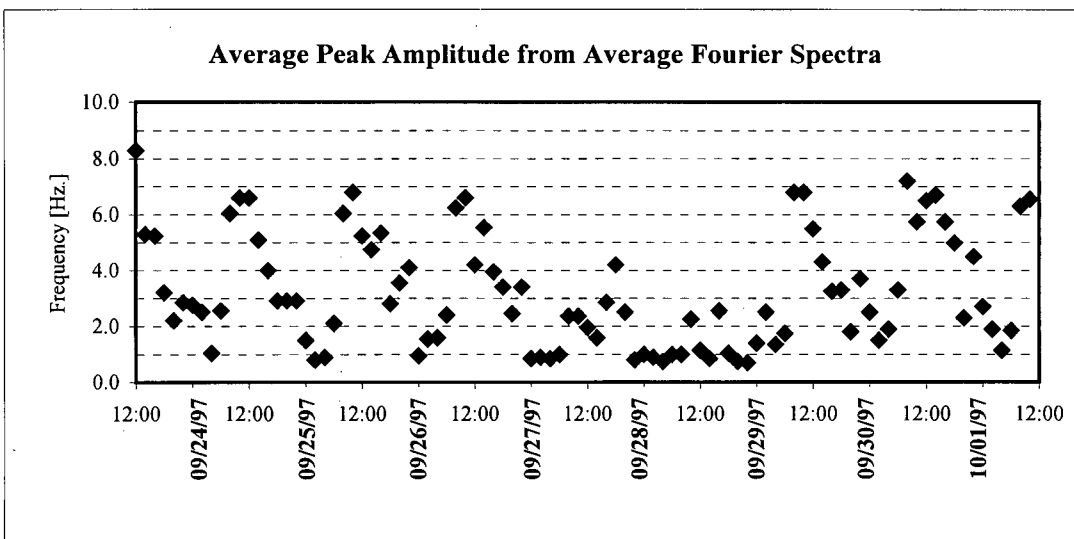
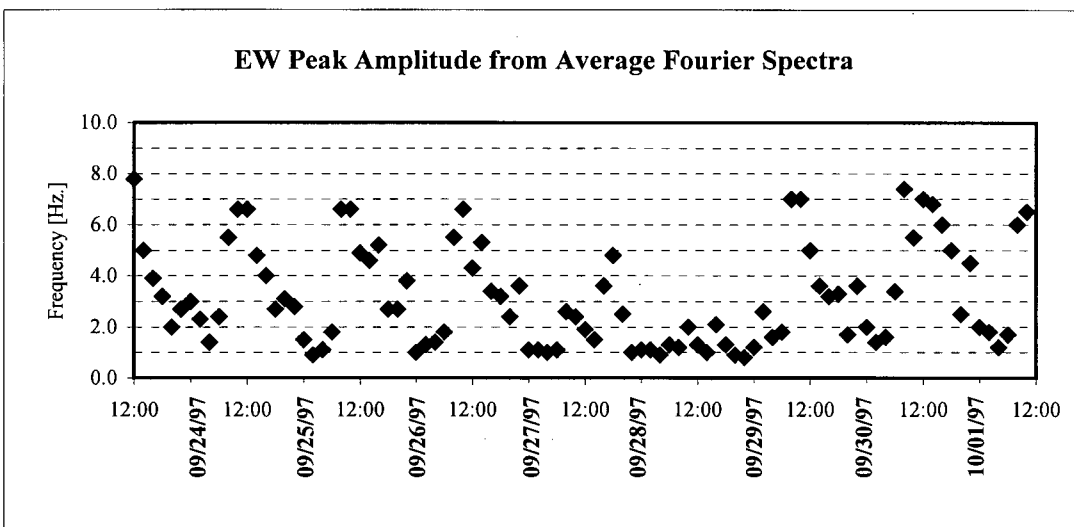
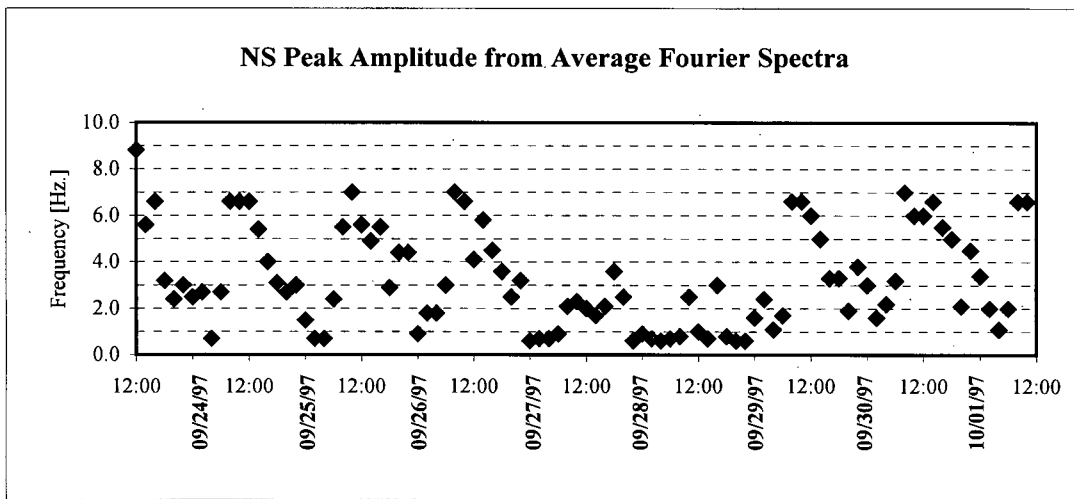


Figure 4.1 Location of MNY Station.



**Figure 4.2** Variations of Predominant Frequencies from Average Fourier Spectra over time.



**Figure 4.3** Variations of Peak Amplitudes from Average Fourier Spectra over time.

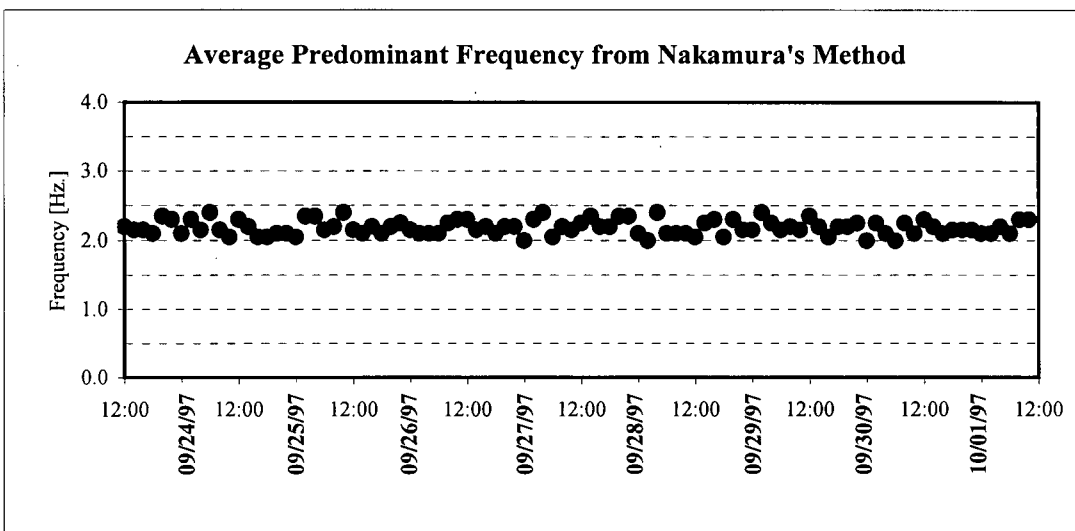
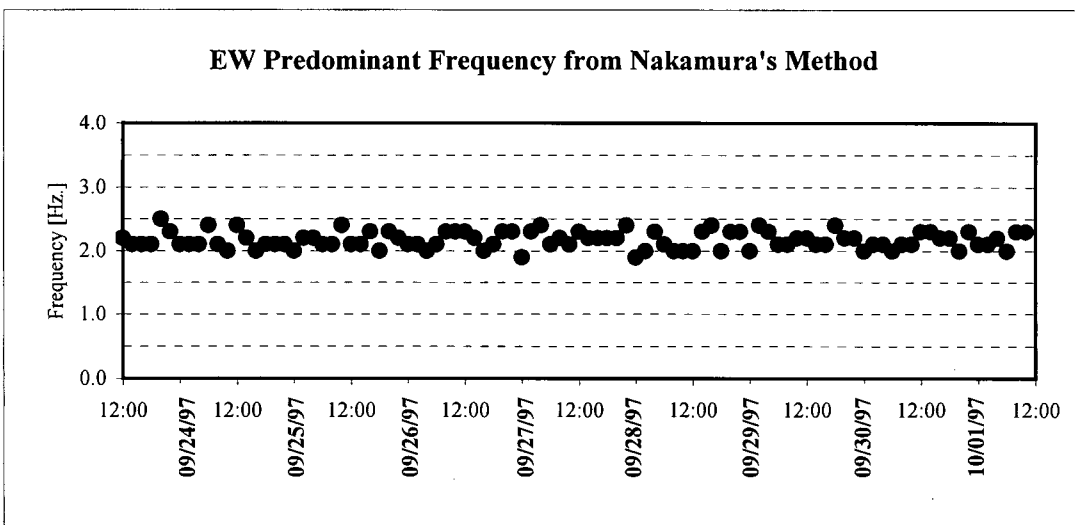
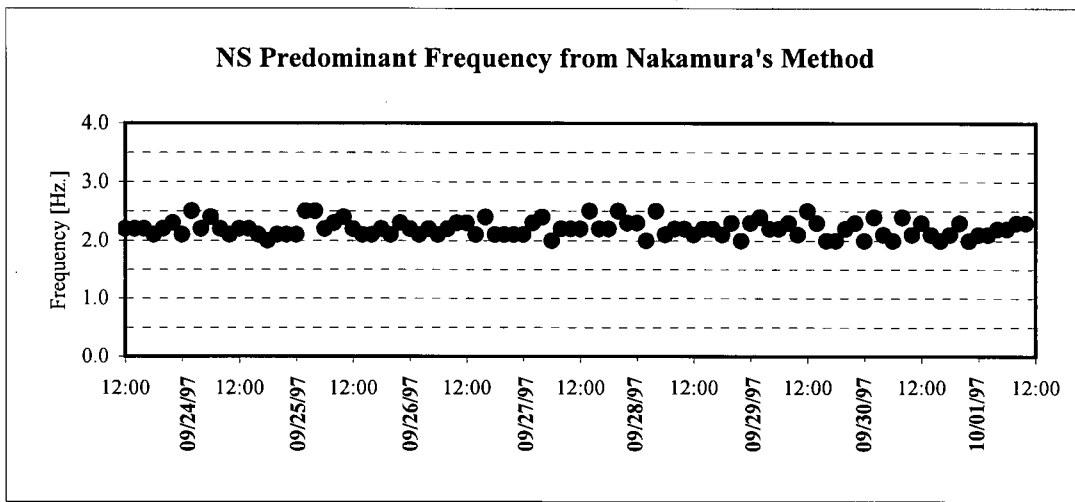


**Figure 4.4** Variations of Predominant Frequencies from Nakamura's Method over time.

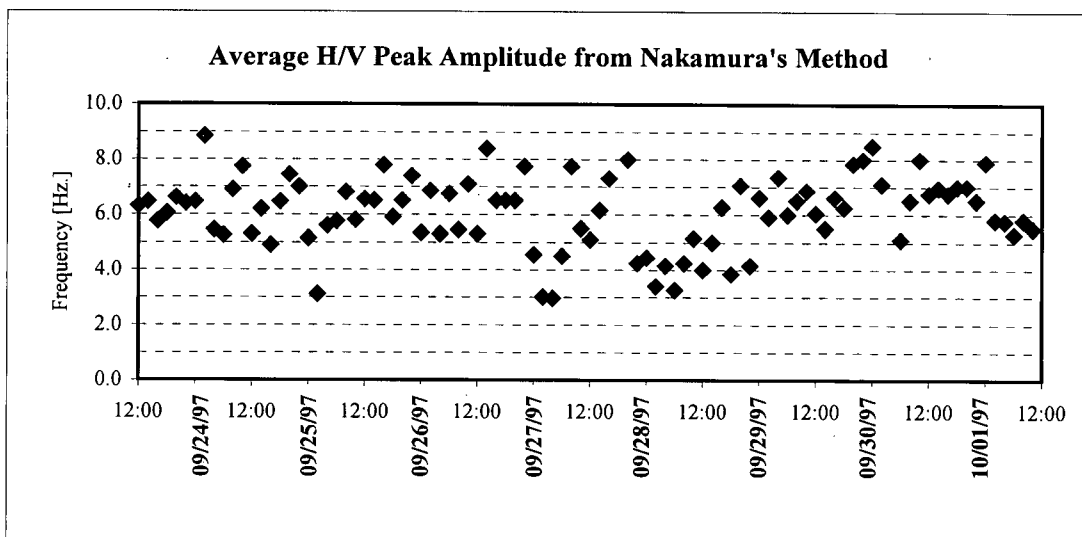
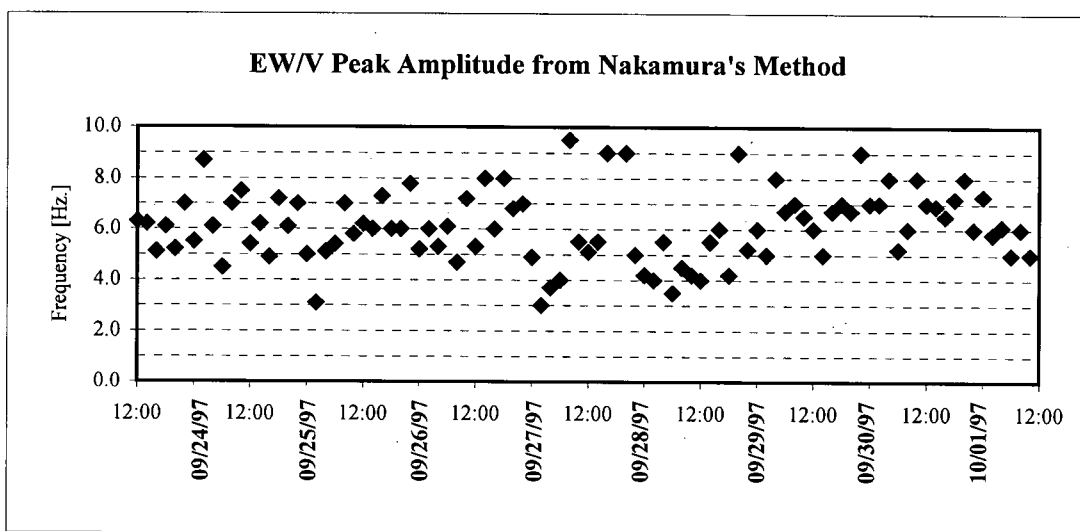
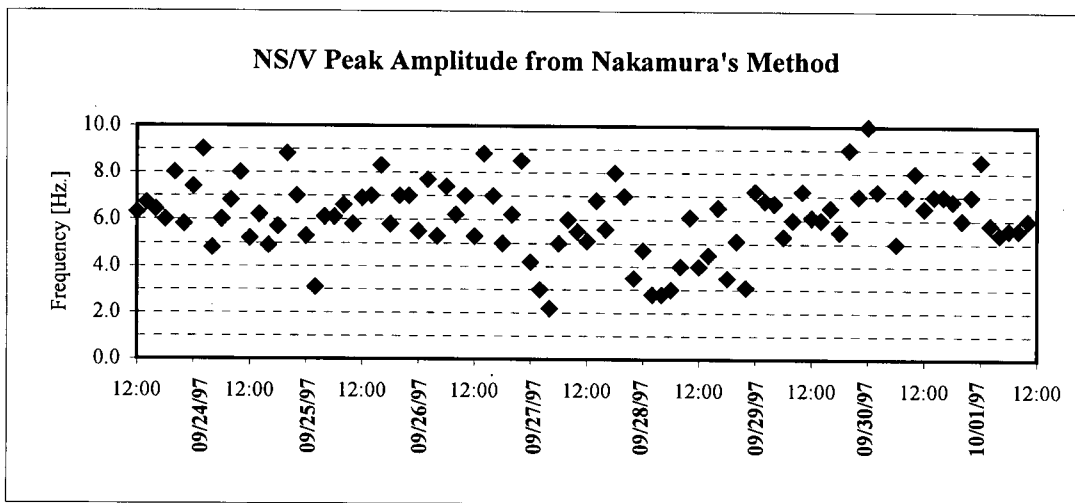


**Figure 4.5** Variations of Peak Amplitudes from Nakamura's Method over time.

# CHAPTER 5

## U.B.C.'S MICROTREMOR MEASUREMENT TECHNIQUE AND DATA ANALYSIS

---

### 5.1 INTRODUCTION

This chapter describes the microtremor measurement technique used at U.B.C. A discussion on the theoretical background and procedures used for the analysis of microtremor records is also included. The determination of site predominant periods and amplification factors from microtremor records using U.B.C.'s technique is based on Nakamura's method, which was described in detail in **Section 3.1**. The microtremor records obtained during the course of this study were analyzed using commercial, signal processing computer program DADiSP. A number of DADiSP macros were written specifically to automate and accelerate the data analysis. Examples of such macros are included in **Appendix C**. A flow chart for data acquisition and analysis is shown in **Figure 5.1**.

### 5.2 MICROTREMOR MEASUREMENTS AND TYPICAL TESTING PROCEDURES

Measurements of microtremors were carried out at selected locations in Lulu Island, New Westminster, and along Shell Road, Richmond. Three velocity-type sensors were used to measure three orthogonal components of ground motions at a point – north-south (N00E), east-west (N90E) and the vertical directions. Program DASam, developed by Seo *et al.*

(1989), was used to record microtremors, extract components, convert measured signals to physical units and perform preliminary data analyses. The following subsections discuss the procedures followed when performing microtremor measurements in the field. Details of the testing procedure can be found in **Appendix A**.

### 5.2.1 EQUIPMENT USED FOR MICROTREMOR MEASUREMENTS

The components of the equipment used for microtremor measurements and their characteristics are described as follows.

- **Sensors** -- Six velocity-type sensors (Model MTKH-1c/V-1c) with a natural period of 1 second and an amplitude range of  $\pm 3000 \times 10^{-6}$  m/s<sup>2</sup> with resolution of  $0.005 \times 10^{-6}$  m/s<sup>2</sup> may be deployed at a time. Three of these sensors -- two for measuring microtremor signals along orthogonal, horizontal directions and one along vertical direction -- were used to record measurement at a point on ground surface at each station. The response characteristics of the sensors at three signal amplification periods of 1, 3 and 5 seconds are shown in **Figure 5.2**.
- **Amplifier** -- The measured signals were amplified and filtered using an amplifier (Model TA-406) with switchable gains. Measured signals can be converted with this amplifier from velocity to displacement measurement before data is recorded. The amplifier can be operated at signal amplification periods of 1, 3 and 5 seconds. Its frequency range is 1 to 70 Hz. The period of signal measurement can be set using the *Period* button on the amplifier (see details in **Section A.5**). If the signals measured were weak, e.g., less than  $10 \times 10^{-6}$  m/s<sup>2</sup>, it was typical to set the period of measurement to 5 seconds so that the details of the measured signals can be recorded.

On the other hand, if the signals measured were strong, e.g., more than  $30 \times 10^{-6} \text{ m/s}^2$ , the period of measurement was usually set to 1 second to ensure that signal saturation did not occur easily and sufficient details of the measured signals were still recorded.

- **Analog-to-digital Converter** -- A 12-bit Analog-to-digital (A/D) converter which can handle up to 8 channels of data was used.
- **Data Acquisition Computer** -- The data acquisition was facilitated by running the program DASam and following the on-screen instructions on a notebook computer (NEC PC-9801 NS/T). In addition, on-site preliminary data analysis was also carried out using this computer.

### 5.2.2 DECIDING SENSOR LOCATIONS

The locations of the sensors were chosen to minimize the possibility of signal saturation due to background artificial noises, and to ensure that the signals measured reflected the characteristics of subsurface geologic conditions instead of those of some underground engineering structures, such as drainage/sewage system or electrical storage systems. The sensors were usually setup near the location of interest but as far away as possible from noticeable local disturbances such as traffic vehicles and heavy machinery facilities. Special care was also taken to avoid carrying out measurements on sites which might contain subsurface engineering structures. This was accomplished by avoiding places with indications of this type of structures, such as steel covers and concrete chambers.

### 5.2.3 TYPICAL TESTING PROCEDURE

Once a measurement station was located in the field, the velocity sensors were setup at the station and connected via cables to the amplifier. A photograph showing a typical arrangement of the data acquisition system is shown in **Figure 5.3**. The sensors were oriented to measure velocity signals along three orthogonal directions. A typical sensor arrangement is shown in **Figure 5.4**.

Once the setup of the sensors was completed, the program DASam was loaded on the data acquisition computer in order to start the data acquisition. The entire data acquisition process was carried out by following the step-by-step on-screen instructions regarding information input. The testing procedure was fairly straightforward. First, the sensors were calibrated to center the signals on the calibration screen by adjusting the calibration button on the amplifier. This was followed by adjustment of the signal amplification level using the attenuation factors on the amplifier. The latter step was to ensure that sufficiently strong signals would be measured, filtered and recorded. Measurement of microtremors was then carried out for about 300 seconds.

Once the measurement was completed, the data was checked for time segments of signal saturation. Signal saturation, which is indicated by top and bottom cut-off of signals, is usually caused by loud noises generated near the data acquisition station, e.g., a heavy truck passing by. Examples of measured microtremor records with: (a) very limited or no signal saturation, (b) some signal saturation, and (c) too much signal saturation are shown in **Figures 5.5(a), (b) and (c)** respectively. If there were many instances of significant

signal saturation such as in **Figure 5.5(c)**, the measurement would be repeated. Once the data had been checked, preliminary data analyses would be performed using a data analysis program developed by Seo *et al.* (1989) which was incorporated into DASam. The same procedure was repeated at every station.

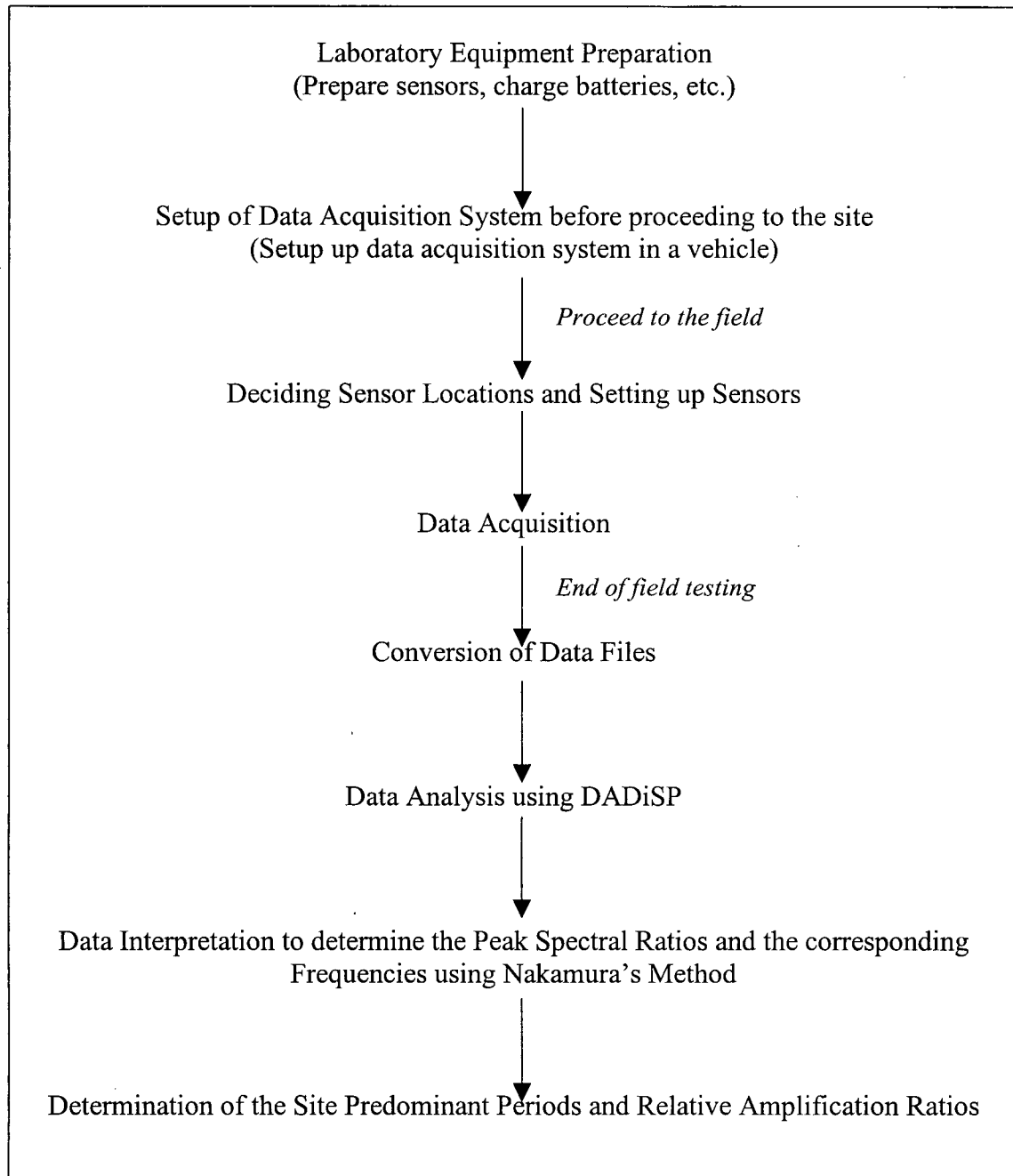


**Figure 5.1** Flow chart of Microtremor Data Acquisition and Analysis.

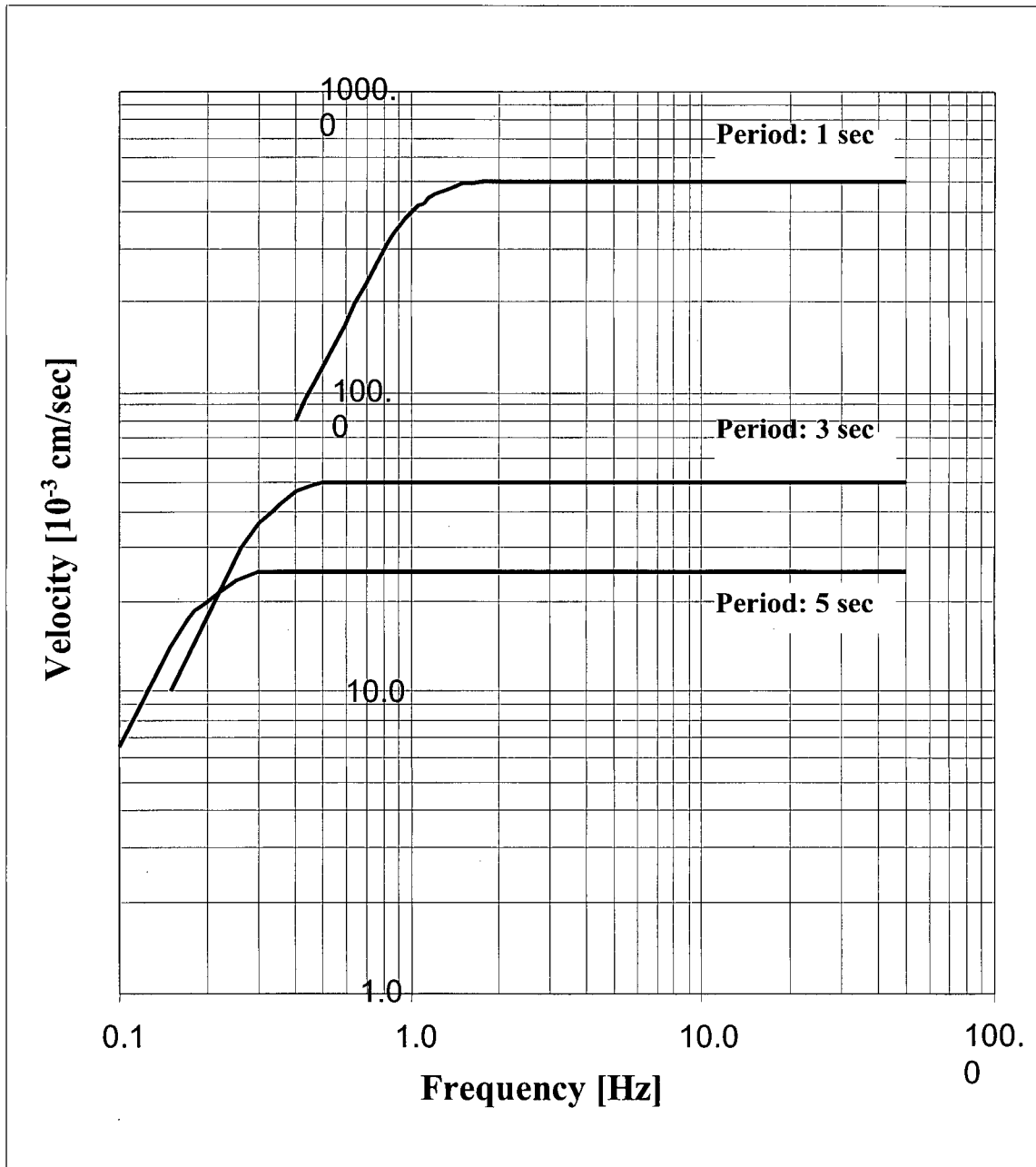


**Figure 5.2** Response Characteristics of Velocity Sensors used for Microtremor Measurements.

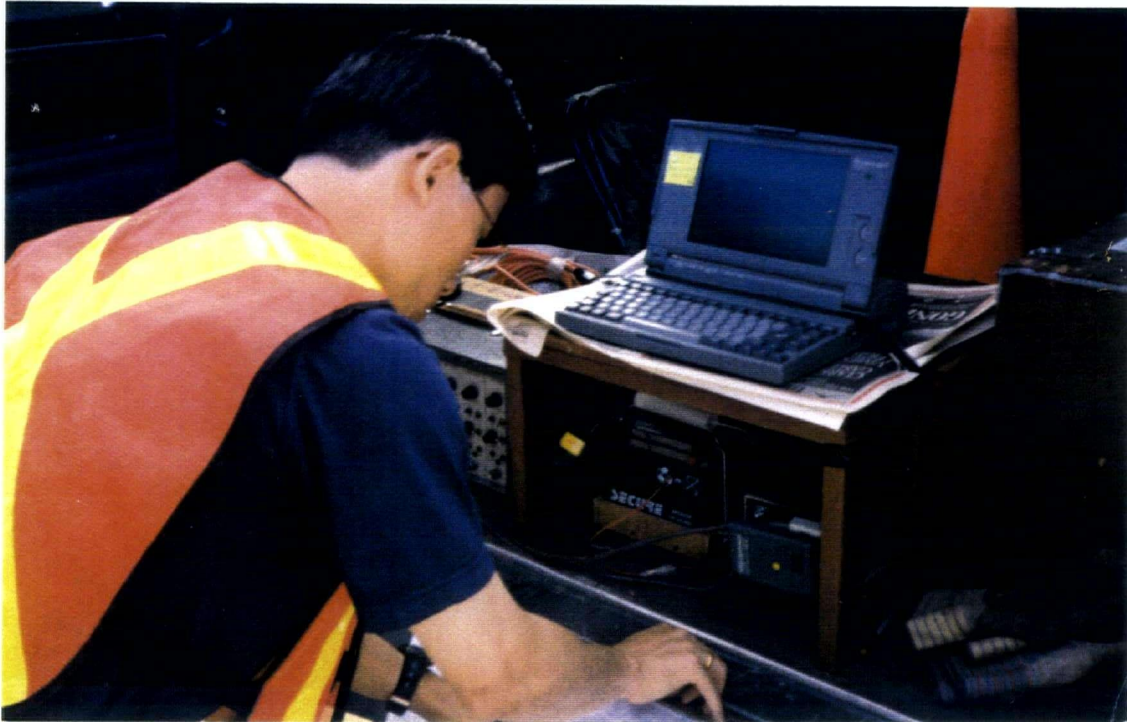


**Figure 5.3** Arrangement of Data Acquisition System.

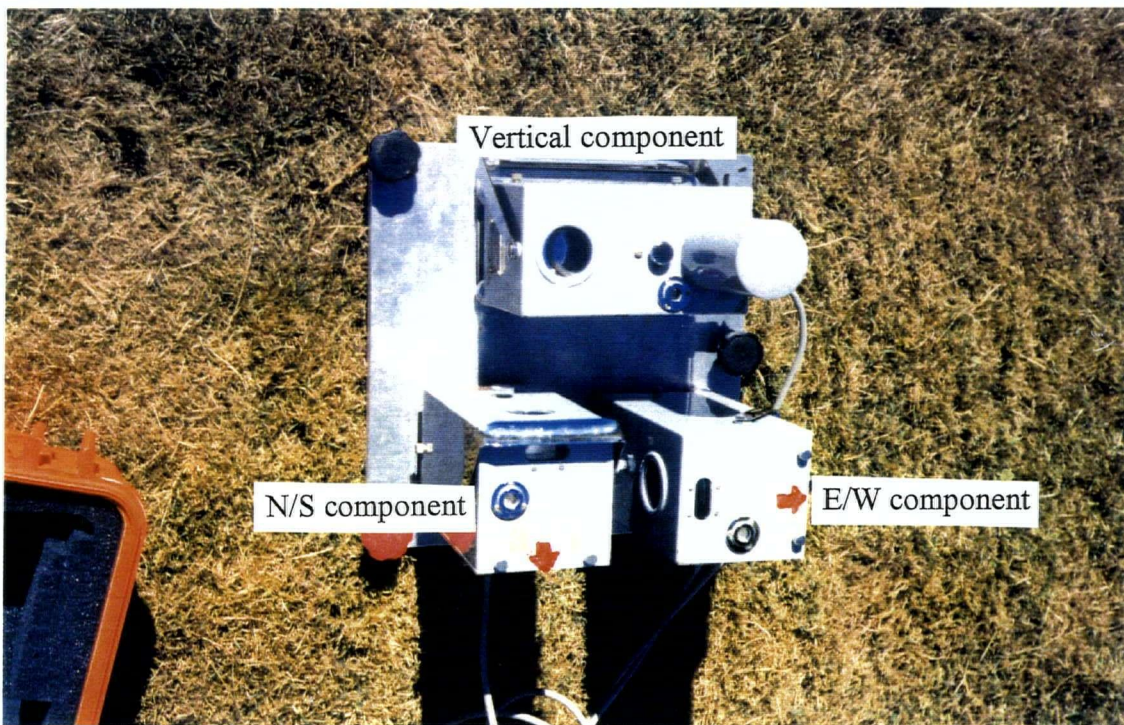
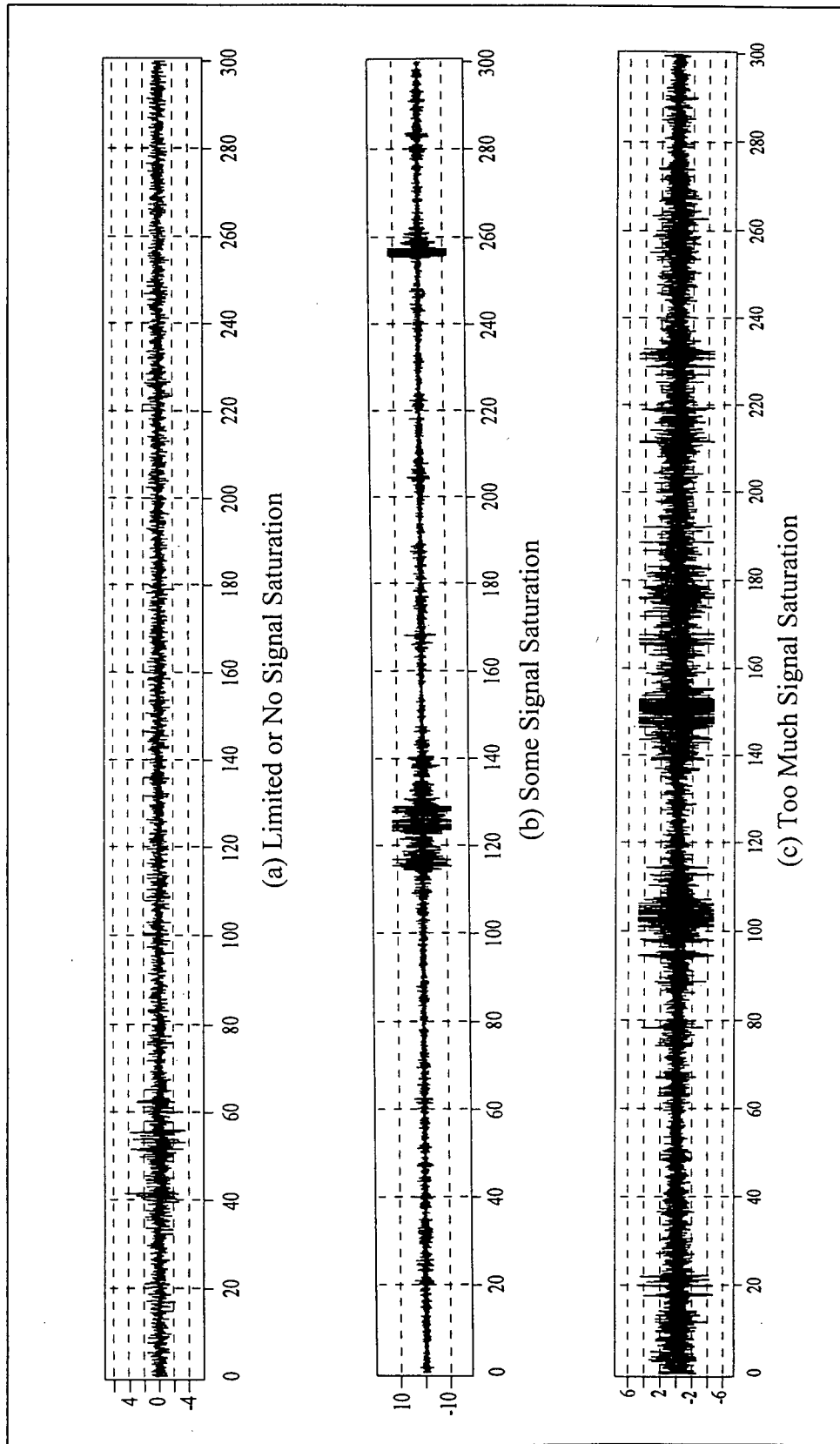


**Figure 5.4** Typical Arrangement of Sensors (Top view).



**Figures 5.5** Examples of Measured Microtremor Records with: **(a)** limited or no signal saturation, **(b)** some signal saturation, and **(c)** too much signal saturation.

## 5.3 METHOD FOR DETERMINING SITE PREDOMINANT PERIODS AND RELATIVE AMPLIFICATION RATIOS

The following subsections discuss the procedure used for determining site predominant periods and relative amplification ratios from microtremor measurements. Each microtremor record (or data file) stored within the data acquisition system is first converted into readable format for analysis using DADiSP (§5.3.1). The converted microtremor record is then processed using DADiSP (§5.3.2). An example of an analyzed record is illustrated in **Figure 5.6**. The record shows the time history of the records obtained (top), the corresponding Fourier spectra in Hertz (bottom) in three orthogonal directions, and the H/V spectral ratios (right column). Finally the site predominant periods and relative amplification ratios were estimated using the procedure described in §5.3.2.

### 5.3.1 CHANNEL DATA EXTRACTION

Prior to any detailed analysis using the program DADiSP, all measured microtremor data files (AD file extension) were first converted into DADiSP readable file format (AMP file extension) using the program *DASam* and the data acquisition computer. Details of data file conversion are presented in **Appendix B**. The purpose of the file conversion was to extract and separate the data from the electrical signals into three channel components, as sampled by the three sensors oriented orthogonally during measurements. During the conversion, the header information containing information on magnitude scaling factors of the ground motions was read into the new file. The header information

was used in subsequent data analysis to adjust the amplitudes of the ground motion measured.

### **5.3.2 DETERMINATION OF SITE PREDOMINANT PERIODS AND RELATIVE AMPLIFICATION RATIOS**

Once the data files were converted into readable format, they were first stored in a directory in the hard disk of the computer used for data analysis. The default storage location of the data files was specified as *c:\dsp4\com* in a DADiSP macro named ADAS.DAT (**Appendix C**) to facilitate batch file processing using DADiSP.

Most of the processes for analyzing each microtremor record were performed by DADiSP using macros (see **Appendix C** for details). First, the measured amplitudes of the ground motions or microtremors were adjusted based on the header information from the corresponding data file using an equation developed by Samano *et al.* (1997). This was followed by determination of average Fourier response spectrum of each record. In order to generate the average Fourier spectra, the three time histories, i.e., three sets of microtremor data measured along three orthogonal directions, were each divided into 8 segments with 50%-overlap; each segment consisting of 4096 points. Data of all the segments were filtered using a Hamming window. Each segment was then Fourier transformed to produce the Fourier response spectrum. An average Fourier spectrum was then calculated based on the Fourier spectra of the eight segments.

Determination of the site predominant periods and amplification factors was based on Nakamura's method. The spectral ratios of horizontal to vertical components were

calculated using the average Fourier spectral components of the two orthogonal horizontal directions and the vertical direction. Once the spectral ratios were calculated, a record similar to that in **Figure 5.6** was then produced. The site predominant frequencies and amplification factors were visually estimated from the most amplified peaks of the horizontal-to-vertical spectral ratios. The amplification factor is the peak amplitude of the spectra ratios and the site predominant frequency is the corresponding frequency. The predominant periods were subsequently calculated by taking the reciprocal of the corresponding site predominant frequencies.

Finally, the relative amplification ratio of each station was calculated by taking the ratio of the site amplification factor to that of a reference hard ground site. For this thesis, the reference hard ground site chosen was station K05 which is located near the intersection of Spruce Street and 13<sup>th</sup> Avenue in Vancouver (see **Figure 5.7**). Based on information from a surface geology map of the Fraser Delta (see **Figure 6.1** for details), station K05 is situated on a shallow, hard ground site. Microtremor measurement was carried out at station K05 and analysis of the measured record indicates that the site predominant period at station K05 to be approximately 0.25 seconds. Shear wave velocity in the Holocene or top surface layers in GVRD have typical average values in the range of 200 to 300 m/s (Hunter, 1995). Using an average shear wave velocity of 300 m/s, the depth of the surface layer is estimated to be approximately 19 metres using the equation:

$$T = \frac{4 \cdot H}{V_s} \Rightarrow H = \frac{T \cdot V_s}{4} \quad (\text{Eqn. 5.1})$$

where  $T$  is the site predominant period,  $H$  is the thickness of the uniform soil layer and  $V_s$  is the average shear wave velocity of the soil layer. **Equation 5.1** is normally applicable to uniform soil layers only, but since an average shear wave velocity was used to estimate the thickness of surface layer(s) at station **K05**, **Equation 5.1** should give a fairly reasonable estimated depth of the surface layer at the site. The average shear wave velocity used in the estimation of the depth of the surface layer is essentially an upper-bound value; hence, the estimated depth at station K05 should be reasonably accurate in indicating it as a shallow site. Since station K05 is a shallow, hard ground site, it can serve as a fairly good reference site for comparison of the relative amplification potential of other sites, many of which have deeper surface layers.

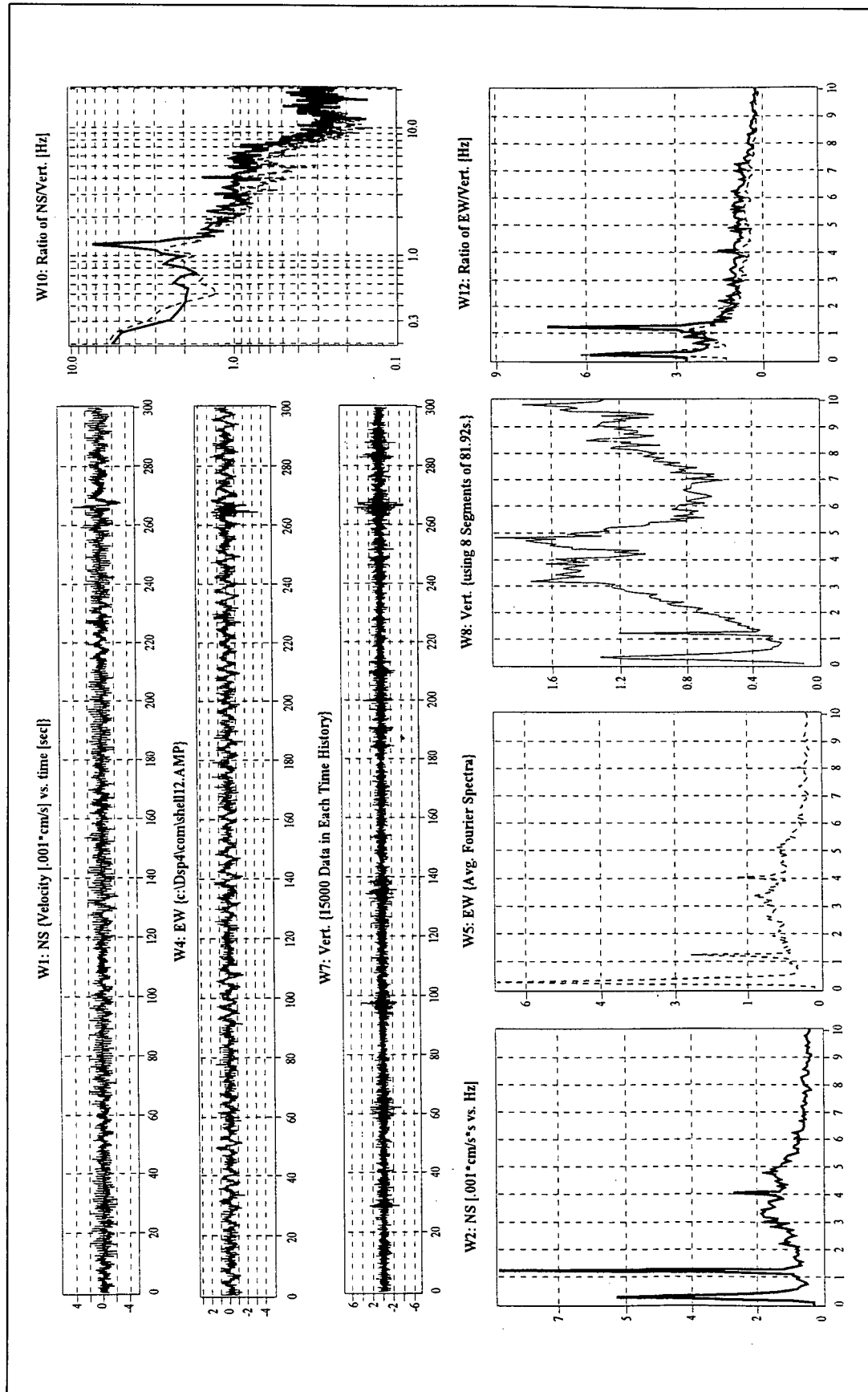


**Figure 5.6** An Example of An Analyzed Record of Microtremor Measurement at Shell Road in Richmond (1999).

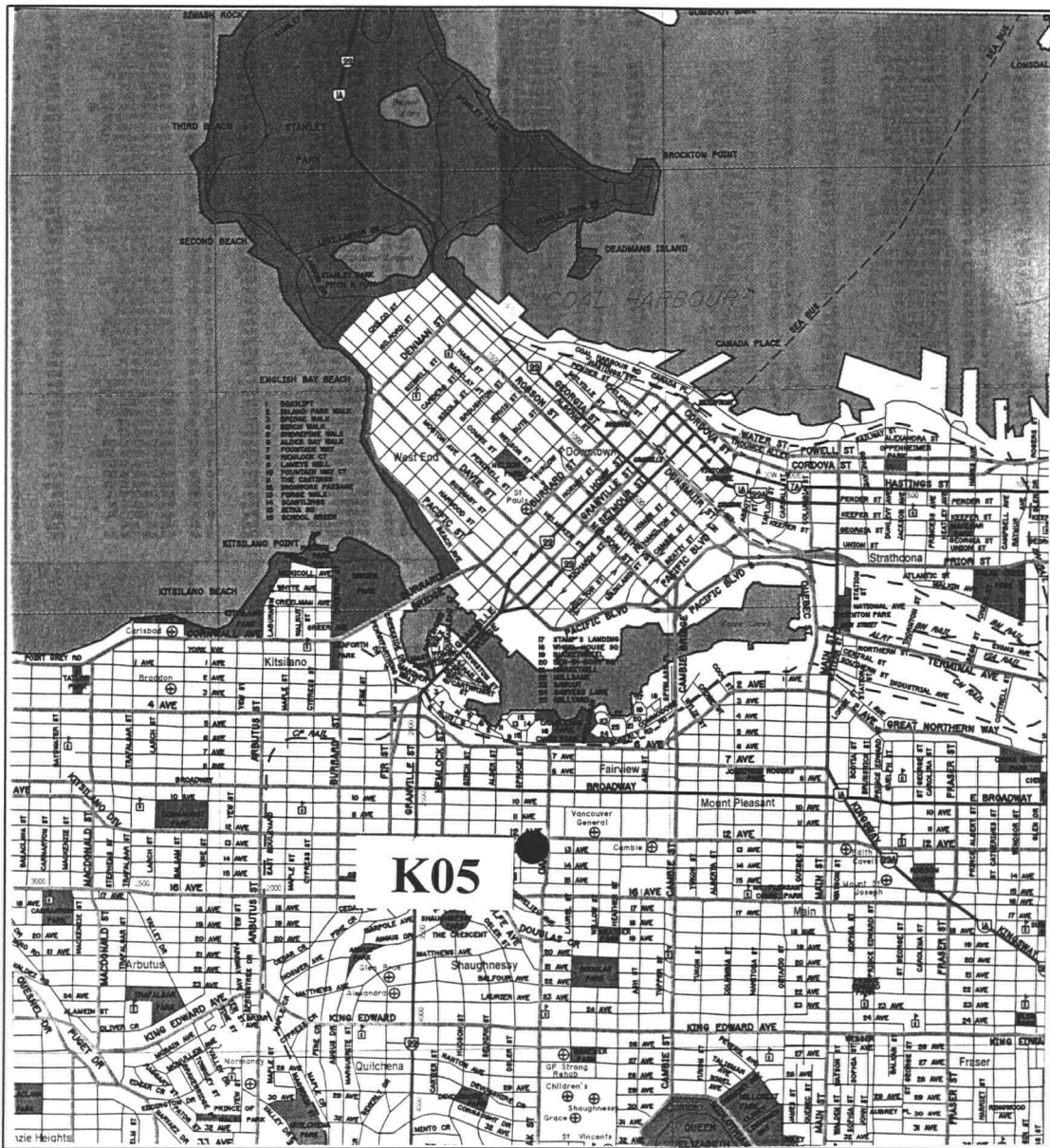


Figure 5.7 Location of the Reference Hard Ground Site: Station K05.

## CHAPTER 6

# APPLICATION OF MICROTREMOR MEASUREMENTS – CASE STUDIES

---

This chapter first describes the geology of the Fraser Delta where the microtremor measurements were carried out. A case study is then presented to compare the Fourier spectral characteristics of low-level earthquake ground motions and microtremor measurements recorded at a site in the GVRD region to determine if microtremors can be used to estimate the dynamic characteristics of the ground for earthquake response studies. This is followed by presentation and discussion of the results of analysis of the microtremor data from Lulu Island and Richmond. Finally, discussion and conclusions based on the results of the several case studies discussed are presented in this chapter. The author carried out microtremor measurements at several sites in the GVRD regions, specifically along Wood Street and Ewen Avenue in Lulu Island, New Westminster, and along Shell Road in Richmond. Additional measurements were performed at various locations in the GVRD region under the leadership of Dr. Hao X.S., and some of the test results were included in this thesis.

### 6.1 GEOLOGY OF THE FRASER DELTA

Most of the microtremor measurements carried out during the field testing phase of this thesis were performed on sites in Richmond and Lulu Island, both of which are located in the Fraser Delta. The Fraser Delta is located just south of Vancouver to the south of the North Arm of the Fraser River. **Figure 6.1** shows the map of geological settings of the

Fraser Delta (inclusive of Vancouver) with the corresponding information about the geological settings tabulated in **Table 6.1**. Most of the measured microtremor sites in Richmond and Lulu Island in New Westminster are located on the Fraser river sediments (**Fc, Fd**) and Quaternary Postglacial sediments (**SAb, SAc** and **SAd**). Most of the sites in the Vancouver area are located in the Postglacial and Pleistocene regions (**VCb** and **Cb**). The Fraser Delta consists of mainly Holocene-age deltaic deposits (top layer) and Pleistocene-age glacial and interglacial deposits which overlie the Tertiary bedrock. The Holocene sediments are up to about 300-m thick (Luternauer and Hunter, 1996) and consist of mainly silts and sands. Depths of the Holocene sediments at several sites in the Fraser Delta are shown on geological map in **Figure 6.1**, with the strong motion instrument stations marked in capital letters in group of three letters, e.g., MNY, RHA (Rogers *et al.*, 1997). The Holocene sediments thin rapidly to the north at the edge of the basin and are about 300-m thick in the basin centre near strong motion station RHA. The north side of the Fraser river near station MNY is relatively shallow with less than 50 metres of Holocene deposits. The shear wave velocity in the Holocene layer increases with depth (Hunter, 1995) with typical average values in the range of 200 to 300 m/s, but about 100 m/s near the surface in many places (Finn *et al.*, 1998). The underlying Pleistocene sediments are mostly ice-compacted tills and glaciomarine silts and sands that overlie tertiary bedrock. The average shear wave velocity in the Pleistocene sediments is about 500 m/s but it varies considerably from place to place.



Table 6.1 Definition of Geological Settings in the Fraser Delta.

<b>DEFINITION OF GEOLOGICAL SETTINGS</b>	
<b>QUATERNARY</b>	
	<b>POSTGLACIAL</b>
	<i>Salish Sediments</i>
<b>SAa</b>	Landfill including sand, gravel, till, crushed stone, and refuse
<b>SAc</b>	Lowland peat up to 1-m thick, underlying Fb (up to 2-m thick)
<b>SAd</b>	Organic-rich sandy loam to clay loam 15- to 45-cm thick overlying Fd
<b>SAe</b>	Upland peat up to 8-m or more thick overlying VC units
<b>SAF</b>	Marine shore sediments; SAF, sand to sandy loam up to 2-m thick overlying Fe
	<i>Fraser River Sediments</i>
<b>Fc</b>	Overbank silty to silt loam normally less than 2-m thick overlying 1.5-m or more
<b>Fd</b>	Deltaic and distributary channel fill (includes tidal flat deposits), 10- to 25-m interbeds
	<b>PLEISTOCENE</b>
	<i>Capilano Sediments</i>
<b>Cb</b>	Raised beach medium to coarse sand 1- to 5-m thick
	<i>Pre-Vashon Deposits</i>
<b>PVa</b>	Pre-Vashon glacial, nonglacial, and glaciomarine sediments; quadra fluvial channel fill and floodplain deposits, crossbedded sand containing minor silt and gravel lenses and interbeds
	<i>Vashon Drift and Capilano Sediments</i>
<b>VCa</b>	Glacial drift, bedrock within 10 m or less of the surface
<b>VCb</b>	Glacial drift, bedrock more than 10 m below surface
	<b>TERTIARY</b>
<b>T</b>	Tertiary bedrock including sandstone, siltstone, shale, etc.; covered by glacial deposits and colluvium

## 6.2 COMPARISON OF MICROTREMOR MEASUREMENTS WITH EARTHQUAKE GROUND MOTIONS AT STATION MNY

A comparison of spectral characteristics of low-level earthquake ground motions and microtremor measurements was performed at station MNY to determine the effectiveness of microtremors in assessing the dynamic characteristics of the ground in GVRD region for earthquake response studies. Several low amplitude earthquake generated ground motions were recorded by a permanent strong motion instrument at station MNY (Hao, Finn, Ventura, Seo and Samano, 1998). The background information of the earthquake ground motions is described and the results of comparison are discussed below.

### 6.2.1 BACKGROUND INFORMATION ON THE EARTHQUAKE GROUND MOTIONS

Two low-level earthquake ground motions were recorded at strong motion station MNY in 1996 and 1997. **Tables 6.2(a)** and **(b)** present information on the earthquake sources and peak ground accelerations of the two earthquakes (Hao *et al.*, 1998). The first earthquake was the May 1996 Duvall, Washington earthquake of magnitude 5.1 (referred to as 96Eq in this thesis), and the second earthquake is the June 1997 Georgia Strait, B.C. earthquake of magnitude 4.5 (referred to as 97Eq). The 1996 earthquake was recorded at an epicentral distance of 186 km with a direction of N330E from the epicenter. It had a large peak ground acceleration of  $15.5 \text{ cm/s}^2$  in the N90E direction. The 1997 earthquake was recorded at an epicentral distance of 37 km with a direction of N95E from the

epicenter. It had peak ground accelerations of  $14 \text{ cm/s}^2$  in the transverse component (N00E) and a smaller PGA of  $9 \text{ cm/s}^2$  in the radial direction (N90E).

### **6.2.2 COMPARISON OF SPECTRAL CHARACTERISTICS BETWEEN MICROTREMORS AND EARTHQUAKE GROUND MOTIONS**

The time histories and average Fourier spectra for each of the three components of the 1996 and 1997 earthquake ground motions are shown in **Figures 6.2** and **6.3** respectively. The average Fourier spectra from the 1996 record indicated that the site frequencies of peak response are approximately 2.0 Hz along north-south direction and 2.2 Hz along east-west direction. From the 1997 earthquake record the site frequencies of peak response are 2.8 Hz along north-south direction and 2.4 Hz along east-west direction. Both horizontal Fourier spectral components from the 1996 and 1997 earthquakes showed the site predominant frequencies of approximately 2 to 3 Hz at station MNY, even though the orientation and epicentral distance of both the earthquakes to station MNY were different. These site predominant frequencies are similar to the site predominant period of 2.3 Hz estimated from microtremor records at station MNY (see §4.1.1 for details).

**Table 6.2(a)** Earthquake Source Information (after Hao *et al.*, 1998).

Code	Earthquake	Date	Time	$M_w$	Location	N. Latitude	W. Longitude
96Eq	Duvall, Washington	03-Mar-96	4:04	5.1	40 km ENE of Seattle	47.76	121.88
97Eq	Georgia Strait, B.C.	24-Jun-97	7:41	4.3	SSW of Gibsons, B.C.	49.24	123.62

**Table 6.2(b)** Earthquake Peak Ground Accelerations Recorded at station MNY (after Hao *et al.*, 1998).

Code	Earthquake	Peak Acceleration ( $\text{cm/s}^2$ )		Epicentral Distance [km]	Azimuth
		N00E(L)	N90E(T) Vert.		
96Eq	Duvall, Washington	-6.2	15.5	186	330
97Eq	Georgia Strait, B.C.	13.58	-8.85	37.28	95

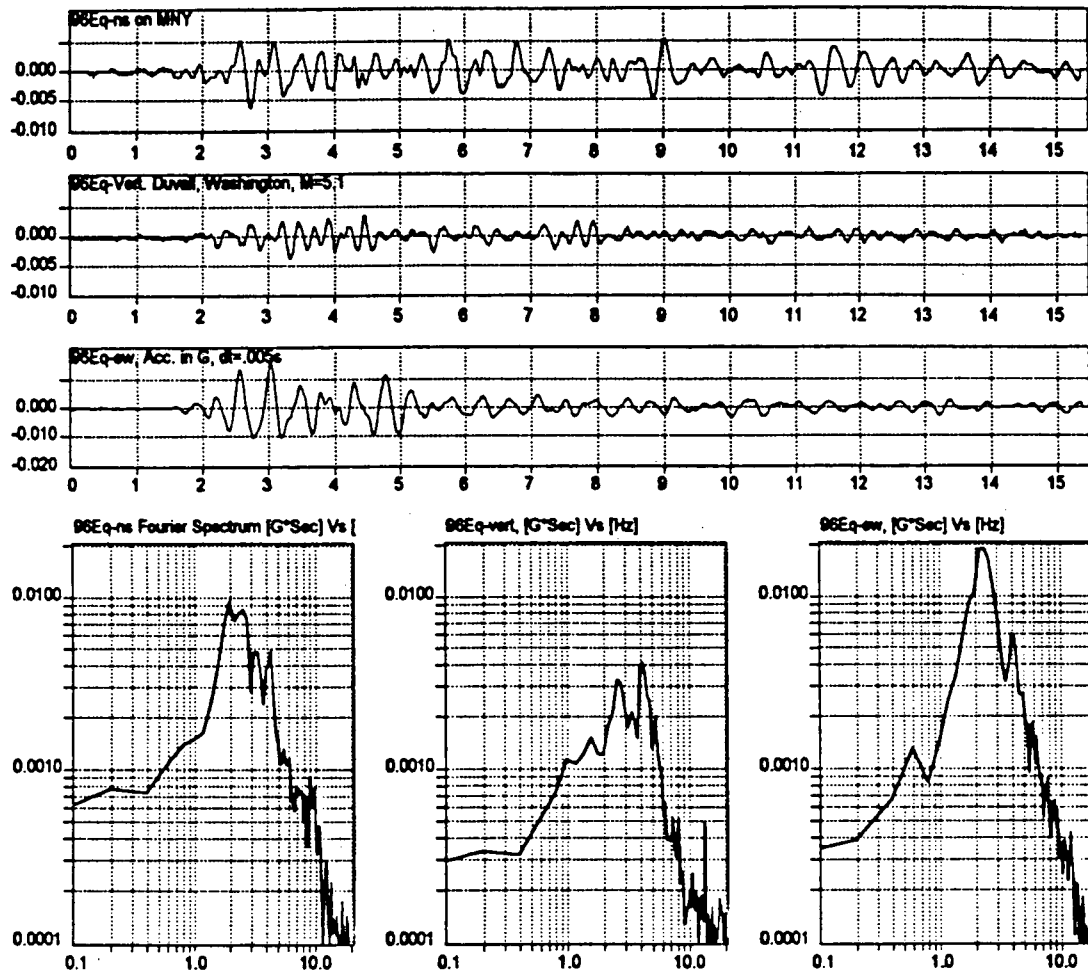
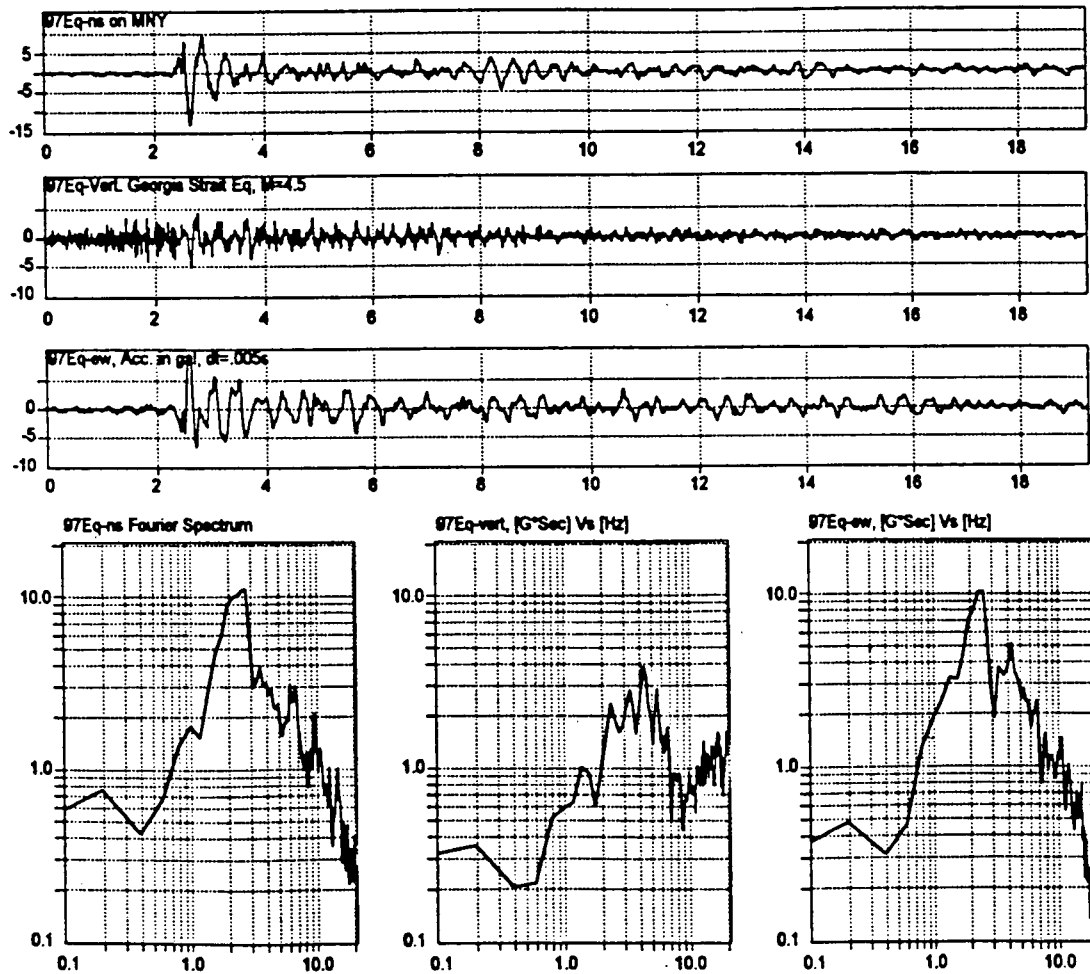


Figure 6.2 Acceleration Records and Fourier Spectra of the 1996 Duvall, Washington Earthquake measured at station MNY (after Hao *et al.*, 1998).



**Figure 6.3** Acceleration Records and Fourier Spectra of the 1997 Georgia Strait, British Columbia Earthquake measured at station MNY (after Hao *et al.*, 1998).

### 6.3 LULU ISLAND, NEW WESTMINSTER

Microtremor measurements were carried out on stations along *Wood Street* (gridline A) and *Ewen Avenue* (gridline B) on September 2 and 3, 1998. The locations of the measurement stations are shown in **Figure 6.4**. The predominant site periods, estimated depths of surface layer(s) based on average shear wave velocity values of 150, 200 and 250 m/s, relative amplification ratios, and number of storeys of buildings likely to suffer the most damage under strong shaking are tabulated in **Tables 6.3(a)** and **(b)**. The distribution of shear wave velocities averaged over the top 30 metres of the ground,  $V_{S30}$ , in Lulu Island and Richmond based on data of seismic cone penetration tests performed by the Geological Survey of Canada (G.S.C.) is shown in **Figure 6.5**. The average  $V_{S30}$  in Lulu Island and Richmond are approximately 200 and 185 m/s respectively. Examples of analyzed microtremor records at Wood Street (station A1) and Ewen Avenue (station B3) are shown in **Figures 6.6** and **6.7** respectively. From **Figure 6.6**, the site frequency of peak response at station A1 is estimated from the horizontal-to-vertical spectral ratios to be 0.9 Hz and the corresponding peak spectral ratio is 3.5. From **Figure 6.7**, the site frequency of peak response at station B3 is estimated to be 1.1 Hz and the corresponding peak spectral ratio is 5.0.

#### 6.3.1 SITE PREDOMINANT PERIODS AND ESTIMATED DEPTHS OF SURFACE LAYER

The distribution of site predominant periods along Wood Street and Ewen Avenue from analyses of the microtremor measurements is shown in **Figure 6.8**. The site predominant periods from microtremor measurements were used to estimate the depth of surface

layer(s) at each station based on estimated values of shear wave velocities and the following equation:

$$T = \frac{4 \cdot H}{V_s} \Rightarrow H = \frac{T \cdot V_s}{4}$$

where  $T$  is the site predominant period,  $H$  is the thickness of the uniform soil layer and  $V_s$  is the average shear wave velocity of the soil layer. The above equation is normally applicable to uniform soil layers only, but for this thesis an approximate average shear wave velocity was used to estimate the thickness of surface layer(s) at each site and hence the estimated depth should reasonably reflect the depth of the surface layer(s) at each site. **Figure 6.9** shows the distribution of estimated depths of surface layer(s) at various stations along Wood Street and Ewen Avenue based on a shear wave velocity value of 200 m/s. The shear wave velocity of 200 m/s was chosen for the estimation of the depths of surface layer(s) for the different sites in Lulu Island because these sites have average  $V_{s30}$  of approximately 200 m/s.

The site predominant periods were found to be longer, with the corresponding estimated depths of soil surface layer deeper, at southeast end of Wood Street, e.g., 1.9 seconds in the vicinity of Salter Street (station A6) and South Dyke Road (station A7), whereas in the northern end of Wood Street next to Queensborough Bridge, the site predominant periods were comparatively shorter at approximately 1.1 to 1.3 seconds. Along Ewen Avenue the site predominant periods are longer at both the northeast and southwest ends at approximately 1.5 to 2.0 seconds, and at Pembina Street near the central region of Ewen Avenue at approximately 1.7 seconds. The predominant periods and estimated

depths of surface layers of sites in Lulu Island indicate that the Lulu Island sites have fairly shallow surface layers of less than 100 metres. A borehole site (FD97-1) near SCPT station 95-31 (**Figure 6.5**), which is located on the north-east region of Annacis Island and approximately 1-km south-east of microtremor station A7, has depth of surface layer to bedrock of approximately 97 metres (Monahan, P.A., 1998). This is also clearly shown in **Figure 6.10** (G.S.C., 1998) which shows the distribution of shear wave velocities and soil profiles with depth at the site; the shear wave velocity increases drastically in the transition of the clay layer to the bedrock layer at about 96-m depth. This known depth of surface layer to bedrock in close vicinity of microtremor stations A6 and A7 near the southern end of Wood Street, with estimated depths of surface layers of 94 and 95 metres respectively, confirmed that microtremor measurements have reasonably predicted the depths of surface layers.

A building will likely experience the greatest resonance and hence the most damage when its fundamental period synchronizes with the site predominant period of the surface layer(s) due to the effect of soil-structure interaction. The number of storeys ( $N$ ) of buildings which are likely to suffer the most damage under strong ground shaking was estimated using an empirical formula from the Building Code for a moment resistant space frame:

$$N = 10 \cdot T$$

where  $N$  is the number of storeys of a building and  $T$  is the fundamental period of buildings. The fundamental periods of the buildings were set at the same value as the site predominant periods for calculations of the number of storeys of the buildings. For

example, site A4 at Wood Street has a measured site predominant period of 1.4 seconds; buildings which will suffer the greatest damage are probably those of 14-storey high during severe ground shaking. The number of storeys (N) of buildings which will likely experience the most damage due to ground shaking at the estimated site predominant period at the sites where microtremor measurements were carried out is included in **Tables 6.3(a) and (b)**. Assuming that the results of microtremor measurements performed along Wood Street and Ewen Avenue are representative of most sites in Lulu Island, buildings between 10- to 20-storey high in Lulu Island will likely to sustain the most damage under earthquake ground shaking.

### **6.3.2 RELATIVE AMPLIFICATION RATIOS**

The distribution of relative site amplification ratios is shown in **Figure 6.11**. For this thesis, the reference hard ground site was station K05 as noted in §5.3.2. The relative amplification ratios along Wood Street and Ewen Avenue were found to vary from 1.2 to 2.0 at most stations. The only exceptions are station B8 (4.5) near the intersection of Stanley Street and Ewen Avenue and station B4 (2.8) near the intersection of Salter Street and Spruce Street. The closeness in amplitudes of the relative amplification ratios of the different sites in Lulu Island, New Westminster indicates that the relative amplification or seismic hazard potential of the sites in Lulu Island are likely to be similar. The similarity in relative seismic hazard potential of the sites in Lulu Island is not surprising because these sites have very similar geological settings of Holocene sediments consisting of silty-to-sandy Fraser River sediments with thin layer of peat near the surface overlying Pleistocene deposits. The reference site K05 is a very shallow, hard ground site (the

upper-bound estimated depth of surface layer overlying bedrock is approximately 19 metres). The relative amplification ratios of greater than 1.0 at most stations in Lulu Island indicate that the relative amplification potential of the various sites is greater than that of the reference site as expected.

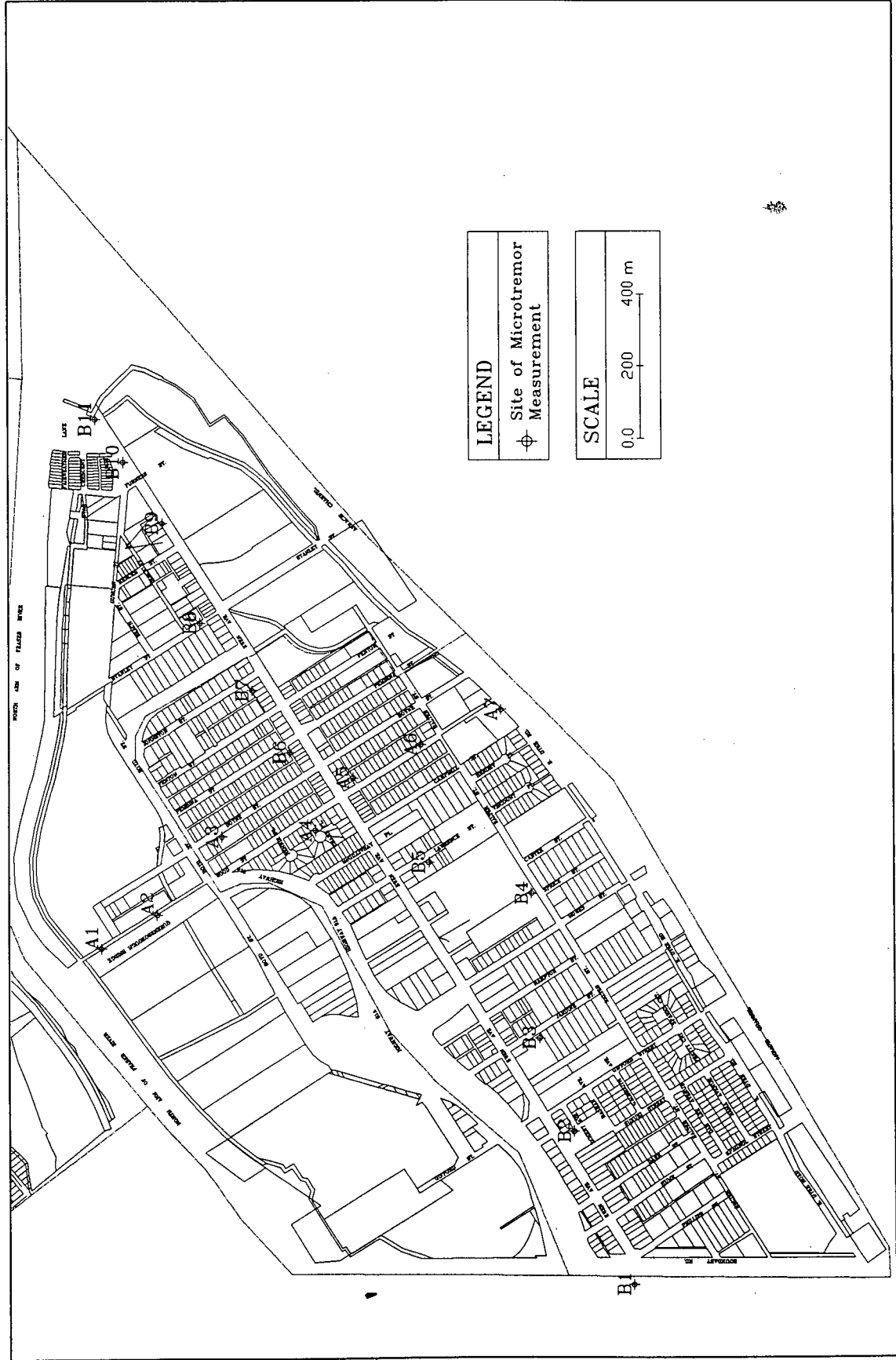


**Figure 6.4** Locations of Microtremor Measurement Stations along Wood Street and Ewen Avenue in Lulu Island, New Westminster, British Columbia.

**Table 6.3(a)** Site Predominant Periods, Estimated Depths of Surface Layer(s), Relative Amplification Ratios and Number of Storeys of Buildings likely to experience the Most Resonance along Wood Street in Lulu Island, New Westminster, British Columbia.

**GRIDLINE A:** *Wood Street*

Site Code	Coordinates		Predominant		Surface Layer Depth, $H = (T/4) \times V_s$			Rel. Amp. Ratio	# of Storeys $N = 10 \times T$
	Longitude	Latitude	Freq. [Hz.]	Period [Sec.]	$V_s = 150 \text{ m/s}$ [m]	$V_s = 200 \text{ m/s}$ [m]	$V_s = 250 \text{ m/s}$ [m]		
A1	-122.9433	49.1957	0.9	1.1	43	57	72	1.2	12
A2	-122.9425	49.1945	0.8	1.3	50	67	83	1.6	14
A3	-122.9400	49.1925	1.1	0.9	34	45	57	2.0	10
A4	-122.9387	49.1900	0.7	1.4	52	69	87	1.6	14
A5	-122.9375	49.1887	1.0	1.1	39	53	66	1.7	11
A6	-122.9358	49.1876	0.5	1.9	71	94	118	1.6	19
A7	-122.9350	49.1853	0.5	1.9	69	93	116	1.2	19

**Table 6.3(b)** Site Predominant Periods, Estimated Depths of Surface Layer(s), Relative Amplification Ratios and Number of Storeys of Buildings likely to experience the Most Resonance along Ewen Avenue in Lulu Island, New Westminster, British Columbia.

**GRIDLINE B:** *Ewen Avenue*

Site Code	Coordinates		Predominant		Surface Layer Depth, $H = (T/4) \times V_s$			Rel. Amp. Ratio	# of Storeys $N = 10 \times T$
	Longitude	Latitude	Freq. [Hz.]	Period [Sec.]	$V_s = 150 \text{ m/s}$ [m]	$V_s = 200 \text{ m/s}$ [m]	$V_s = 250 \text{ m/s}$ [m]		
B1	-122.9558	49.1825	0.7	1.4	54	71	89	1.6	15
B2	-122.9508	49.1842	0.5	2.0	75	100	125	1.8	20
B3	-122.9475	49.1850	1.1	0.9	34	45	57	1.9	10
B4	-122.9447	49.1850	1.2	0.8	31	42	52	2.8	9
B5	-122.9400	49.1873	1.0	1.1	39	53	66	1.4	11
B6	-122.9358	49.1908	0.6	1.7	63	83	104	1.6	17
B7	-122.9333	49.1917	1.0	1.0	38	50	63	2.3	10
B8	-122.9308	49.1933	1.0	1.0	38	50	63	4.5	10
B9	-122.9283	49.1937	1.1	0.9	34	45	57	1.9	10
B10	-122.9250	49.1950	0.6	1.8	68	91	114	1.4	19
B11	-122.9217	49.1963	0.7	1.5	58	77	96	1.7	16

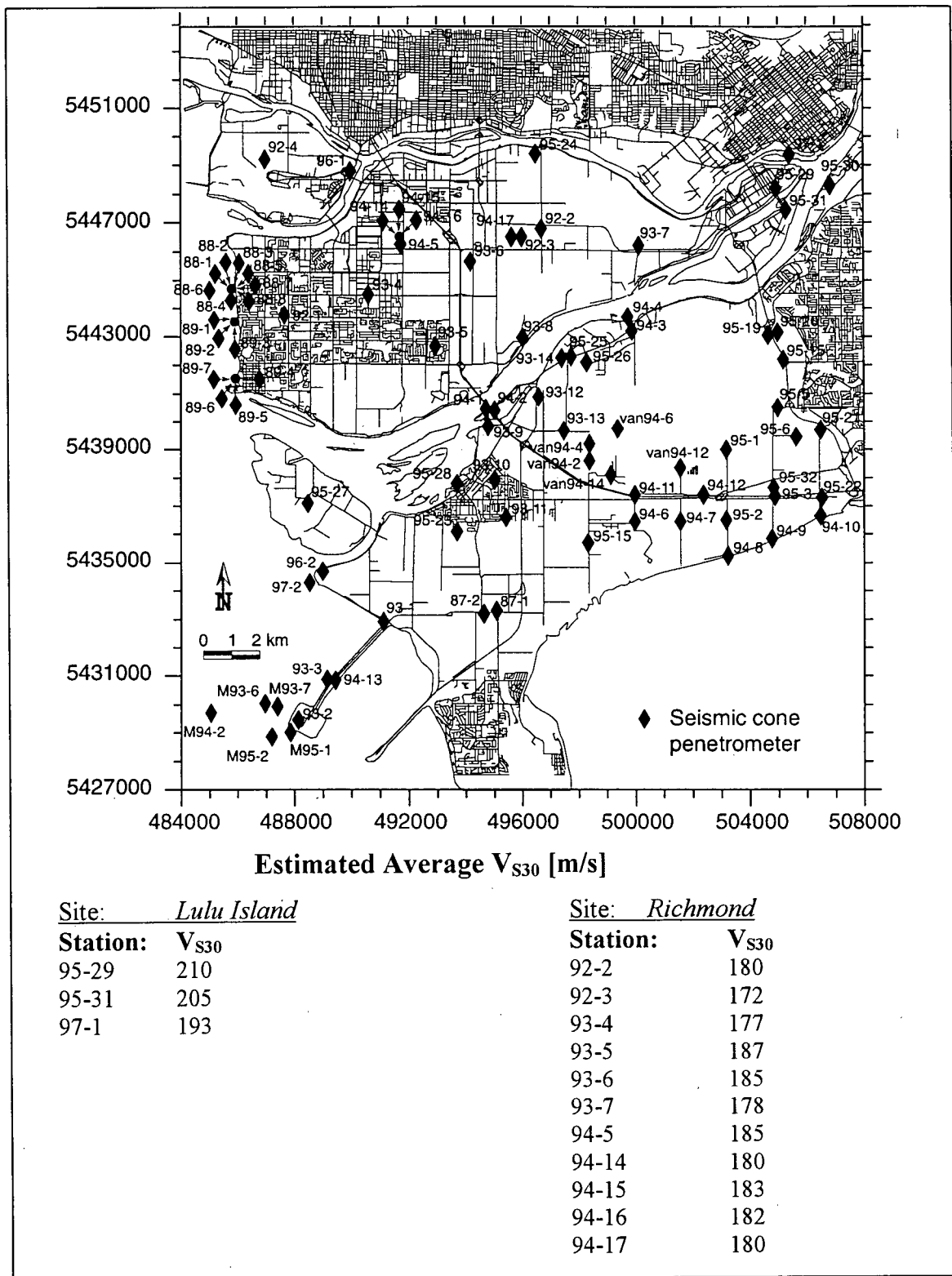


**Figure 6.5** Distribution of  $V_{S30}$  in Lulu Island, New Westminster and Richmond from Seismic Cone Penetration Tests carried out by Geological Survey of Canada (after Hunter *et al.*, 1998).

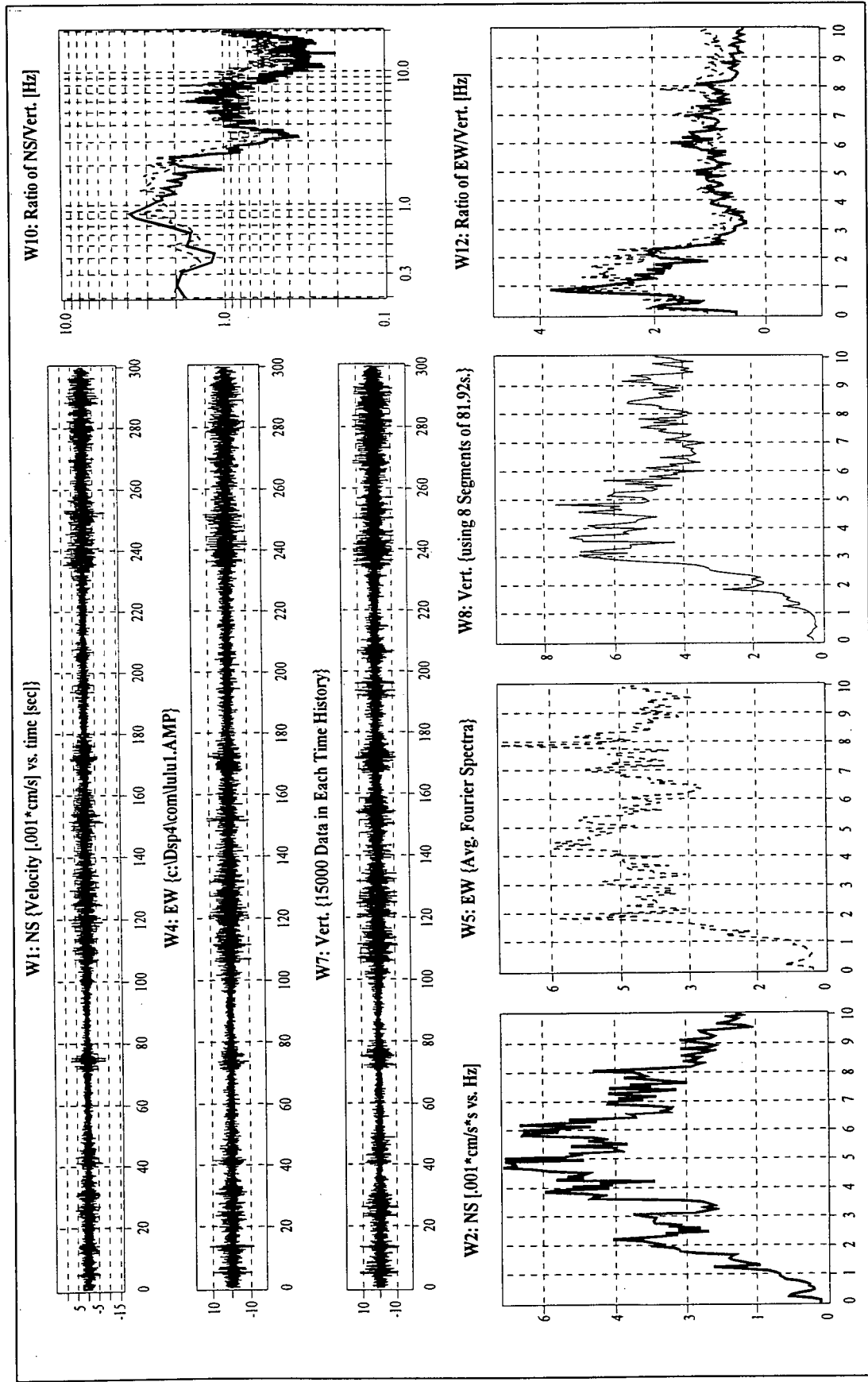


**Figure 6.6** An Example of Records of Microtremor Measurements at sites along Wood Street in Lulu Island (1998).

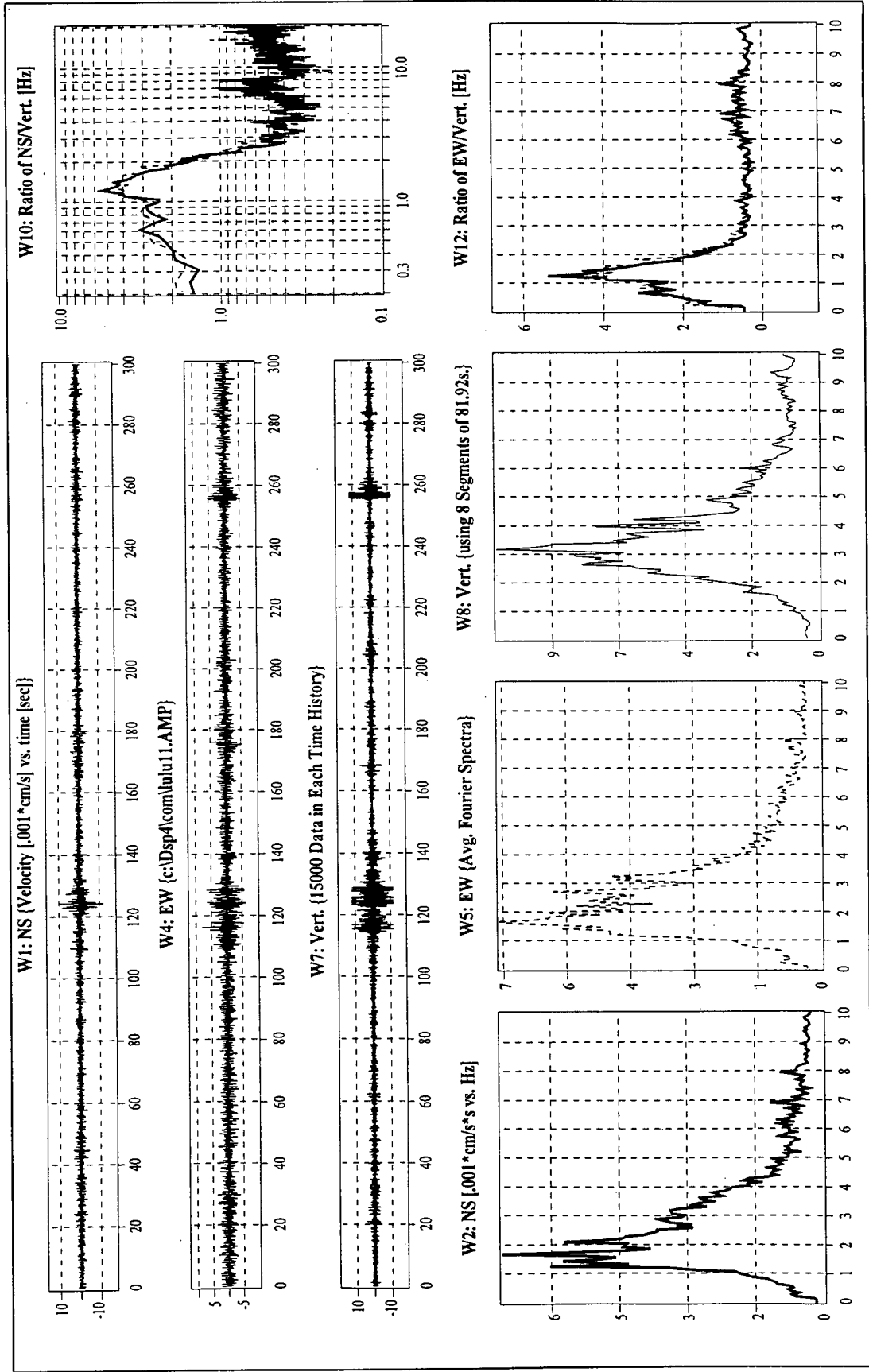
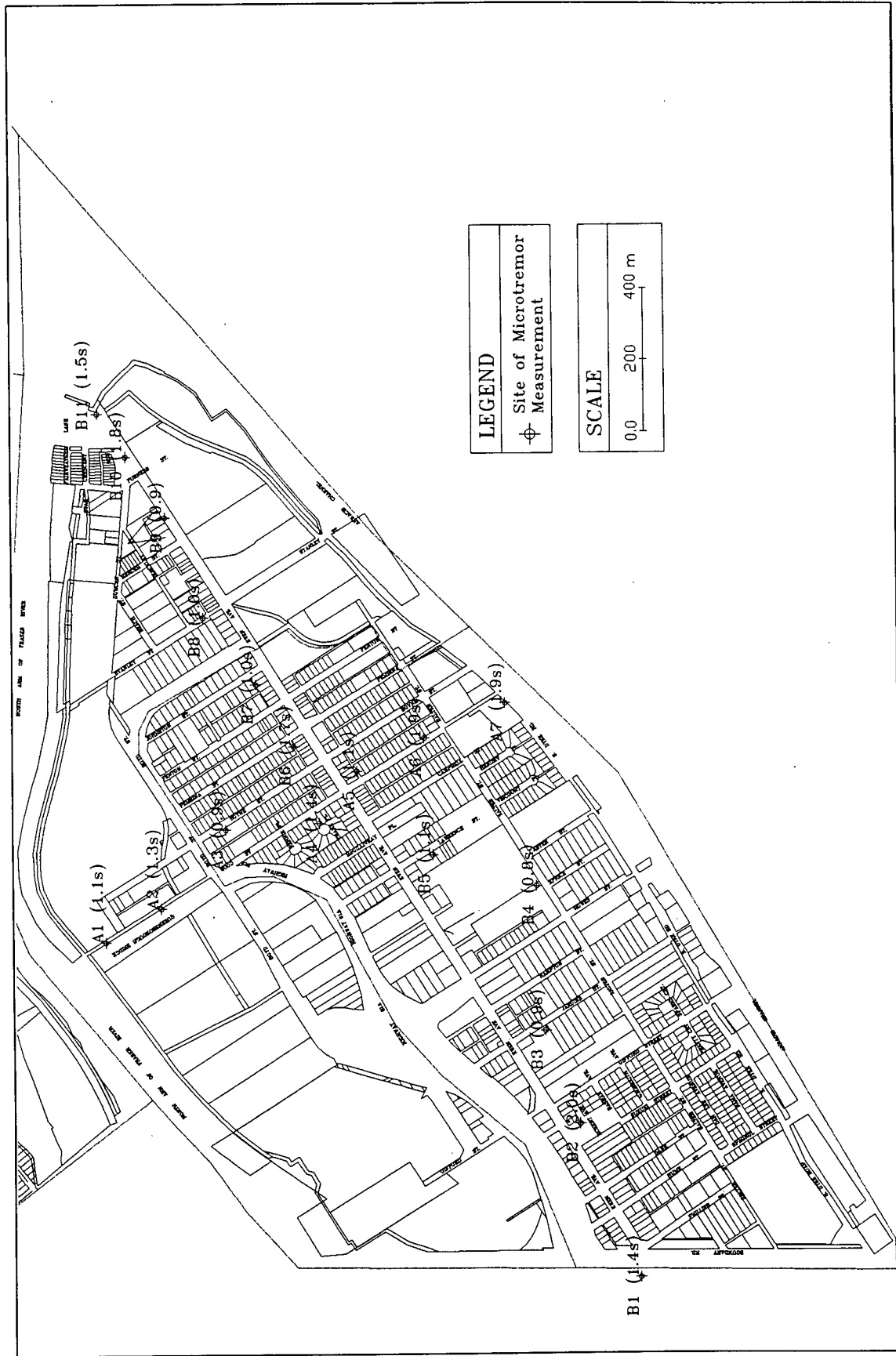
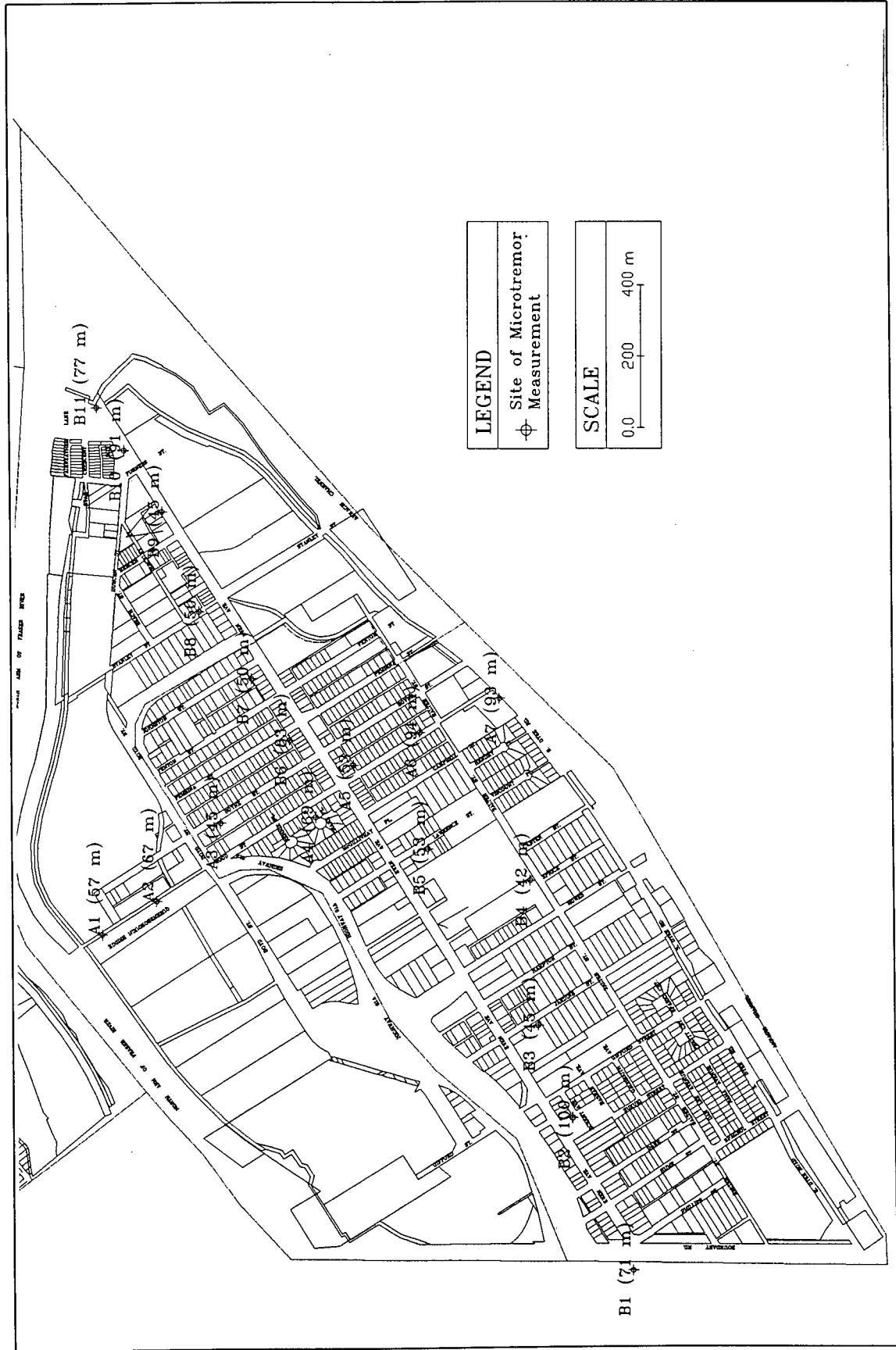


Figure 6.7 An Example of Records of Microtremor Measurements at sites along Ewen Avenue in Lulu Island (1998).



**Figure 6.8** Distribution of Site Predominant Periods (in seconds) along Wood Street and Ewen Avenue in Lulu Island, New Westminster, British Columbia.



**Figure 6.9** Distribution of Estimated Depths (in metres) of Surface Layer(s) based on  $V_s$  of 200 m/s along Wood Street and Ewen Avenue in Lulu Island, New Westminster, British Columbia.

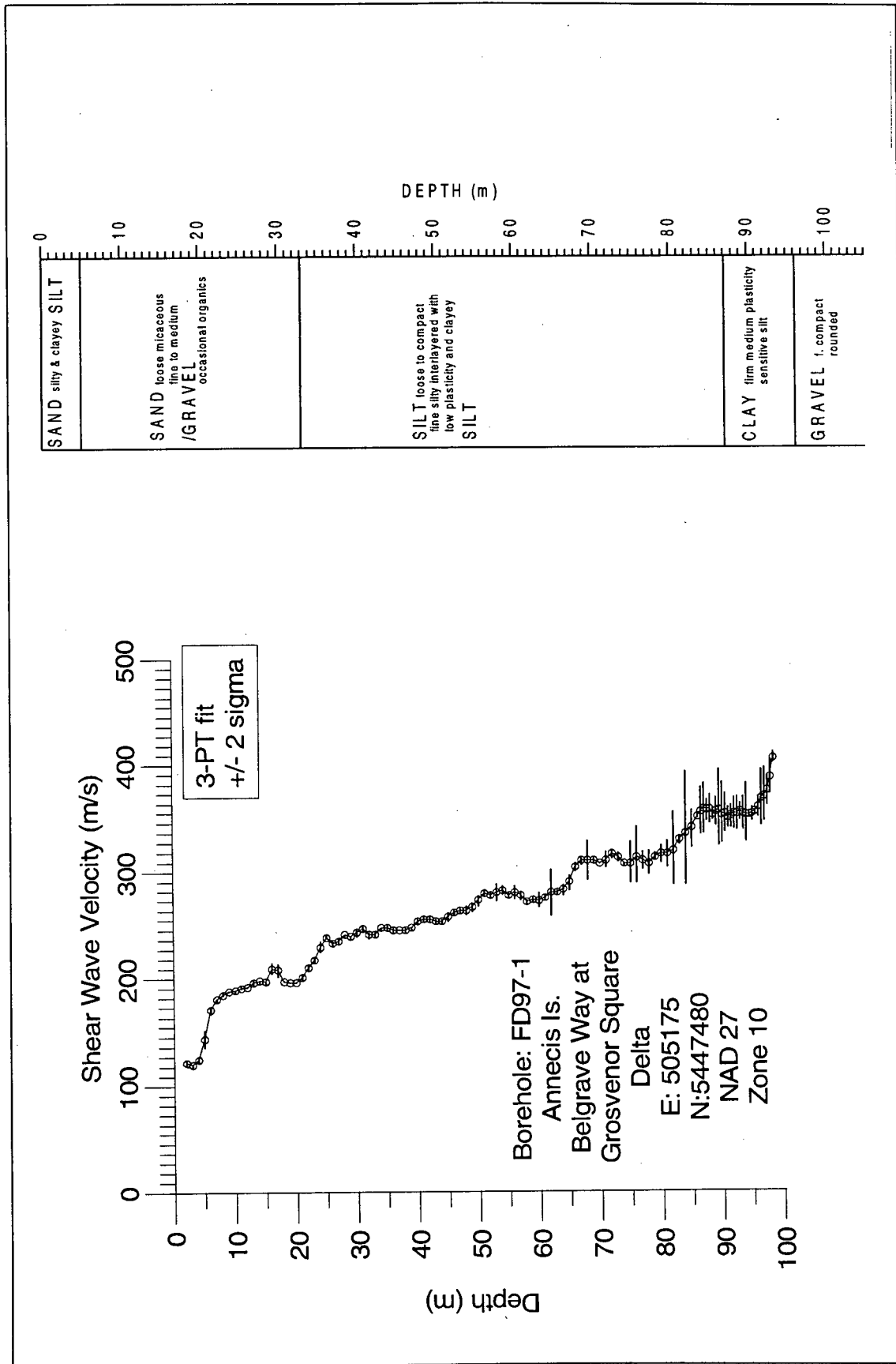


**Figure 6.10** Distribution of Shear Wave Velocities and Soil Profiles with Depth at Borehole station FD97-1 (after Geological Survey of Canada, 1998).



**Figure 6.11** Distribution of Relative Amplification Ratios along Wood Street and Ewen Avenue in Lulu Island, New Westminster, British Columbia.

## 6.4 RICHMOND

Microtremor measurements were carried out in Richmond on October 30, 1998 along Shell Road (gridline S) and on September 19, 1997 along Westminster Highway (gridline K). The locations of the measurement stations are shown **Figure 6.12**. The primary (or most amplified) site predominant periods, secondary (or second most amplified) periods, estimated surface layers, and relative amplification ratios, as well as the number of storeys of buildings which will likely experience the most damage are tabulated in **Tables 6.4(a)** and **(b)**. Examples of analyzed microtremor records at Shell Road (station S2) and Westminster Highway (station K25) are shown in **Figures 6.13** and **6.14** respectively. From **Figure 6.13**, the site frequency of peak response at station S2 was estimated from the horizontal-to-vertical spectral ratios to be 0.3 Hz and the corresponding peak spectral ratio was 7.0. The secondary site predominant frequency at station S2 was approximately 0.9 Hz and the corresponding spectral ratio was 4.0. From **Figure 6.14**, the site frequency of peak response at station K25 was estimated to be 1.0 Hz and the corresponding peak spectral ratio is 5.0. The secondary site predominant frequency at station K25 was approximately 0.4 Hz and the corresponding spectral ratio was 3.0. The existence of a secondary site predominant frequency will be discussed below.

### 6.4.1 SITE PREDOMINANT PERIODS AND ESTIMATED DEPTHS OF SURFACE LAYER

The distribution of site predominant periods along Shell Road and Westminster Highway in Richmond based on results of microtremor measurements is shown in **Figure 6.12**.

The site predominant or most amplified periods from microtremors vary from 0.8 to 5.0 seconds along Shell Road, with most stations along Shell Road having site periods of 3.4 to 5.0 seconds. The low site period of 0.8 seconds was found at the southern end of Shell Road near Williams Road. Along Westminster Highway the site periods were fairly constant at approximately 4.0 seconds towards the west side from Richmond Nature Park and Green Acres Public Golf Course. There was a sudden drop in site periods from 3.3 to 0.5 seconds from No. 5 Road and towards the east the site predominant periods were found to range from 0.5 to 1.0 seconds. With the exception of a few locations, most sites in Richmond were found to have periods of peak response greater than the typical microtremor period response of 2 to 3 seconds. These longer site periods are representative of the sites in Richmond which have deep Holocene layers in excess of 200 metres (see **Figure 6.1**). In addition to the periods of peak response, the second most amplified site periods were also included in **Tables 6.4(a)** and **(b)**. These site periods are probably due to resonance in one of the upper strata when the site periods are shorter than the periods of peak response or the excitation of one of the higher periods of the sites.

**Figure 6.15** shows the distribution of estimated depths of surface layer(s) at various stations along Shell Road and Westminster Highway based on an estimated average shear wave velocity,  $V_{s30}$ , of 185 m/s as indicated by the results of G.S.C.'s SCPT testing (**Figure 6.5**). Along Shell Road the estimated depths of the surface layers at most sites were found to be greater than 150 metres. At the southern end of Shell Road, the surface layers were estimated to be greater than 200-m deep, e.g., 231 metres at stations S7 and S8. The western end of Westminster Highway near Minoru Park to the east of No. 3

Road has significantly deeper estimated depth of the ground surface layer(s) at approximately 185 metres, whereas sites from No. 5 Road and to the east have shallower estimated depths of surface layers ranging from 21 to 51 metres. The geological map in **Figure 6.1** shows that the depths of Holocene deposits near microtremor stations K22, K23 and K24 to be approximately 26, 19 and 62 metres respectively. The depths of surface layers at these stations were estimated from results of microtremor measurements to be 36, 23 and 51 metres, respectively. Microtremor measurements fairly accurately predicted the shallow depths of the Holocene layers at these sites. On the other hand, station K20 has estimated depth of surface layer of about 154 metres but the depth of Holocene deposits in the vicinity of K20 is about 236 metres. **Figure 6.16** shows the distribution of shear wave velocities and soil profiles with depth near station K20 (borehole FD94-4). Up to a depth of 300 metres the site still consists of mainly clayey layers, although the sharp increase shear wave velocities at about 240-m depth indicates the existence of a dense layer directly underlying the thick clay layer extending from 110-m to 240-m depths. The discrepancy between the estimated depths of surface layers and the depths of Holocene deposits may be due to either the excitation of upper strata within the Holocene deposits or the amplitude of the average shear wave velocity used in the estimation. Shear wave velocities at Richmond do vary from site to site, and an average shear wave velocity ( $V_{S30}$ ) of 185 m/s was used to estimate the depths of surface layers at different sites in Richmond. If an average shear wave velocity of 250 m/s which is representative of the shear wave velocity in the Holocene sediments (Finn *et al.*, 1998) was used in the estimation, the estimated depth of surface layer at station K05 would be approximately 200 metres and more closely reflect the depth of the Holocene layer.

Since the depths of surface layers were estimated using the periods of peak response, it confirms the notion that on deep sites (>150 metres to the depth of bedrock) microtremor measurements indicate the peak response of surface layer(s) or the top strata most resonated by the ground motions, instead of those of the entire layers above the bedrock. The predominant periods estimated based on microtremor measurements are therefore the periods of peak response instead of the fundamental periods of the sites.

Finally, based on the results from microtremor measurements along Shell Road and New Westminster Highway, taller buildings of 35 to 50 storeys along most parts of Shell Road and east of Westminster Highway will likely suffer the most damage during strong earthquake shaking. At the south end of Shell Road and the east side of Westminster Highway, the number of storeys of buildings likely to suffer severe damage is 10 storeys or less.

#### **6.4.2 RELATIVE AMPLIFICATION RATIOS**

The distribution of relative site amplification ratios is shown in **Figure 6.17**. The relative amplification ratios along Shell Road range from 1.0 to 1.6, and those along Westminster Highway range from 0.9 to 1.8. By comparison to the relative amplification ratios at sites in Lulu Island, the smaller range in values of the relative amplification ratios of the sites along Shell Road and Westminster Highway indicates that the relative seismic hazard potential along Shell Road and Westminster Highway are likely to be smaller. The closeness in values of the relative amplification ratios also indicates that the relative seismic amplification or hazard potential at sites along Shell Road and Westminster

Highway are likely to be very similar. On the other hand, the existence of relative amplification ratios of 1.0 such as at stations S4 and S6 essentially means that the relative seismic hazard potential at these soft ground sites and that of the reference hard ground site K05 are similar, which is unlikely. Thus, the relative amplification ratios might not be a good indicator of the relative seismic damage potential of different sites or of different geologic units.

The relative amplification ratios were plotted against the estimated depths of surface layers from microtremor analysis for sites in Lulu Island and Richmond as shown in **Figures 6.18**. The purpose is to verify if any correlation exists between the two parameters of peak response. **Figures 6.18** did not show any perceivable trend or correlation between the relative amplification ratios and estimated depths of surface layers. The relative amplification ratios remain fairly constant at  $1.5 \pm 0.5$  regardless of the estimated depths of surface layers at most of the sites.



**Figure 6.12** Locations of Microtremor Measurement Stations and Distribution of Site Predominant Periods along Shell Road and New Westminster Highway in Richmond, British Columbia.

**Table 6.4(a)** Site Predominant Periods, Estimated Depths of Surface Layer(s), Relative Amplification Ratios and Number of Storeys of Buildings likely to experience the Most Resonance along Shell Road in Richmond, British Columbia.

GRIDLINE S: Shell Road												
Site Code	Coordinates		Predominant <sup>1</sup>		Predominant <sup>2</sup>		Surface Layer Depth, H = (T/4) × V <sub>s</sub>		Rel. Amp.		# of Storeys N = 10 × T	
	Easting	Northing	Freq. [Hz.]	Period [Sec.]	Freq. [Hz.]	Period [Sec.]	V <sub>s</sub> = 150 m/s [m]	V <sub>s</sub> * = 185 m/s [m]	V <sub>s</sub> = 250 m/s [m]	Ratio		
S1	492,600	5,449,150	0.25	4.0	0.90	1.1	150	185	250	1.2	40	
S2	492,500	5,447,870	0.29	3.4	1.00	1.0	129	159	216	1.5	35	
S3	492,550	5,447,050	0.25	4.0	1.00	1.0	150	185	250	1.6	40	
S4	492,600	5,445,430	0.25	4.0	0.90	1.1	150	185	250	1.0	40	
S5	492,600	5,444,700	0.25	4.0	1.20	0.8	150	185	250	1.3	40	
S6	492,650	5,443,600	0.20	5.0	0.85	1.2	188	231	313	1.0	50	
S7	492,700	5,442,730	0.20	5.0	1.00	1.0	188	231	313	1.2	50	
S8	492,550	5,442,800	0.20	5.0	0.90	1.1	188	231	313	1.0	50	
S9	492,950	5,442,800	1.20	0.8	0.20	5.0	31	39	52	1.6	9	
S10	493,350	5,441,300	1.20	0.8	0.20	5.0	31	39	52	1.6	9	

**Note:**

1. Predominant<sup>1</sup> Frequency/Period is the most amplified period of the site.
2. Predominant<sup>2</sup> Frequency/Period is the next most amplified period of the site.
3. Rel. Amp. Ratio is the Relative Amplification Ratio.
4. V<sub>s</sub>\* is the estimated average shear wave velocity of the site based on results of seismic cone penetration tests.

**Table 6.4(b)** Site Predominant Periods, Estimated Depths of Surface Layer(s), Relative Amplification Ratios and Number of Storeys of Buildings likely to experience the Most Resonance along Westminster Highway in Richmond, British Columbia.

**GRIDLINE S:** *Westminster Highway*

Site Code	Coordinates		Predominant <sup>1</sup>		Predominant <sup>2</sup>		Surface Layer Depth, H = (T/4)×V <sub>s</sub>		Rel. Amp. Ratio	# of Storeys N = 10×T
	Easting	Northing	Freq. [Hz.]	Period [Sec.]	Freq. [Hz.]	Period [Sec.]	V <sub>s</sub> = 150 m/s [m]	V <sub>s</sub> = 250 m/s [m]		
K16	489,375	5,445,900	0.25	4.0	0.27	3.7	150	250	1.1	40
K17	490,000	5,445,450	0.25	4.0	0.27	3.7	150	250	0.9	40
K18	490,050	5,445,500	0.25	4.0	0.27	3.7	150	250	1.4	40
K19	490,675	5,445,775	0.25	4.0	0.27	3.7	150	250	1.4	40
K20	491,850	5,446,825	0.30	3.3	1.00	1.0	125	208	1.4	33
K21	493,200	5,446,225	2.20	0.5	0.28	3.6	17	28	1.5	5
K22	494,550	5,446,350	1.30	0.8	0.30	3.3	29	48	1.1	8
K23	495,925	5,446,500	2.00	0.5	0.25	4.0	19	31	1.3	5
K24	496,750	5,446,900	0.90	1.1	0.30	3.3	42	69	1.8	11
K25	498,400	5,446,875	1.00	1.0	0.40	2.5	38	63	1.6	10

**Note:**

1. Predominant<sup>1</sup> Frequency/Period is the most amplified period of the site.
2. Predominant<sup>2</sup> Frequency/Period is the next most amplified period of the site.
3. Rel. Amp. Ratio is the Relative Amplification Ratio.
4. V<sub>s</sub><sup>\*</sup> is the estimated average shear wave velocity of the site based on results of seismic cone penetration tests.

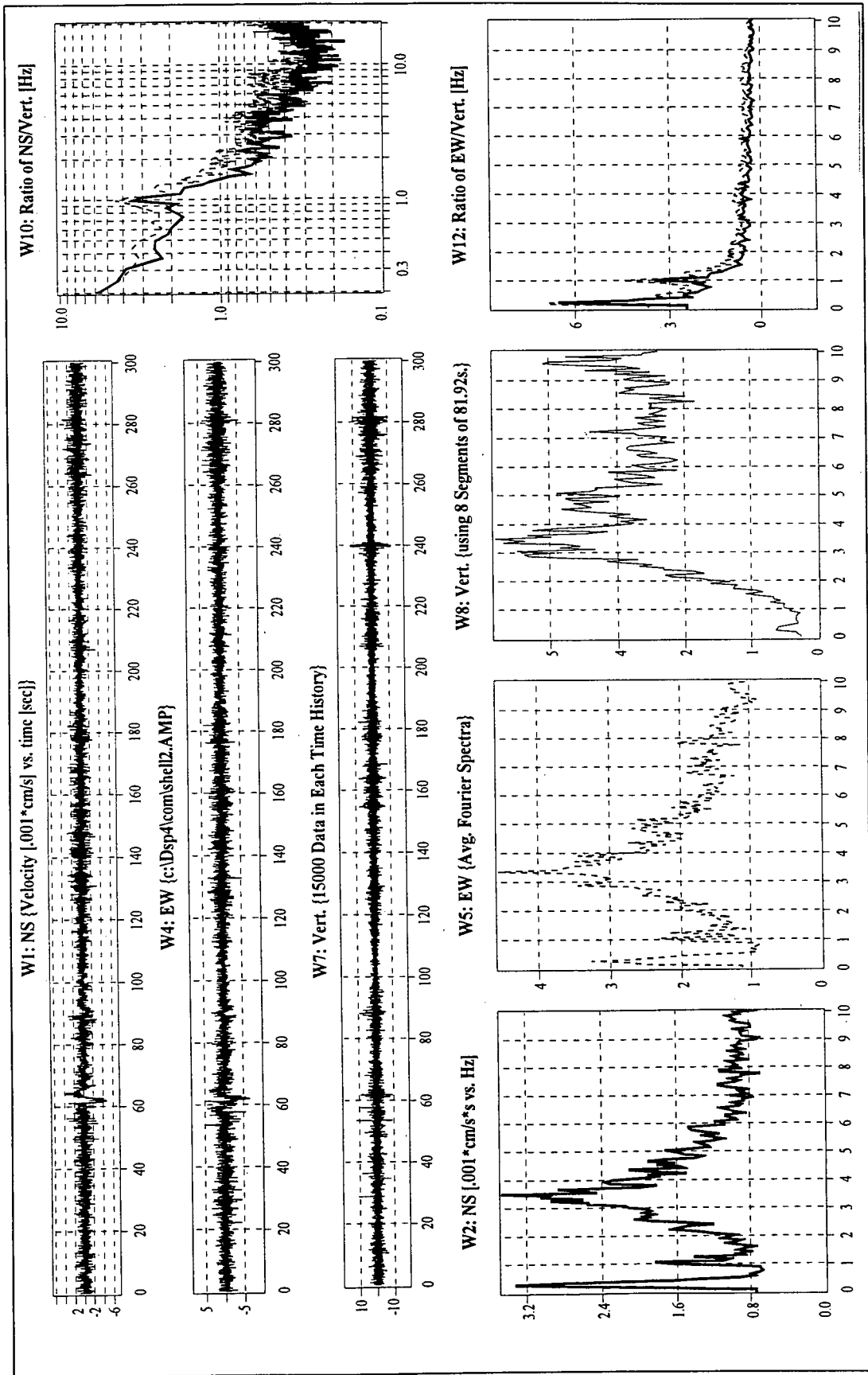


Figure 6.13 An Example of Records of Microtremor Measurements at sites along Shell Road in Richmond (1998).

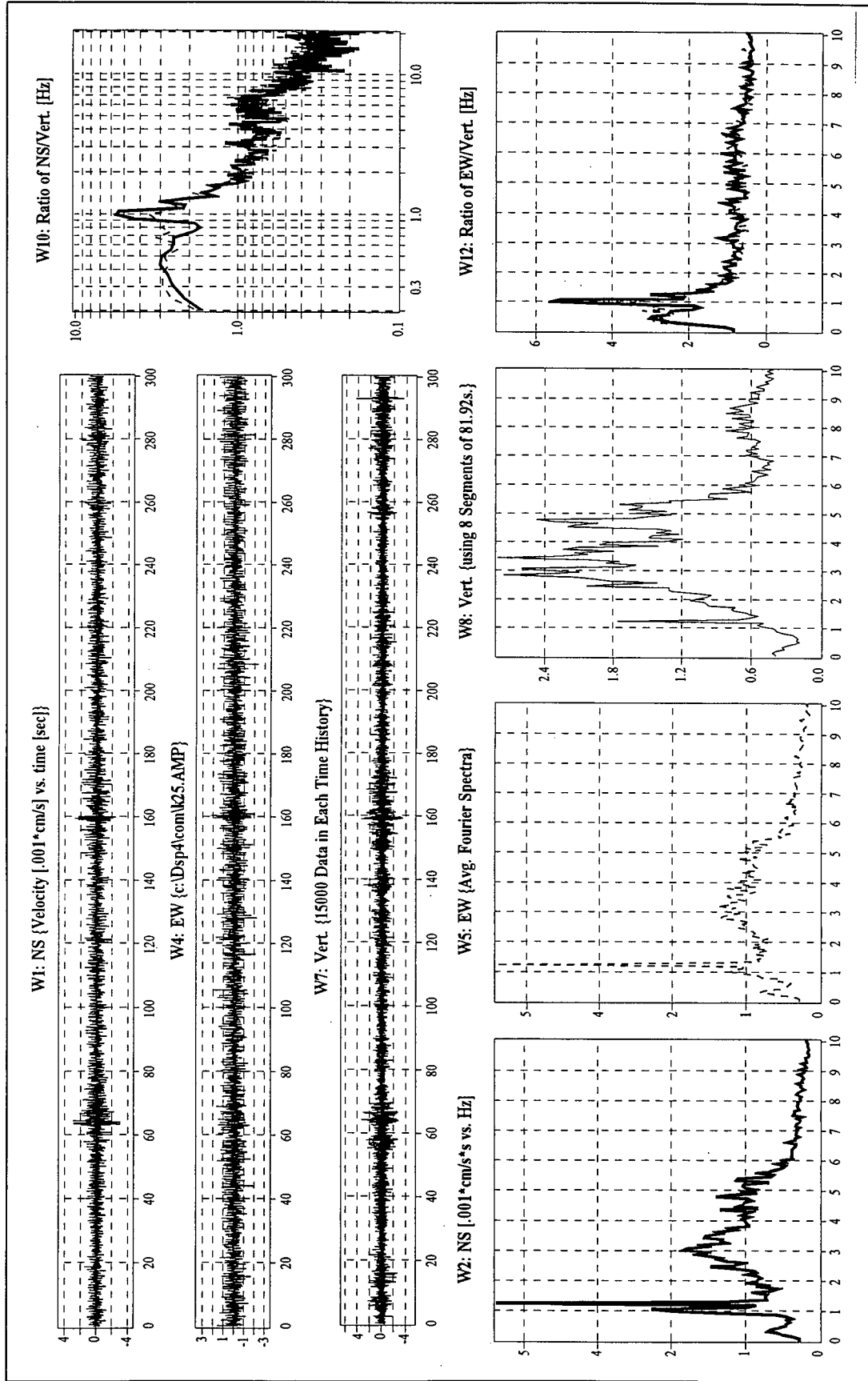
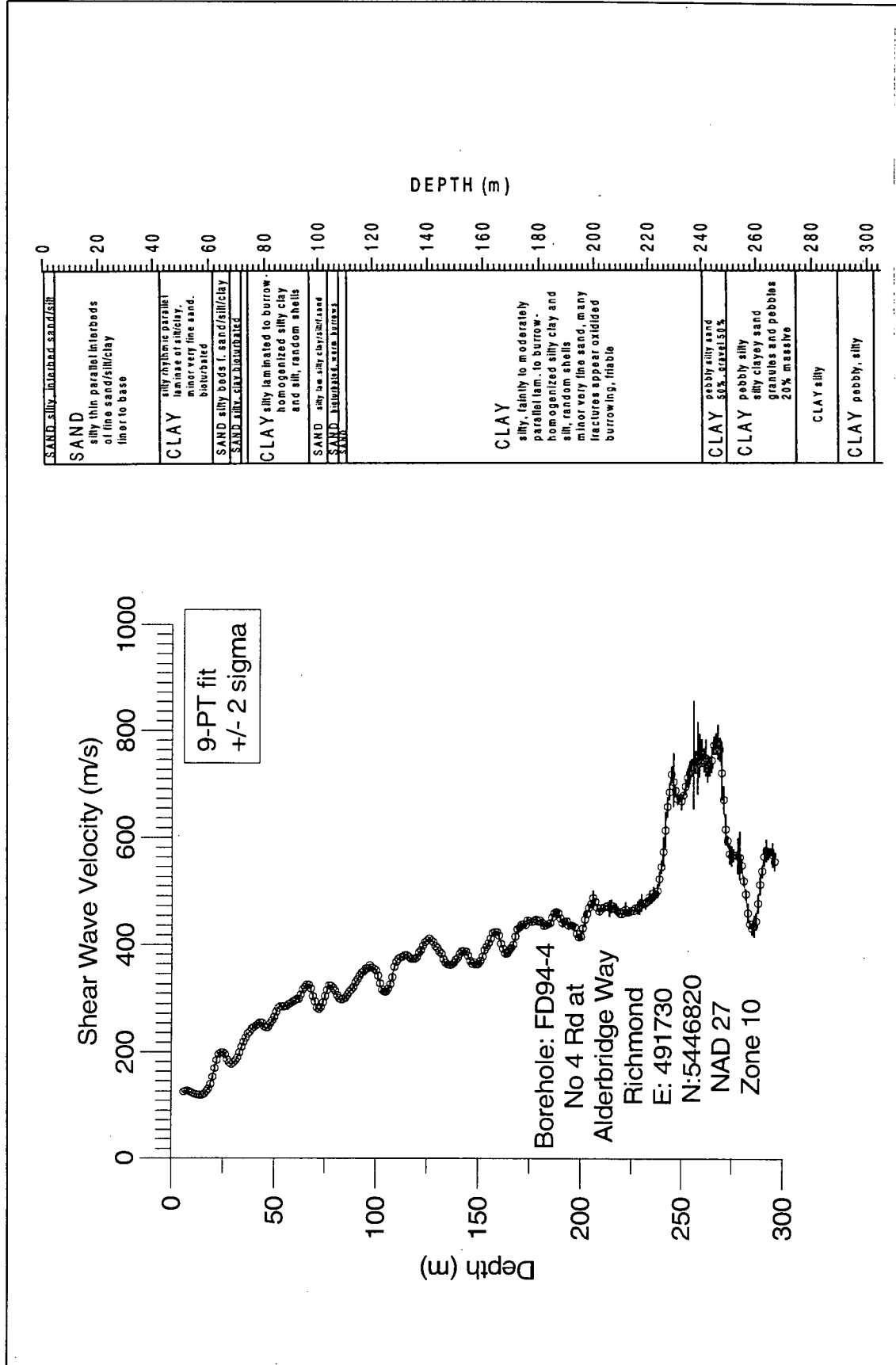


Figure 6.14 An Example of Records of Microtremor Measurements at sites along Westminster Highway in Richmond (1998).

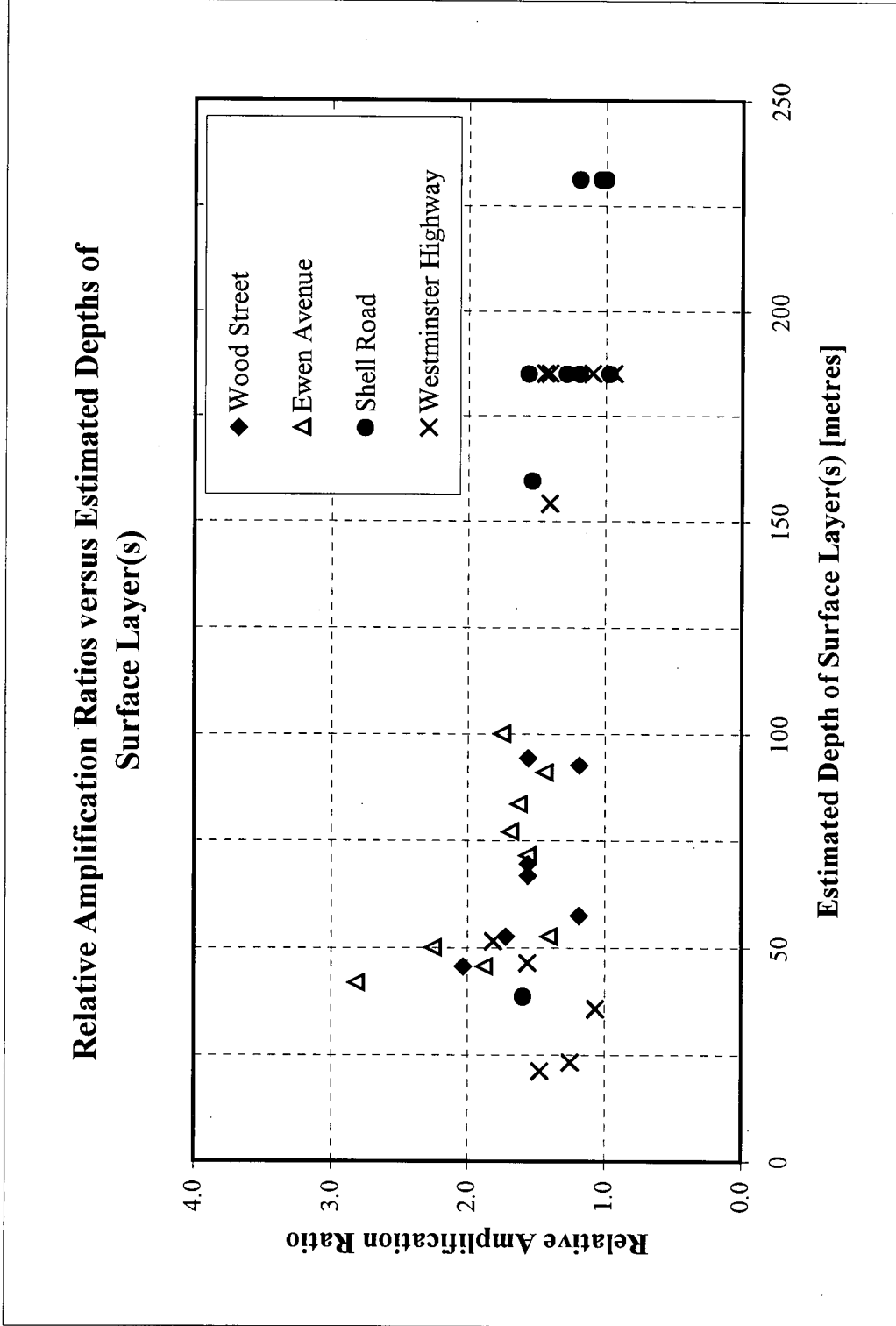


Figure 6.15 Distribution of Estimated Depths (in metres) of Surface Layer(s) based on  $V_s$  of 185 m/s along Shell Road and Westminster Highway in Richmond, British Columbia.



**Figure 6.16** Distribution of Shear Wave Velocities and Soil Profiles with Depth at Borehole station FD94-4 near station K20 (after Geological Survey of Canada, 1998).





**Figure 6.18** Plot of Relative Amplification Ratios versus Estimated Depths of Surface Layer(s).

## 6.5 CONCLUSIONS

The following conclusions can be drawn based on the results of the several case studies presented above regarding the effectiveness of microtremor measurements as a method of assessing seismic hazard potential of different sites.

1. Comparison of spectral characteristics of low-level earthquake ground motions and microtremor measurements at station MNY shows that the predominant frequency from microtremor measurements is similar to those from earthquake ground motions.
2. In Lulu Island and Richmond sites, microtremor measurements were used to estimate the periods of peak response, depths of surface layers, relative amplification ratios and number of storeys of buildings which are likely to suffer the most damage under strong ground shaking due to soil-structure interaction. Seismic hazard maps showing distribution of the above parameters were developed.
3. On shallow sites ( $\leq 150$  metres to depth of bedrock) such as those in Lulu Island, New Westminster, the estimated depths of surface layers were found to agree with the depths to bedrock based on comparison with borehole data. This is probably because periods of peak response coincide with fundamental periods of the sites.
4. On deeper sites ( $> 200$  metres to depth of bedrock) such as at many sites in Richmond, microtremor measurements indicate site periods of peak response but not the fundamental periods of the sites. In addition, the estimated depths of surface layers seem to indicate the depths of the Holocene deposits or those of the upper strata which are resonated by ground motions.
5. The relative amplification ratios which were calculated using the spectral ratio of a reference hard ground site were fairly constant at  $1.5 \pm 0.5$  for most sites and indicate

that the relative hazard potential for the sites are similar. This result is probably because both the Lulu Island and Richmond sites are of similar geological settings. However, the existence of several deep, soft ground sites with relative amplification ratios of approximately 1.0 essentially means that the relative seismic damage potential of these sites are similarly to that of the reference hard ground site. Since it is unlikely that a hard ground site would have similar seismic hazard potential to a soft ground site, more research is therefore required to determine whether the relative amplification ratios can be a good indicator of relative seismic hazard potential between different sites or for different geologic units.

## CHAPTER 7

# **SUMMARY, CONCLUSIONS AND RECOMMENDATIONS FOR FUTURE RESEARCH**

---

### 7.1 SUMMARY

The research work carried out during the course of this study is summarized as follows.

- Investigating the theory and background information of microtremors, as well as the use of microtremor measurements in engineering applications;
- Carrying out field microtremor measurements in Lulu Island and Richmond and various other sites, and performing the analyses and interpretation of the measured microtremor records;
- Investigating the stability characteristics of microtremors at station MNY in Vancouver in terms of the most amplified period and the corresponding peak amplitude based on Fourier response spectra and Nakamura's method;
- Comparing the spectral characteristics of microtremors and those of low-level earthquake ground motions to determine whether microtremors can be used to estimate the periods of peak response for seismic response studies;
- Developing seismic hazard maps based on periods of peak response and other parameters from results of microtremor measurements for sites in Lulu Island and Richmond, and determining the reasonableness of the results based on available seismic or geological data as well as whether the relative amplification ratios can be used as a reasonable indicator of relative seismic hazard potential between different sites.

## **7.2 CONCLUSIONS**

A number of conclusions can be drawn from the results of this investigation. These have been grouped into three sections; namely Stability of Dynamic Characteristics of Microtremors, Surface Microtremor Measurements, and Analytical Analysis and Interpretation.

### **7.2.1 STABILITY OF DYNAMIC CHARACTERISTICS OF MICROTREMORS**

- The site predominant frequencies (or periods) of microtremors were found to be stable in the GVRD region.
- Even in the absence of strong source effects, Nakamura's method was found to provide a site predominant frequency with a smaller standard deviation in comparison to the determination of the frequency of peak response based on the average Fourier spectra.
- The peak Fourier spectral amplitudes and the peak spectral ratios were found to be unstable and highly dependent on the strength of input sources.

### **7.2.2 SURFACE MICROTREMOR MEASUREMENTS**

- Comparing to the more traditional site investigation or seismic microzonation methods, microtremor measurements provide a relative inexpensive and fast way of determining the periods of peak response of sites for site response studies.

### 7.2.3 ANALYTICAL ANALYSIS AND INTERPRETATION

- The frequency of peak response from microtremor measurements is very similar to those obtained from Fourier spectral analysis of two low-level earthquake ground motions recorded at a GVRD site; this result indicates that microtremor measurements may be an effective means of determining site period/frequency for earthquake response studies in the GVRD region.
- Seismic hazard maps were developed for sites in Lulu Island and Richmond, British Columbia based on site predominant periods, estimated depths of surface layers and relative amplification ratios from results of microtremor measurements. The number of storeys of buildings likely to suffer the most damage under strong ground shaking due to soil-structure interaction was estimated and tabulated.
- Results of microtremor measurements on deep and shallow sites showed that microtremor measurements are effective in delineating the periods of peak response instead of the fundamental periods of the sites. The estimated depths of surface layers are therefore the depths of upper strata of the ground which are most resonated by the ground motions instead of the depths of the entire soft soil layers overlying the bedrock at the sites. On shallow sites ( $\leq 100$  metres to depth of bedrock or dense layers) microtremor measurements have been reasonably good in indicating the depths of the surface layers to the underlying bedrock or dense layers. This is most likely because the periods of peak response are similar to the fundamental periods of the sites.
- The relative amplification ratios were found to be fairly constant for most sites in Lulu Island and Richmond, and this is most likely due to these sites having

similar geological settings of soft Holocene overlying dense Pleistocene deposits. The small magnitudes of the relative amplification ratios for most of the sites, many of which are of deep, soft ground sites especially those in Richmond, at approximately  $1.5 \pm 0.5$  indicated that these soft ground sites have essentially very similar seismic hazard potential to that of the reference hard ground site, which is highly unlikely. Hence, it may be concluded that the relative amplification ratios may not be a good indicator of relative seismic hazard potential between different sites or geologic units, or at the least, more research is necessary to determine the effectiveness of using the relative amplification ratios for such purpose. The relative amplification ratios were also found to have no correlation with the estimated depths of surface layers at different sites.

### **7.3 RECOMMENDATIONS FOR FUTURE RESEARCH**

While this thesis explored many aspects of the applications and effectiveness of using microtremor measurements in assessing the dynamic characteristics for seismic response studies, there are several additional aspects worth studying. First, a stability test could be performed at another location different from station MNY in the GVRD region. The stability of characteristics of microtremors was assumed applicable to all sites in the GVRD region based on results of stability test at one site (station MNY) which showed stable site predominant period over time. The additional stability test would serve as an important check of the reasonableness of the assumption that the microtremor characteristics are stable in the GVRD region. Second, since during the course of this thesis microtremor measurements were carried out in the Fraser Delta where the different

sites have very similar geological settings of soft Holocene sediments overlying dense Pleistocene deposits, it would be worthwhile to carry out microtremor measurements at sites which are located on geological settings different from those in Richmond and Lulu Island, such as the shallow, hard ground sites in North Vancouver. The results from microtremor measurements at these sites would be useful in further assessing the effectiveness (or lack) of using the relative amplification ratio as a means for determining the relative seismic damage potential of different sites or different geologic units.

## NOMENCLATURE

---

$A_n$	Amplitude of H/V peak
$A_s$	Maximum amplitude of vertical shear wave amplification function
$E_S$	Transfer function for vertical motions
EW	East-west
F	Foundation or amplification factor
$f$	Frequency
$F(f)$	Wave motion radiation characteristics at the source
$f_n$	Frequency corresponding to H/V peak
$f_s$	Frequency of vertical shear wave resonance
H	Thickness of uniform soil layer
H/V	Horizontal-to-vertical spectral ratios
NS	North-south
$R_B$	Horizontal-to-vertical spectral ratio of base-layer ground motions
$R_S$	Horizontal-to-vertical spectral ratio of surface ground motions
$S(f)$	Surface layer characteristics
SCPT	Seismic cone penetration test
$S_{HB}$	Spectral ordinate of the horizontal motions at the base layer
$S_{HS}$	Spectral ordinate of the horizontal motion at the surface
SPT	Standard penetration test
$S_T$	Transfer function for horizontal motions
$S_{TT}$	Modified transfer function
$S_V$	Vertically incident shear waves
$S_{VB}$	Spectral ordinate of the vertical motions at the base layer

$S_{vs}$	Spectral ordinate of the vertical motions at the surface
T	Site Predominant Period or Fundamental Period of Moment Resistant Frame
$T(f)$	Wave propagation characteristics
$V_s$	Average shear wave velocity [m/s]
$V_{s30}$	Average shear wave velocity [m/s] of the top 30 metres of the ground

## **ABBREVIATIONS**

---

G.S.C.	Geological Survey of Canada
GVRD	Greater Vancouver Regional District
NBCC	National Building Code of Canada
NEHRP	National Earthquake Hazards Reduction Program
U.B.C.	University of British Columbia

## REFERENCES

---

1. Bard, P.Y., Duval, A.M., Lebrun, B., Lachet, C., Riepl, J., Harzfeld, D. (1997) "Reliability of the H/V Technique for Site Effects Measurement: An Experimental Assessment," **Proceedings of Earthquake Conference in Istanbul (July 1997)**, pp.1-8.
2. Bendat, J.S. and Piersol, A.G. (1993), **Engineering Applications of Correlation and Spectral Analysis**, 2<sup>nd</sup> Edition. John Wiley and Sons, Inc., New York, U.S.A.
3. Cassidy, J.F., Rogers, G.C. and Weichert, D.H. (1997), "Soil Response on the Fraser Delta to the MW = 5.1 Duvall, Washington Earthquake," **Bulletin of the Seismological Society of America**, Vol. 87, pp. 1354-1361.
4. Cassidy, J.F., Rogers, G.C., Weichert, D.H. and Little, T.E. (1998), "Strong Ground Motion Recordings of the June 1997, Strait of Georgia Earthquake," Geological Survey of Canada, Open File.
5. DSP Development Corporation (1996) **The DADiSP Worksheet: Function Reference Manual**. One Kendall Square, Cambridge, MA, U.S.A.
6. Finn, W.D.L. (1991) "Geotechnical Engineering Aspects of Microzonation," **Proceedings of 4<sup>th</sup> International Conference on Seismic Zonation**, Vol. 1, pp. 236-250.
7. Finn, W.D.L. (1994), "Effect of Foundation Soils on Seismic Damage Potential," **Proceedings of Tenth World Conference on Earthquake Engineering**, Madrid, Spain, pp.6493-6506.
8. Finn, W.D.L. (1997) "Effects of Local Soil Conditions on Site Response," **Class Notes of CIVL 504**, University of British Columbia.
9. Haile, M. (1998) "Study of Site Effects at Axum Obelisk Site by using Microtremors," **The Effects of Surface Geology on Seismic Motion**, 1998 Ed., pp. 665-671.
10. Hao, X.-S. (1992) "Local Geologic Effects on Ground Motions and Low Damage Anomaly of the 1976 Tangshan, China, Earthquake," **Ph.D. thesis**, Tokyo Institute of Technology.
11. Hao, X.-S., Finn, W.D.L., Ventura, C.E., Seo, K., Samano, T. (1998) "Microtremor Measurements in the Vancouver Regional District, Canada," **Conference Paper**.
12. Hao, X.-S., Hagio, K., Maeda, T., and Hibino, H. (1995) "Evaluation of Predominant Period of Ground Motions based on Microtremor Measurements," **Taisei Technical Research Report**, No. 28, pp. 69-76, (in Japanese with English abstract).

13. Hao, X.-S., Hagio, K., Maeda, T., Hibino, H. and Yamanaka, R. (1994) "*A Site Response Estimation in Kushiro City based on a Comparison between Microtremors and Weak Motions*," **Proceedings of 9<sup>th</sup> Japan Earthquake Engineering Symposium**, 2, E67-72.
14. Hunter, J.A., Monahan, Patrick (1998a). A CD-rom compilation of shear wave velocity data for unconsolidated sediments in the Fraser River Delta, **Proceedings of the 12<sup>th</sup> Annual Vancouver Geotechnical Society Symposium on Site Characterization**.
15. Kagami, H., Duke, C.M., Liang, G.C. and Ohta, Y. (1982) "*Observation of 1- to 5-Second Microtremors and Their Application to Earthquake Engineering. Part II. Evaluation of Site Effect Upon Seismic Wave Amplification Due to Extremely Deep Soil Deposits*," **Bulletin of the Seismological Society of America**, Vol. 72, No. 3, pp. 987-998.
16. Kanai, K. and Tanaka, T. (1961) "*On Microtremors. VIII*," **Bull. ERI**, Tokyo University, Vol. 39, pp. 97-114.
17. Kobayashi, H., Seo, K. and Midorikawa, S. (1986) "*Measurement of Microtremors in and around Mexico D.F.*," **Report on Seismic Microzoning Studies of the Mexico Earthquake of September 19, 1985, Part. 1**, Tokyo Institute of Technology, pp. 1-98.
18. Lachet, C. and Bard, P.Y. (1994) "*Numerical and theoretical investigations on the possibilities and limitations of the 'Nakamura's technique'*," **Journal of Physics of the Earth**, Vol. 42, pp. 377-397.
19. Monahan, P.A. (1998) Private communication.
20. Monahan, P.A., Byrne, P.M., Watts, B.D., and Naesgaard, E. (1998) "*Engineering Geology of the Fraser River Delta*," **Proceedings of the 8<sup>th</sup> IAEG Congress**, pp. 3-21.
21. Nakamura, Y. (1989) "*A Method for Dynamic Characteristics Estimation of Subsurface using Microtremor on the Ground Surface*," **QR of RTRI**, Vol. 30, No.1, pp. 25-33.
22. Navarro, M., Sanchez, F.J., Posadas, A.J. and Luzon, F. (1998) "*Evaluation of Surface Soil Effects using Geotechnical Data and Microtremor Measurements in Almeria City*," **The Effects of Surface Geology on Seismic Motion, 1998 Ed.**, pp. 635-642.
23. Seo, K. (1992) "*A Joint Work for Measurements of Microtremors in the Ashigara Valley*," **Proceedings of the International Symposium on the Effects of Surface Geology on Seismic Motion**, pp.282-291.

24. Seo, K. (1992), "*A Joint Work for Measurements of Microtremors in the Ashigara Valley,*" **Proceedings of the International Symposium on ESG**, Vol. II, pp. 43-52.
25. Seo, K. (1994), "*On the Applicability of Microtremors to Engineering Purposes: Preliminary Report of the Joint ESG Research on Microtremors after the 1993 Kushiro-oki (Hokkaido, Japan) Earthquake,*" **Proceedings of 10<sup>th</sup> European Conference on Earthquake Engineering**, Vol. 4, pp. 2643-2648.
26. Seo, K. (1995) "*On the Applicability of Microtremors to Engineering Purposes: Preliminary Report of the Joint ESG Research on Microtremors after the 1993 Kushiro-oki (Hokkaido, Japan) Earthquake,*" **Proceedings of the 10<sup>th</sup> European Conference on Earthquake Engineering**, pp. 292-297.
27. Seo, K. (1997) "*Comparison of Measured Microtremors with Damage Distribution,*" **Technical Report of JICA Research and Development Program on Earthquake Disaster Prevention**, Japan.
28. Seo, K. (1998) "*Application of Microtremors as a Substitute of Seismic Motion – Reviewing the Recent Microtremors Joint Research in Different Sites,*" **The Effects of Surface Geology on Seismic Motion**, 1998 Ed., pp. 577-586.
29. Udawadia, F.E. and Trifunac, M.D. (1973), "*Comparison of Earthquake and Microtremor Ground Motions in El Centro, California,*" **Bulletin of Seismological Society of America**, Vol. 63, pp. 1227-1253.

## APPENDIX A

# MICROTREMOR MEASUREMENTS

---

### A.1 OVERVIEW

This appendix describes the microtremor measurement requirements and procedures. The measurements are carried out with the aid of the program DASam which was developed by Seo *et al.* (1989). There are two versions of DASam -- one is used for data acquisition and hence labeled "DASam 1- Observation System"; the other is used to convert microtremor data into readable format for data analysis and it is labeled "DASam 2 - Data Analysis".

### A.2 EQUIPMENT CHECK LIST

The following items should be included for each microtremor measurement field trip:

1. Two sets of microtremor measurement sensors – 3 velocity sensors per set;
2. Notebook computer for data acquisition and preliminary data analysis;
3. Diskette containing the data acquisition program DASam 1 – Observation System, which contains the step-by-step onscreen instructions for carrying out data acquisition;
4. PC connector for connecting the data acquisition computer to the A/D converter;
5. Notebook PC adapter;
6. AC/DC converter;
7. Amplifier;
8. Cables for amplifier-sensor connection;

9. Cable connector (found on an orange triangular holder) with 30' extension cables for amplifier-sensor connection;
10. Two batteries (Secure SB12250 12V);
11. Detailed map of sites;
12. Camera and films;
13. Fine screw-driver set for calibration of sensors;
14. Steel plate for seating sensors during field testing;
15. Level for leveling the steel platform;
16. Six traffic cones to setup boundaries of measurement station;
17. Three (or more) life vests, depending on the number of people going on the field trip;
18. Miscellaneous equipment (i.e., duct tape, papers, markers, etc.).

### **A.3 PREPARATION AND STORAGE OF SENSORS**

The sensors for both horizontal (two sensors) and vertical measurements should be prepared before field testing by performing the steps indicated below. The names of various parts of the sensors are as shown in **Figures A.1, A.2 and A.3**. **Figure A.1** shows the three sensors used for microtremor measurements. **Figures A.2 and A.3** show the sensors (with external case removed) used to measure vibrations along the horizontal and vertical directions respectively. The key steps are first summarized, followed by the detailed descriptions of the steps.

#### Summary of key steps:

1. Take sensors out of safekeeping box, remove the sensor cases and unlock the internal locks of the sensors.

2. Put sensor cases back on and lock the external locks of the sensors.
3. Level steel plate and then level the sensors on the steel plate.
4. Put sensors back in the safekeeping box, or after use, lock the internal locks and leave the external locks in open/unlocked position.

Detailed preparation steps:

1. Remove the three sensors from the storage box. Make sure that the external lock is unlocked. To check if the external lock of each sensor is unlocked, make sure that the horizontal line mark on the lock is in vertical position.
2. For each sensor, loosen the case screws and remove the sensor case. Once the case is removed, loosen the internal lock completely. Give the brass coil disc a slight perturbation to make sure that it can move freely.
3. Carefully put the sensor case back on. It is important to ensure that the movement of the brass coil disc is not restricted by the internal lock after the case is put back on since ground vibrations are measured using the brass coil disc through its vibrating mechanism. Press and release the external lock or tilt the sensor slightly to check (through the lense external to the brass coil disc as shown by **B** in **Figure A.1**) that the brass coil disc can move freely. If the brass coil disc is stuck, remove the case and adjust the internal lock to ensure the lock does not restrict the movement of the disc. Repeat the previous step.
4. Lock the brass coil disc in position by locking the external coil lock, i.e., turning the line mark on the lock to horizontal position.
5. Place the small steel plate for the sensors on the floor and level it using a level by adjusting the base screws. Place the three sensors on the steel plate by aligning the arrow marks on top of the sensors with those on the steel plate to ensure the sensors are measuring signals along three orthogonal directions. Next, adjust the two base screws of the sensors to level the sensors by centering the bubble within the level of the sensor. Since on-site setup of the sensors will be done on the same steel plate,

this step will minimize the amount of time required to level the sensors if the plate is leveled.

6. After the sensor is leveled, unlock the external coil lock and check through the lense to see if the brass coil disc can move freely. For the sensor measuring vibrations in the vertical direction, the movement of the brass coil is seen through a small mirror which can be seen through the lense external to the brass coil disc.
7. Lock the external lock and place the sensors back into the storage box. The sensors are ready to be used for field testing.

After field measurement, it is important to put the sensors away by performing the following steps.

1. Before putting the sensor back into the storage box, remove the sensor case. Adjust the internal lock plate by pressing the handle down until the plate is under the internal lock. Next, tighten the internal lock and put the sensor case back on. Also, make sure that the external lock is unlocked because only one of the two locks – internal or external -- should be locked at any time.
2. Finally, put the sensor back into the storage box for safe storage.

#### **A.4 SETUP OF DATA ACQUISITION SYSTEM**

1. Before each field trip, make sure that the batteries are charged. Use a charger to check if the batteries are charged, and to charge the batteries. Gather all equipment listed in the equipment check list of **Section A.3**.
2. Arrange the equipment – amplifier, data acquisition computer, batteries, cables, etc. -- for microtremor measurements in the vehicle where the equipment will be transported. A good arrangement of the equipment is as shown in **Figure 5.3**.
3. Hook up the amplifier to the A/D converter using the three amplifier-converter cables (black in colour). Use the first three channel slots (starting from the left) of the amplifier. Check the tags on the various cables if unsure which cables to use. Connect the PC connector to the data acquisition computer and connect the other end

of the connector to the A/D converter. Connect both the amplifier and data acquisition computer to the portable battery via an AC/DC converter. For the data acquisition computer, use the PC adapter.

4. Set all channel attenuation factors on the amplifier to maximum, i.e.,  $\times 200$  and  $\times 10$ . There are two attenuation factors: attenuation 1 has settings of  $\times 1$ ,  $\times 2$ ,  $\times 5$ ,  $\times 20$ ,  $\times 50$  and  $\times 200$ , and attenuation 2 has settings of  $\times 1$  and  $\times 10$ . For each of the three channel slots, set the "Vel./Dis." Switch to [velocity] for measurement type and set the "Calibration/Measurement" switch to [calibration]. The relevant parts of the channel slots of the amplifier are shown in **Figure A.4**.
5. Make sure that the diskette labeled "**DASam 1: Observation System**" is in the disk drive of the data acquisition system.
6. Switch on the AC/DC converter and check that the data acquisition system is working properly by switching on the amplifier and the data acquisition computer.
7. After the computer is turned on, the screen should show the main menu for the data acquisition program as shown in **Figure A.5**. Use *Space Bar* to select *Option 0: End* and press the *Enter* key. The screen should show *ok*. Type *system* and press the *Enter* key to go to the DOS screen. At the DOS prompt, i.e., **A:¥>**, check the date and time using the **date** and **time** commands. If the date or time is inaccurate, make appropriate changes. Note that the computer is using Japanese DOS system and hence the DOS prompt looks slightly different from that of the North American DOS system. Next, make a new directory for storing the data files using the **md** command, i.e., **C:¥>md directory name**.
8. Turn off the amplifier, data acquisition computer and AC/DC converter.

## A.5 TYPICAL TESTING PROCEDURES

The typical testing procedures are as follows. Note that selection of options when operating the data acquisition computer can be done using either the *Space Bar* or the

up/down arrow keys. The key steps are summarized below, followed by detailed descriptions of the testing procedures.

Summary of key steps:

1. Setup the sensors at a location.
2. Level the sensors and centre the internal brass coils of the sensors.
3. Run **DASam1: Observation System** in notebook computer.
4. Connect sensors to amplifier.
5. Follow the step-by-step on screen instructions to key in inputs, perform calibration of sensors, and record microtremor data.
6. Check records for signal saturation and perform preliminary spectral analysis using notebook computer.

Detailed descriptions of testing procedures:

1. Setup a measurement station near the site where the intended measurement is to be carried out. A suitable location should have minimum traffic or other artificial vibration noises such as construction activities in close vicinity (less than 5 metres) of the station.
2. Setup the sensors at the station by first leveling the steel plate before leveling the sensors on the steel plate. The steel platform serves to facilitate the leveling process.
3. For optimal measurement condition, the brass coil disc in each sensor should be approximately centered. This is achieved when the center of the brass coil disc (marked by the edge of the brass coil near the centre of the disc) approximately 1 to 2 mm off the top of the magnetic hollow cylinder. Note that the brass coil disc vibrates in and out of the magnetic hollow cylinder near the cylinder top. Since the sensor is approximately leveled, the brass coil disc should be approximately centered. If the brass coil disc is not centered, adjust the base screws to approximately center the disc.

Also, make sure that sensor is still leveled by ensuring the bubble is within the red circle in the sensor level. For the vertical sensor, if the above steps fail to center the brass coil disc, adjust the vertical spring lock to center the disc. Note that it is highly unlikely that the brass disc cannot be centered through the adjustment of the base screws.

4. The amplifier and data acquisition computer should already be setup in the vehicle. Check to make sure that the diskette labeled **DASam 1: Observation System** is inserted in the disk drive of the data acquisition computer. Switch on the AC/DC converter, amplifier and data acquisition computer.
5. Hook up sensors to the cable connector using the 30' extension cables. Check the tags on the cables to ensure that the appropriate cables are connected to the sensors. The cable tags should have numbers corresponding to the numbers marked on the top of the sensors. Next, connect the amplifier to the cable connector using the amplifier-sensor cables.
6. The data acquisition computer, which was switched on in step 4 should show the <<A/D Conversion Program Menu>> on its screen. Select *Option 1: Temporary Measurement* if it is not already highlighted and press the *Enter* key.
7. In the ensuing <<A/D Conversion Screen>>, make sure that the screen is in English mode, or else press the *Help* key to switch to English format. Select **Start** and press the *Enter* key. Next, highlight **NS/T** for the type of PC-notebook and press the *Escape* key.
8. In the <<A/D Condition>> screen, make appropriate entries at the prompts as illustrated below. The range of allowable values or upper bound is shown in closed square brackets. The default values are also shown following the brackets. Make sure that the *Enter* key is pressed after each entry. Typical values for microtremor measurements are provided as examples as well.
  - # of input channels [1 – 8]: 3 ⇒ 3 [Enter]
  - Channel # of clock signal [none: 0]: 0 ⇒ 0 [Enter]

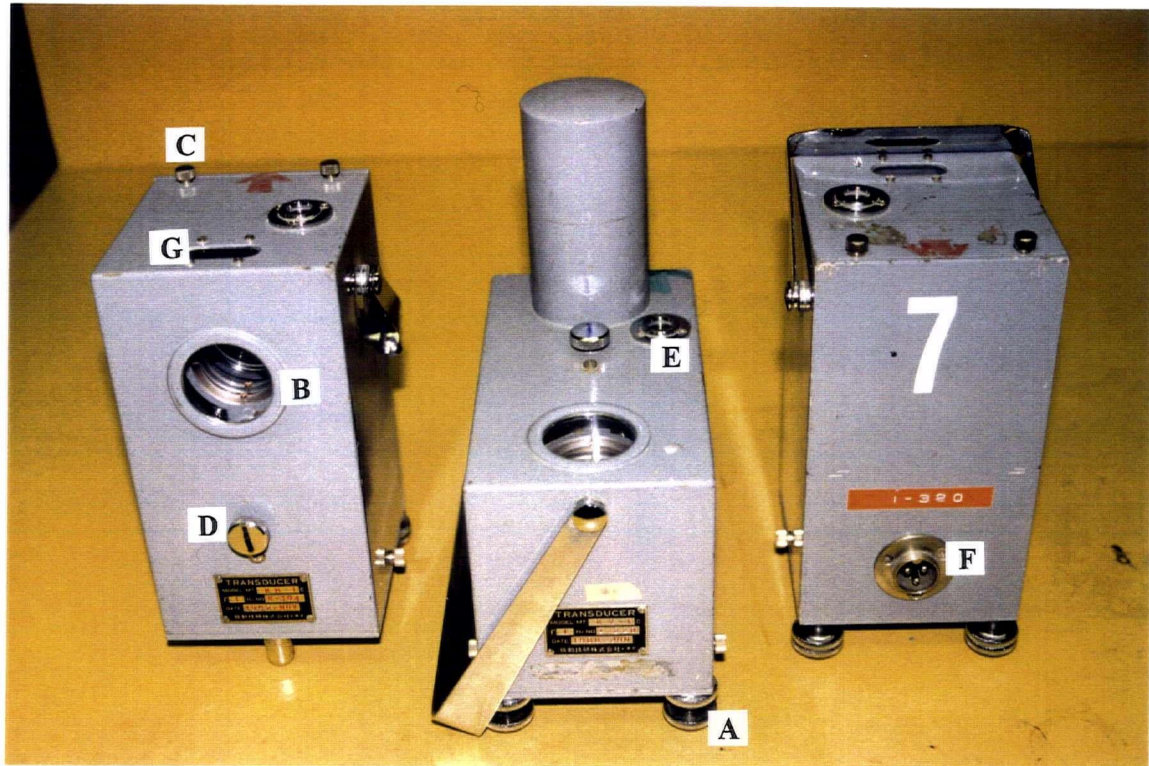
- Sampling rate [max. 500 pts/sec]: 50 ⇒ **50** [Enter]
- Duration of sampling [max. 873 sec]: 50 ⇒ **300** [Enter]
- Duration of display on 1 stage [sec]: 10 ⇒ **10** [Enter]

Press the *Space Bar* to make corrections or changes, and/or press the *Escape* key when the correct entries have been made. Note that typical recording of microtremor signals is carried out for 5 minutes or 300 seconds.

9. In the following screen, specify the signal components – N00E, N90E, Vert. – and select **[5]: TAISEI** to specify the amplifier type. The entries under the headings “pickup” and “amplifier” should automatically show **MTK-1C** and **TA-406** respectively. Press the *Escape* key to accept the entry.
  
10. The next screen shows the switch settings for sensor calibration. The settings for amplifier **TA-406** are shown in the last column. Check that all the amplification factors on the amplifier type TA-406 are set to the maximum. This should have been done in step 4 of the setup of data acquisition system as described in **Section A1.5**. At the “Do you need to check calibration signal?” prompt, select **Yes** and press the *Escape* key. The operator should see Calibration screen on the screen. The calibration factors of the three channels are shown on the top right corner of the screen. Check that the calibration factors are approximately 2000 mV ±20 mV; else, adjust the “gain” button (**H** in **Figure A.4**) using a 1.4-mm screw-driver. Also ensure that the sinusoidal signals are approximately centered, i.e., the maxima and minima of the signals are at ±1000 mV. Otherwise, adjusting the “zero” switch on the amplifier (**G** in **Figure A.4**) using a 1.4-mm screwdriver to center the signals. Wait for the signals to stabilize and then press the *Escape* key to complete the calibration process. Sensor calibration should be checked or repeated at every measuring station.
  
11. Initialize the measurement mode by flipping the “calibration/measurement” switch of the three channel slots of the amplifier to [measurement]. Adjust the period (1, 3 or 5 seconds) and amplification factors of each of the three channels until the screen shows a reasonable magnitude of signals. Note that most measurements are performed with the period of the sensors set at 5 seconds, attenuation 2 (×1 or ×10)

set at  $\times 1$  and attenuation 1 ( $\times 1$ ,  $\times 2$ ,  $\times 5$ ,  $\times 20$ ,  $\times 50$  or  $\times 200$ ) set at  $\times 1$ ,  $\times 2$  or  $\times 5$ . Press the *Escape* key once the adjustment is complete.

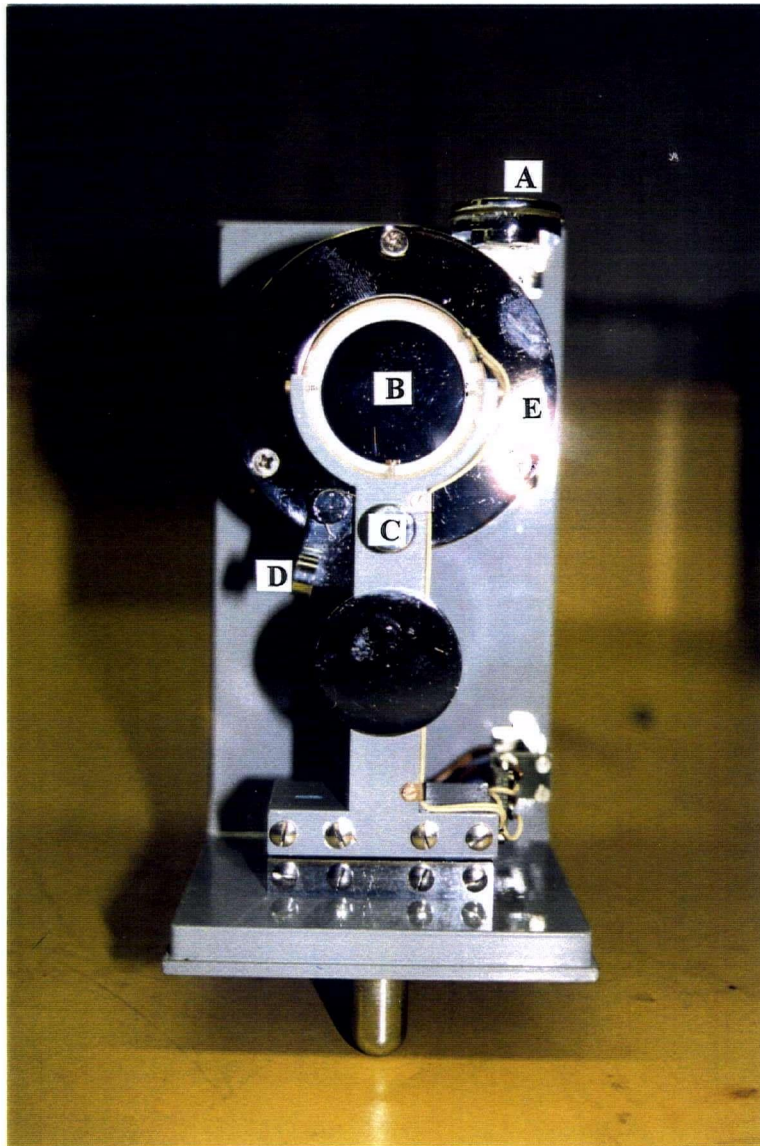
12. In the <<Calibration-amplification (p-p)>> screen, press the *Enter* key
13. In the following screen, input the *Site Name*, *period* and *amplification factors* for each sensor. Press the *Escape* key to confirm entries.
14. The operator can decide whether to start sampling immediately or 10 seconds later by making the appropriate on-screen selection. Once sampling begins, it will last for the entire duration specified in step 8. If at any time during sampling the signals become saturated, e.g., due to a heavy truck passing by, the measurement should be repeated.
15. After sampling is completed, the data acquisition computer will give out beeping sounds to alert the operator. The operator can then choose to display the entire record by pressing the *Space Bar*, or move on to check the spectrum and spectral ratio.
16. After use, set all amplification factors to maximum and set the “Calibration/Measurement” switch to [Calibration].
17. Switch off the data acquisition computer, amplifier and AC/DC converter.
18. Repeat from step 1 for next measurement.



**Legend:**

- |                                    |  |
|------------------------------------|--|
| <i>A: Base screws;</i>             | <i>B: Lense external to brass coil disc;</i> |
| <i>C: Case screws;</i>             | <i>D: External lock;</i>                     |
| <i>E: Level;</i>                   | <i>F: Cable connector;</i>                   |
| <i>G: Lense top of brass disc.</i> |  |

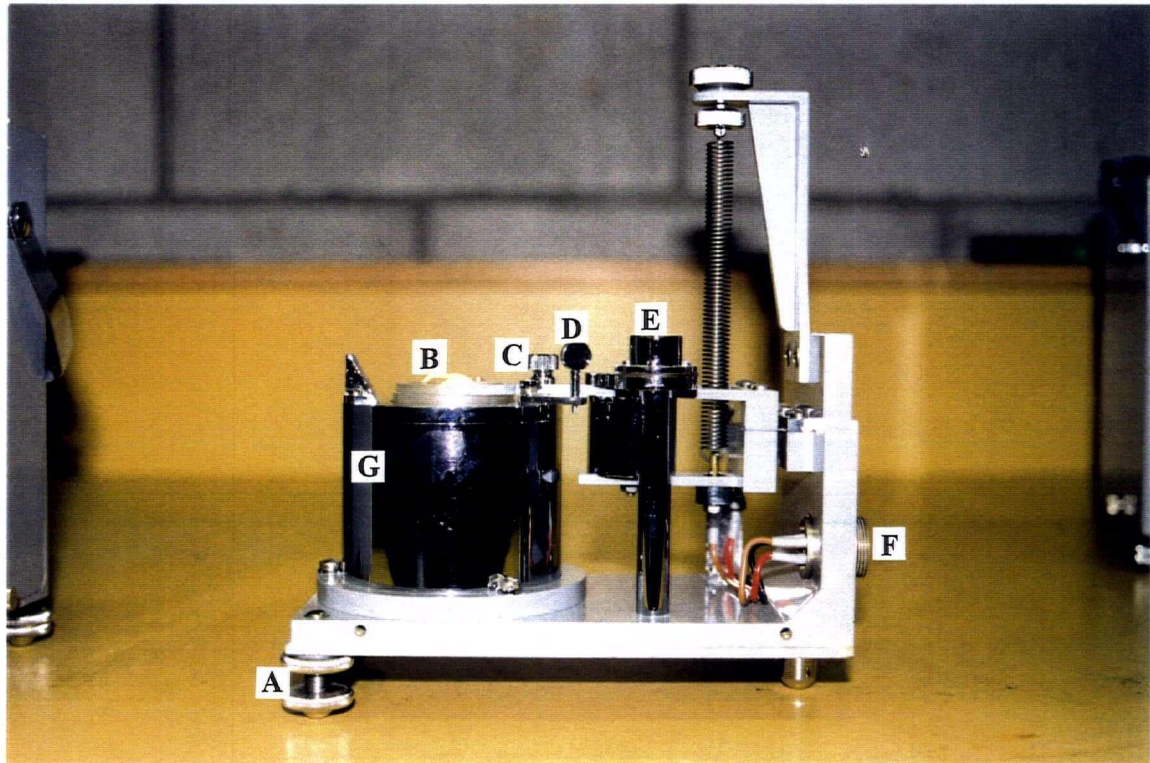
**Figure A.1** Sensors used to measure vibrations in Horizontal (Sensors on Left and Right) and Vertical (Sensor in the middle) directions.



**Legend:**

- |                                     |                                |
|-------------------------------------|--------------------------------|
| <i>A: Level;</i>                    | <i>B: Brass coil disc;</i>     |
| <i>C: Internal lock;</i>            | <i>D: Internal lock plate;</i> |
| <i>E: Magnetic hollow cylinder.</i> |                                |

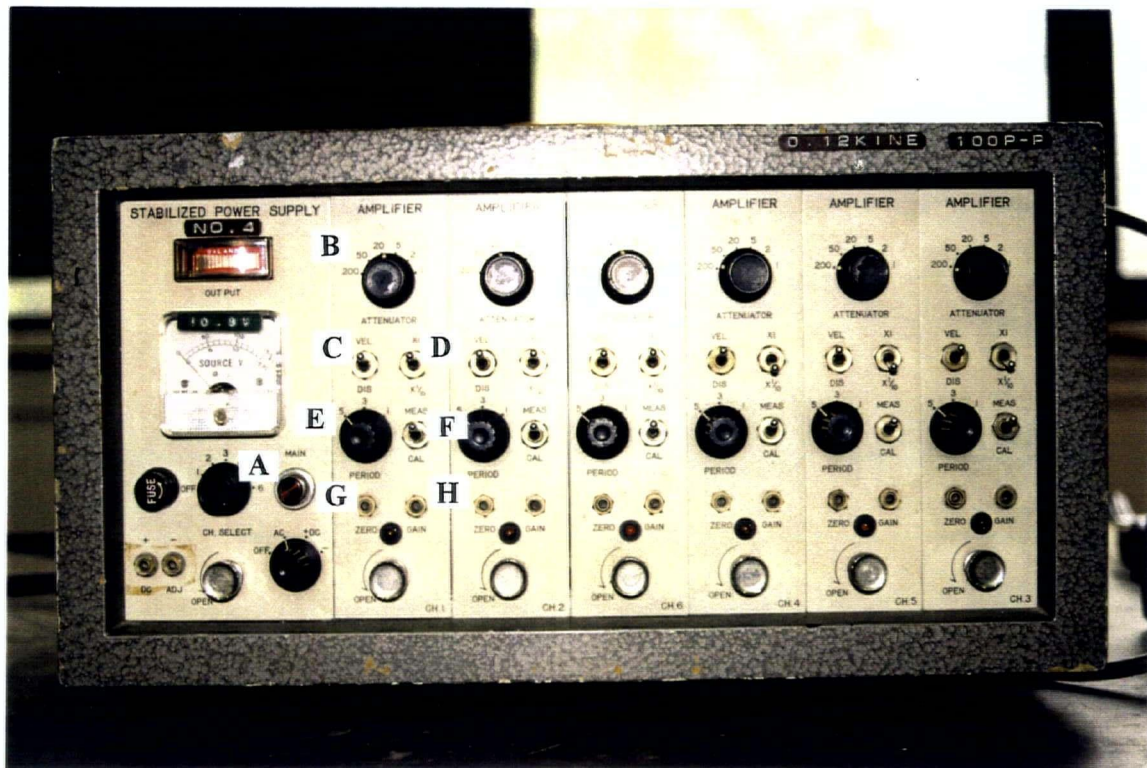
**Figure A.2** Sensor (with case removed) used to measure vibrations in the Horizontal direction.



**Legend:**

- |           |                                  |           |                             |
|-----------|----------------------------------|-----------|-----------------------------|
| <i>A:</i> | <i>Base Screw;</i>               | <i>B:</i> | <i>Brass coil disc;</i>     |
| <i>C:</i> | <i>Internal lock;</i>            | <i>D:</i> | <i>Internal lock plate;</i> |
| <i>E:</i> | <i>Level;</i>                    | <i>F:</i> | <i>Cable connector;</i>     |
| <i>G:</i> | <i>Magnetic hollow cylinder.</i> |           |                             |

**Figure A.3** Sensor (with case removed) used to Measure Vibrations in the Vertical Direction.



**Legend:**

- |           |                          |           |                          |
|-----------|--------------------------|-----------|--------------------------|
| <i>A:</i> | <i>Power switch;</i>     | <i>B:</i> | <i>Attenuation 1;</i>    |
| <i>C:</i> | <i>Vel./Dis. switch;</i> | <i>D:</i> | <i>Attenuation 2;</i>    |
| <i>E:</i> | <i>Period switch;</i>    | <i>F:</i> | <i>Cal./Mea. switch;</i> |
| <i>G:</i> | <i>Zero switch;</i>      | <i>H:</i> | <i>Gain switch.</i>      |

**Figure A.4** Amplifier Model TA-406.

```

*****A/D Conversion Program Menu***** (for PC-Note)*****
**
**      1: temporary measurement                [ADV0]      **
**      2: continuous measurement (regular interval) [AUTV0]    **
**      3: continuous measurement (trigger start)  [EQV0]     **
**      4: plank hammering test                  [ITAV0]    **
**      5: A/D conversion (replay analog recorder) [ADREPLY]  **
**      6: display wave-form of A/D file          [ADPLTV0]  **
**      7: calculate fourier spectra of A/D file  [ADPLTV0]  **
**      8: calculate fourier spectra & spectra ratio [FRTOADV0] **
**      9: edit A/D file                          [AEDTV0]   **
*****[0:END]*****<X.Hao | Dep. Of Civil Eng. | UBC>*****
      Select menu by <space> key then enter <RTN> key

```

**Figure A.5** Main Menu of Data Acquisition Program.

## APPENDIX B

# MICROTREMOR DATA FILE CONVERSION

---

### B.1 DESCRIPTION

Before the measured microtremor records can be read into the DADiSP program for data analyses, the input/data files (extension AD) must be converted to DADiSP readable format (extension AMP). This appendix describes the data file conversion procedures.

Note that during the operations of the data acquisition computer, the selection of options can be made by using either the *Space Bar* or the up/down arrow keys on the keyboard of the data acquisition computer.

### B.2 CONVERSION PROCEDURES

1. Insert the diskette labeled "**DASam 2: Analysis System**" into the disk drive of the data acquisition computer. Switch on the computer by pressing on the *POWER* switch on the top left corner of the computer.
2. After the initial boot-up sequence, a DOS screen emerges to prompt the user for date and time. Note that most of the on-screen instructions are given in Japanese but the key words are given in English. Press the *Enter* key or enter a new date and time to change the default values.
3. An A/D File Conversion screen is then loaded onto the screen. If the first A/D File Conversion screen that appears is in Japanese, press the *Help* key (located to the right of the *Enter* key) to switch to the English A/D File Conversion screen. The screen is titled <<Menu of A/D Data Analysis>>.

4. Select *Option 2. Calculate Real Amplitude using A/D-File* using the *Space Bar* and press the *Enter* key. Note that the other options shown on screen can be used to display waveforms and perform preliminary data analysis of microtremor records.
5. In the following screen of <<Convert A/D File to AMP File Program>>, select *A/D+* as the subscript of A/D (or AD) data files and press the *Enter* key. The user will be prompted for the drive and directory of the location of the AD data files, followed by the drive and directory of the location of the intended AMP data files. Input the required information and press the *Enter* key. Next, select *Manual* at the *Data Input* prompt and press the *Enter* key.
6. The screen should now show all the files in the specified drive and directory of the AD file location. Enter the common name of the input files. For example, if the input files are Shell01 to Shell20 (extension AD), the common part of the filenames is Shell. Press the *Enter* key. The screen will prompt the user for filename number of each input file and output file. Specify all the input files intended to be converted and press the *Enter* key when the specification is completed.
7. In the screen that follows, choose *Option 2: Microtremor Explosion* for data type. Next, select *Vel.* (velocity) for the dimension type. Press the *Escape* key.
8. The new screen shows the information about the microtremor measurement, including the filename, date and time of the measurement, settings of measurements – amplification factors and duration of measurement, sensitivity of the three channels/components of data. Continue to press the *Enter* key to confirm the conversion of the three components of the microtremor data.
9. The waveform of the microtremor record is shown on the screen, and the user is asked to specify the first and end points of the part of the time history to be deleted. Enter the specific points and press the *Enter* key, or press the *Enter* key to skip.
10. The file conversion begins and the entire process can take up a lot of time, with each file requiring about 10 minutes to convert. When the file conversion ends, the user is prompted to select whether to end the file conversion or to choose another input file

for conversion. The converted data files with extension AMP can be found the drive and directory specified in **step 5**.

- 11.** The converted data files can then be copied using low capacity (712 kb) diskettes to a data analysis computer for further data processing and analysis. Low capacity diskettes are used because the data acquisition from Japan which is used for data file conversion can only read diskettes in low-capacity format.

## APPENDIX C

# MICROTREMOR DATA ANALYSIS – PROGRAM OPERATING INSTRUCTIONS AND DOCUMENTATION

---

### C.1 DESCRIPTION

Most steps of the microtremor data analysis are performed using the DADiSP software. The final step of estimating site predominant period and relative amplification ratio is performed through visual inspection of the processed results of the microtremor record. This appendix describes the installation of the DADiSP program and macros files, program requirements and operating instructions of using DADiSP to carry out batch processing of the microtremor data. A set of macros, modified based on the Automated Data Analysis System (ADAS) developed by Hao *et al.* (1995), are used to automate and facilitate the entire data analysis processes, such as reading in microtremor data<sup>1</sup>, extracting header information and time histories of microtremor data, performing Fourier transformation of the data, calculating average Fourier spectra and spectral ratios, printing output files and etc. The DADiSP macros are consisting of the following files, and their respective functions are described as follows. Copies of the macro files are also enclosed in sequence listed below following **Section C.3.1**.

- **MIC2.DSP** initializes all SPL (Serial Processing Language) functions, macros and the file called *ADAS.DAT* (see next file);
- **ADAS.DAT** specifies parameters required for Fourier spectral analysis, as well as location of the source data files; it also controls batch processing of the data files;

---

<sup>1</sup> The microtremor data files which can be read into DADiSP have extension AMP.

- **FLNMTIT2.COQ** calculates the Fourier spectra by calling the macro files: SMOOTH, SP, SSET, and performs Fourier transformation of the data by automating DBLTIT.COQ and MAXTIT.COQ; finally, it controls the printing of the output files;
- **DBLTIT.COQ** reads in header file information and scales amplitudes of the three channels of microtremor data for each measured microtremor record, returns time histories of microtremor data, and setups window headings;
- **MAXTIT.COQ** calculates Fourier spectral ratios based on Nakamura's H/V method;
- **SMOOTH.MAC** smoothes curves of Fourier spectra using Hamming windows;
- **SP.MAC** – calculates Fourier response spectrum of each segment of data and calculates the average Fourier spectrum;
- **SSET.MAC** specifies formats for displaying windows of the Fourier spectral ratios;
- **M\_FRAME.COP** specifies display formats of the general windows;

! Filename: MIC2.DSP

```
!*****  
! Functions: Initializes all DADiSP SPL functions and macros, and runs ADAS.DAT  
! to initialize batch processing of microtremor data files.  
!*****
```

```
removewin(-1) @cr  
clearall @cr  
Addwindow(15) @CR          ! Add 15 Windows
```

```
@CNTL_HOME          ! go to W1
```

```
! Declare location of SPL functions and macros  
Dsploc = strcat("c:\Dsp4\com") @cr
```

```
! Initialize macros  
macread(strcat(Dsploc,"SSET.MAC")) @cr  
macread(strcat(Dsploc,"sedtitAM.MAC")) @cr  
macread(strcat(Dsploc,"SP.mac")) @cr  
macread(strcat(Dsploc,"Smooth.MAC")) @cr
```

```
! Run ADAS.DAT to start batch processing of data files  
call (strcat(Dsploc,"adas.dat")) @cr
```

```
@return
```

```

! Filename: ADAS.DAT

!*****
! Functions: Declares locations of DADiSP and data files, specifies parameters
!             required for Fourier Spectral Analysis, and controls batch processing
!             of data files.
!*****

! Declare the location of DADiSP program
      Dsploc = strcat("c:\Dsp4\com\") @cr

! Declare data set location and name without series #
      flnmcats = strcat("c:\Dsp4\com\shell") @cr

! Declare the number of characters in the parameter: flnmcats
! Ex. There are 17 characters in the string "c:\Dsp4\com\shell"
      sensors = strextract(flnmcats,17,1) @cr

! Declare the number of data per channel
      chnum = 15000 @cr ! Number of each channel

! Declare data range in time histories of microtremor records
      bg = 1 @cr ! The start of data set
      be = chnum @cr ! The end of data set

!*****
! Declare parameters for Fourier Spectral Analysis
      sptm = 8 @cr ! sptm is # of segments
      splnum = 50 @cr ! splnum is frequency
      spnum = 4096 @cr ! spnum is # of points per segment
      ddurs = (spnum/splnum) @cr ! ddurs is duration of segments
      adcat = strcat(".AMP") @cr ! adcat is data filename extension
      defmacro("Nb",1) @Cr

! Declare the first data file's series number as N
      defmacro("N",3) @CR

! Declare the # of data files to be processed
      call(strcat(Dsploc,"flnmtit2.coq"),1) @cr

      moveto(w1) @cr

! Write results of analysis to output file
      writetable("k18.dat",w15) @cr

      @return

```

! Filename: FLNMTIT2.COQ

```
!*****  
! Functions: Controls data processing by calling DBLTIT.COQ and MAXTIT.COQ,  
! generates average Fourier spectra using SMOOTH, SP and SSET  
! macros, and prints results of analysis.  
!*****
```

```
defmacro("j",1) @cr
```

```
! Call DBLTIT to read in header information, scale amplitudes of microtremor  
! time histories, and setup windows of time histories  
call(strcat(Dsploc,"dbltit.coq"),3) @cr
```

```
! Call MAXTIT to generate Fourier spectral ratios based on Nakamura's H/V  
! method  
call(strcat(Dsploc,"maxtit.coq"),1) @cr
```

```
moveto(w1) @cr
```

```
! Call M_FRAME to specify general formats of windows in worksheet  
call(strcat(Dsploc,"m_frame.cop")) @cr
```

```
! Print worksheet containing results of analysis  
printws @cr
```

```
! Reset worksheet for processing of next data file  
pause(5) @cr  
clear(w1..w15) @cr  
display(w1..w15) @cr
```

```
! Define new values for Nb and N  
defmacro("Nb",Nb+1) @cr  
defmacro("N",N+1) @cr
```

```
@return
```

```

! Filename: DBLTIT.COQ

!*****
! Functions: Adjust amplitudes of time histories of microtremor records based on
!            header information and returns correct time histories, and generate
!            Fourier spectra.
!*****

! Scale amplitudes of data based on header information
! Calculate amplitude correction factors
    akm = 256+((J-1)*256*INT(1.99+chnum*2/256)) @cr
    Amax = GETPT(Readb(strcat(flnmcat, strnum(N), adcat), UINT, 2, akm), 1) @cr
    Kmax = GETPT(Readb(strcat(flnmcat, strnum(N), adcat), UINT, 2, akm), 2) @cr
    Rmax = Amax*10^(-kmax) @cr
    Akf = rmax/Amax @cr

! Nbbt information confirmed by T. Samano
    Nbbt = 512+((J-1)*256*INT(1.99+chnum*2/256)) @cr

! Extract data from time histories and adjust amplitudes of data
    extract(readb(strcat(flnmcat, strnum(N), adcat), SINT, chnum, nbbt)*Akf, bg, be)
@CR

    STWAVE2 @CR

    if(splnum == 100, stwave, getwcolor) @cr
    Setplotstyle(0) @cr

! Setup titles for windows w1, w4 and w7
    if((J*3-2)==1, PROTECT(w1, strcat("NS {Velocity [.001*cm/s] vs. time
[sec]}")), getwcolor) @cr
    if((J*3-2)==4, PROTECT(w4, strcat("EW {" , flnmcat, strnum(N), adcat, " } ")),
getwcolor) @cr
    if((J*3-2)==7, PROTECT(w7, strcat("Vert. {" , strnum(be), " Data in Each Time History"
)), getwcolor) @cr

    defmacro("JJ", strcat("w", strnum(J*3-2))) @cr
    wincolor(JJ, lred) @cr

    @rt ! Move to next window, e.g., w2, w5, w8

! Calculate Fourier response spectra
    TMT1(ddurs*Sp(JJ, splnum, sptm)) @cr STFFT2 @cr

    if(splnum==100, setdeltax(0.1219512), getwcolor) @cr

```

! Continuation of **DBLTIT.COQ**

!\*\*\*\*\*

! Specify window display format for Fourier spectra

```
setvunits("cm/s*s") @CR setx(0.0,10.0) @CR sety(0.0,max) @cr setxtic(1)
@CR
setytic(Int(max+.91)/5) @cr
```

! Setup titles for Fourier response spectra

```
if(J*3-1==2,PROTECT(w2,strcat("NS [.001*cm/s*s vs. Hz]" )),getwcolor) @cr
if(J*3-1==5,PROTECT(w5,"EW {Avg. Fourier Spectra}"),getwcolor) @cr
if(J*3-1==8,PROTECT(w8,strcat("Vert. {using ",strnum(sptm)," Segments of ",
strnum(ddurs),"s.}")),getwcolor) @cr
```

@rt

@rt

```
defmacro("J",J+1) @cr
```

@return

```

! Filename: MAXTIT.COQ

!*****
! Functions: Returns Fourier spectral ratios based on Nakamura's H/V method
!            using horizontal to vertical spectral components.
!*****

      moveto(w10) @cr

! Calculate spectral ratio using NS to vertical component
      w2/w8 @cr STFFT2 @cr
      @rt

! Setup title for Fourier spectral ratio
      PROTECT(W10,strcat("Ratio of NS/Vert. [Hz]")) @cr

      Setplotstyle(4) @cr

      @rt

! Calculate spectral ratio using EW to vertical component
      W5/W8 @cr STFFT2 @cr @rt

! Setup title for Fourier spectral ratio
      PROTECT(W12,"Ratio of EW/Vert. [Hz]") @cr Setplotstyle(4) @cr

! Specify W2 as bold and solid line chart
      moveto(w2) @cr nscolor @cr
! Specify W5 as thin and dotted line chart
      moveto(w5) @cr ewcolor @cr

      moveto(w10) @cr nscolor @cr

! Turn on log scale for spectral ratios in W10
      rtFFT @cr

      moveto(w12) @cr ewcolor @cr

! Overplot W10 in W12 - normal scale
      overplot(w10,9) @cr ! blue
      if(max<2,setytic(Int(max+.91)/5),setytic(int(Int(max+.91)/2))) @cr

      moveto(w10) @cr

```

! Continuation of MAXTIT.COQ

!\*\*\*\*\*

! Overplot W12 in W10 - log scale  
overplot(w12,14) @cr ! yellow

@RETURN

! Filename: SMOOTH.MAC

!\*\*\*\*\*

! Functions: *Filters data and smooth curves.*

!\*\*\*\*\*

```
REGRAV(wn)region(ravel(wn,10,1,5),1,10,1,500) ! 0.012207*5
TG      transpose(ghamming(10,.012207))
MM(wn)  mmult(TG,REGRAV(wn))
TM(wn)  transpose(MM(wn))/5      ! to ravel(wn,10,1,5)
TMT1(wn) concat(extract(TM(wn),1,1), TM(wn)); setdeltax(0.0610351)
```

! Filename: SP.MAC

!\*\*\*\*\*

! Functions: *Calculates average Fourier response spectrum.*

!\*\*\*\*\*

! SP = average FFT spectrum  
! DC = mean-value  
! RV = ravel function to ravel specified series into multiple segments  
! which overlaps the previous segment by some specified points  
! RG = region define numbers of groups  
! HM = hamming window to filter time-history  
! SSP = Fourier spectrum of each segment  
! SP = rowreduce(SSP(wn,sl,sn),"+)/sn; returns average of FFT spectrum

DC(wn) wn-mean(wn)  
RV(wn,sl) ravel(DC(wn),sl,1,int(sl/2))  
RG(wn,sl,sn) region(RV(wn,sl),1,sl,1,sn)  
HM(wn,sl,sn) hamming(RG(wn,sl,sn))  
SSP(wn,sl,sn) spectrum(HM(wn,sl,sn))  
SP(wn,sl,sn) rowreduce(SSP(wn,sl,sn), "+")/sn

! Filename: SSET.MAC

```
!*****  
! Functions: generates formatting functions for windows of spectral ratios.  
!*****
```

```
STWAVE2  setxoffset(0.0); sety(min,max); setdeltax(0.02); griddot; gridhv;  
setplotstyle(3); setxtic(20)
```

```
RtFFT    setxlog(1); setylog(1); setxtic(1); setytic(1); setx(0.2,20);  
sety(.1,10)
```

```
STFFT2   setxlog(0); setylog(0); setx(0,10); sety(min,max); griddot; gridhv;  
setxtic(1); setytic(5); setplotstyle(0)
```

```
Nscolor  setlinewidth(4); setline(1); setcolor(9)  
Ewcolor  setlinewidth(2); setline(3); setcolor(14)
```

! Filename: M FRAME.COP

!\*\*\*\*\*

! Functions: *specifies general display formats of windows.*

!\*\*\*\*\*

display(w1,w2,w4,w5,w7,w8,w10,w12) @cr

collayout(2,2,2,2) @cr

Setwsize(w1,0.01,0.01,.735,.16,-1) @cr

Setwsize(w4,0.01,0.17,.735,.16,-1) @cr

Setwsize(w7,0.01,0.34,.735,.16,-1) @cr

@CNTL\_HOME

! go to W1

## C.2 INSTALLATION AND SYSTEM REQUIREMENTS

The DADiSP software, version 4.1, should run on any computer with a 80486 processor or higher, a SVGA monitor and sufficient amount of disk space (>20 Mb). The author found that DADiSP works well in both Microsoft Windows 95 and Windows 98 operating systems.

### C.2.1 Installation of DADiSP 4.1

The installation of the DADiSP software is fairly straightforward. The setup of the DADiSP software can be done by running the setup file (filename: **setup.exe**) on the setup disk which contains the DADiSP software. The remaining steps are carried out by following the on-screen instructions. It should be noted that the location of DADiSP installation is referred to in the DADiSP macro files used to automate the microtremor data analyses. For the DADiSP macro files used by the author to process the microtremor data, the specified location of DADiSP installation is “**c:\dsp4**”, i.e., directory “**dsp4**” on hard disk **C**. If the DADiSP 4.1 is installed in a location other than “**c:\dsp4**”, the user should make appropriate changes in the parameter called *DSPLOC* in the macro files called ADAS.DAT and MIC2.DSP.

### C.2.2 Installation of DADiSP Macro Files

The installation of the DADiSP macro files is carried out by copying all the macro files as described in **Section C.1** into the subdirectory called “**com**” under the directory where DADiSP 4.1 was installed. The complete path to which the macro files should be kept is: “**c:\dsp4\com**”.

## C.3 PROGRAM EXECUTION

### C.3.1 Storing the Data Files for Batch Processing

Prior to running the data analyses using DADiSP, the data files (of extension .AMP) which contain the measured microtremor records must first be stored into a subdirectory specified by the parameter called *flnmc* in the file ADAS.DAT. The directory path specified in the file ADAS.DAT is “c:\dsp4\com”. In addition, minor modifications must be made to the codes in ADAS.DAT as follows. Examples of modifications are shown assuming a collection of three data files: shell01.amp, shell02.amp and shell03.amp.

- To specify the common part of the filenames of the data files:

**flnmc = strcat(“c:\dsp4\com\*common part of filenames*”)**

e.g., since the data files are shell01.amp, shell02.amp and shell03.amp, the *common part of filenames* is *shell*.

- To specify the first data file number:

**Defmacro(“Nb”, *first data file number*) @cr**

e.g., using the same example as before, the *first data file number* is 1 (or 01).

- The number of times the data analyses are to be performed equals the number of data files to be processed. To specify the number of data files:

**Defmacro(“N”, *number of data files*) @cr**

e.g., using the same example as before, the *number of data files* is 3.

### **C.3.2 Running the Programs**

The data analyses of the microtremor data files are performed by first loading/starting the DADiSP program. This can be done by double-clicking the DADiSP program icon on the desktop (if it is there already) or click on Start/Programs/DADiSP for computer systems using Window 95/98 operating system. A DADiSP worksheet would be loaded onto the computer screen (see **Figure C.1**). Assuming that the microtremor data files are stored in the location specified in the macro files and appropriate modifications have been made to the macro files as described in **Section C.3.1**, only one final step is required to begin the data analyses using DADiSP – click on the command line box on top of the worksheet and type: **Call("c:\dsp4\com\mic2.dsp")** and press the *Enter* key. The data processing for the entire batch of data files should be carried out automatically, with each output file printed after each data file is processed. Once the output files are ready, the remaining work is to estimate the site predominant periods and relative amplification ratios from the output files through visual inspection.

### **C.3.3 Example of Experimental Analytical Results**

An example of a processed microtremor output file is shown in **Figure C.2**. The location of the site, K15, is near the entrance to the Northeast wing of the Civil and Mechanical Engineering Building, University of British Columbia as shown in **Figure C.3**. The site predominant frequency is estimated from the peak Fourier spectral H/V ratios to be 0.8 Hz, whereas the peak spectral ratio is approximately 3.0. Both of these values are very similar to those obtained by Dr Hao X.-S. on a different occasion for the same K15 station.

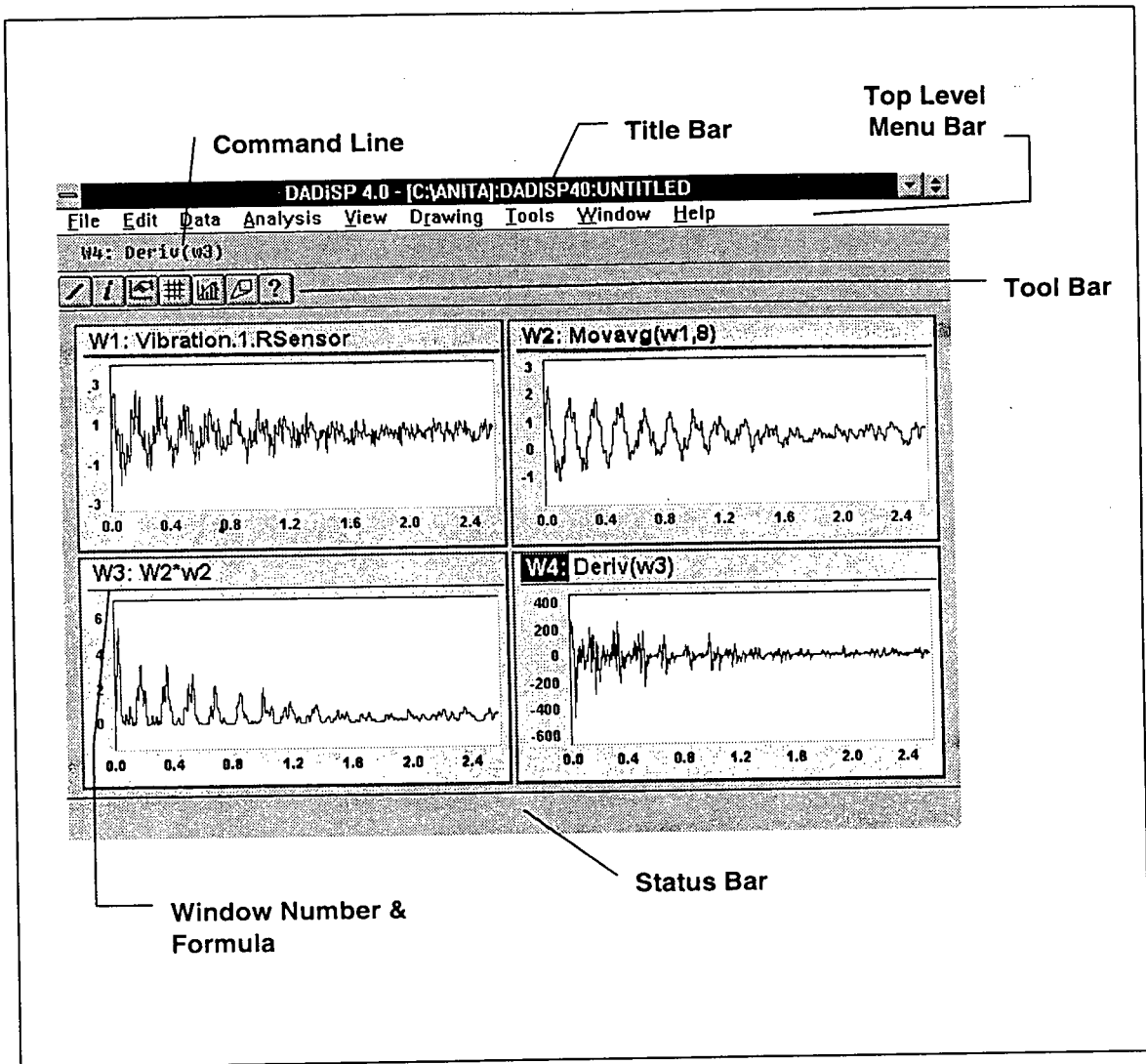


Figure C.1 DADiSP Worksheet Layout.

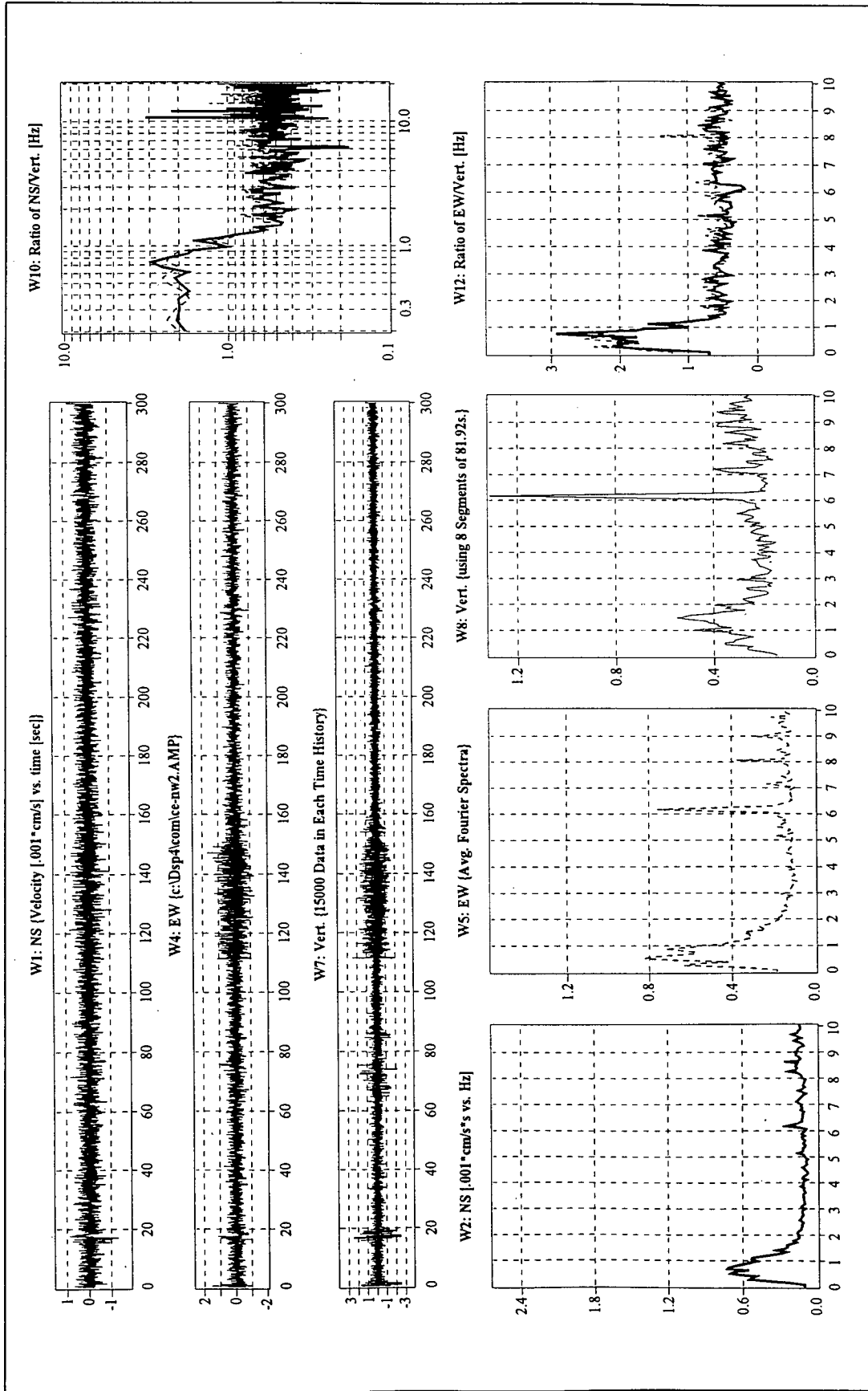


Figure C.2 An Example of An Analyzed Record of Microtremor Measurement at Station K15 in U.B.C. (1998).

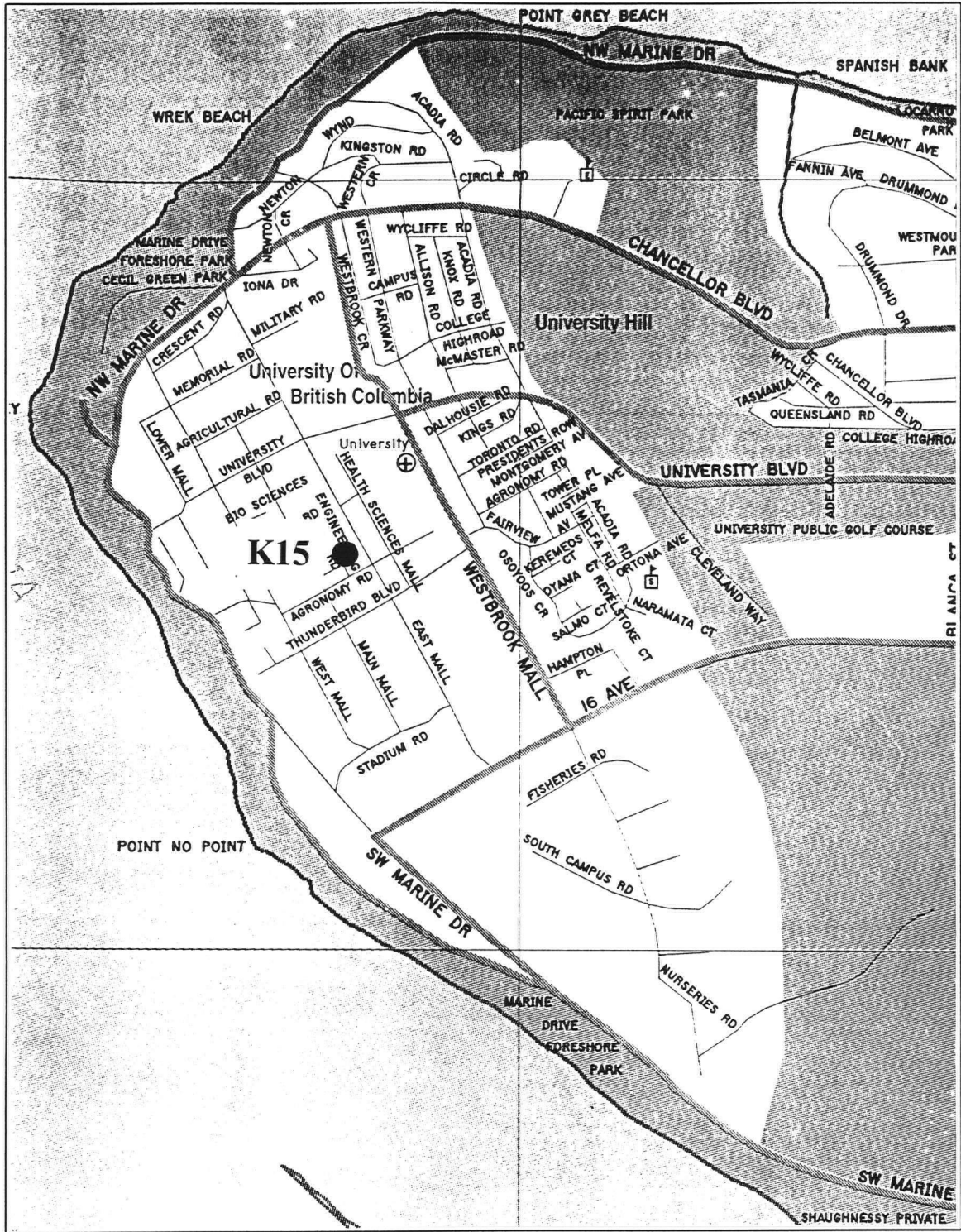


Figure C.3 Location of Microtremor Measurement Station K15.